GCA Technical Report 65-23-N

UPPER ATMOSPHERE CHEMICAL RELEASE STUDY

J. Pressman A. Sharma J. Padur H. K. Brown C. Rosen

FINAL REPORT

Contract No. NASw-985

August 1965

GCA CORPORATION
GCA TECHNOLOGY DIVISION
Bedford, Massachusetts

NATIONAL AERONAUTICS AND SPACE ADMINISTRATION
Headquarters
Washington 25, D.C.

TABLE OF CONTENTS

Section	Title	Page
	INTRODUCTION	1
	A. Purpose of Contract	1
	B. Outline of Program	2
	C. Reports	3
	D. Review of Chemical Release Studies of Upper Atmosphere	3
2	OUTLINE OF PROJECTED ROCKET SERIES AND PRIORITIES	5
	A. List of Priority Experiments	5
	B. Suggested Rocket Experiments	5
3	ANALYSIS IN DEPTH OF ROCKET EXPERIMENT RELEASING OXYGEN	31
	A. Introduction	31
	B. Short History of the 6300Å Emission Line Research	31
	C. Theoretical Discussion of Possible Mechanisms	32
	D. Approximate Calculations	33
	E. More Accurate Calculations from Full Differential Equations	41
4	LABORATORY STUDIES	57
	A. Introduction	57
	B. Experimental	60
	C. Results of Survey Experiments	62
	D. Low Pressure Study	86
5	RECOMMENDATIONS	93
	REFERENCES	95
Appendix A	RESUME OF THE MATHEMATICAL DEVELOPMENT SPECIFIED IN THE "SNOWPLOW" AND "INTERPENETRABILITY" MODELS FOR THE 6300Å PERTURBATION ROCKET EXPERIMENT	97

LIST OF ILLUSTRATIONS

Figure	Title	Page
1	Fraction dissociated as function of temperature and pressure.	9
2	Heat content of 2 gm of hydrogen as a function of temperature and pressure.	10
3	Heat content of hydrogen gas containing one mole of hydrogen atoms as a function of pressure and temperature.	11
4	Container volume as a function of temperature and pressure.	12
5	Visible spectrum of chemiluminescent reaction of nitric oxide with atomic oxygen and ozone.	23
6	Rate of excitation, $O^*(^1D) = \alpha\,[e]\,[O_2^+]$ as a function of time.	34
7	Center-point values of concentration fields of several species for Snowplow model.	50
8	Integrated line density $S^{(1)}_{[O^*]}$ of O* for Snowplow model, $\epsilon = 0$, and $\epsilon = 1$.	53
9	Integrated line density $S_{[O^*]}(t,h)$ of O* for Interpenetrability model.	54
10	Medium pressure reaction system.	61
11	Low pressure reaction chamber.	63
12	Block diagram of apparatus for observation of chemiluminescence.	64
13	Ozone-handling system.	65
14	An arrangement for transferring organometallic liquid.	66
15(a)	Chemiluminescence spectrum of acetylene and atomic oxygen.	71
(b)	Chemiluminescence spectrum of ethylene and atomic oxygen.	71

LIST OF ILLUSTRATIONS (continued)

Figure	Title	Page
16	Chemiluminescent spectrum of carbon disulfide, carbonyl sulfide and hydrogen sulfide reaction with atomic oxygen and comparison with sulfur dioxide afterglow.	72
17	Corrected spectrum of the chemiluminescence produced during the reaction of boron trichloride and atomic oxygen.	74
18	The spectrum of the chemiluminescent reaction of germane with atomic oxygen.	76
19	The spectra of the chemiluminous reactions of some organometallic compounds with atomic oxygen: the relative intensity of the different chemiluminous reactions is shown.	77
20	The spectrum of the chemiluminescence produced during the reaction of trimethyl aluminum and atomic oxygen.	78
21	The spectrum of the chemiluminous reactions of triethyl boron and atomic oxygen.	79
22	The spectrum of the chemiluminous reaction of diethyl zinc and atomic oxygen.	80
23	The spectrum of the chemiluminous reaction of trimethyl antimony and atomic oxygen.	81
24	The spectrum of the chemiluminous reaction between hydrocarbon and atomic nitrogen.	82
25	The spectrum of the chemiluminescence produced during the reaction of boron trichloride and atomic nitrogen.	83
26	Intensity vs flow rate variation at low pressure.	91

UPPER ATMOSPHERE CHEMICAL RELEASE STUDY

By J. Pressman, A. Sharma, J. Padur, H.K. Brown, and C. Rosen
GCA Corporation, GCA Technology Division

INTRODUCTION

A. Purpose of Contract

The objective of this program of research has been to conduct a series of laboratory and theoretical studies in the general area of chemical release experiments in the upper atmosphere. These studies had for their purpose the design of a program of chemical release experiments for obtaining scientific data on the upper atmosphere of the earth. It was considered further that a chemical release program before moving into field operation should be based on as accurate as possible laboratory data and a full theoretical analysis insuring a solid foundation. Before the chemical release occurs in the upper atmosphere the fundamental microscopic numbers such as reaction rates, quantum efficiency, emission spectrum, etc. will have been carefully measured.

Further, in chemical release experiments there is a necessary chain of argument and mathematics from the observations to the final result. In general an appropriate system of equations including the kinetics of the reactions and diffusion must be solved in some degree of complexity allowing for initial conditions. If the modelling is unrealistic or the mathematics intractable, the reduction of data to meaningful results may be poor or even impossible. Consequently, this theoretical aspect has been carefully investigated for one experimental concept. There are additional theoretical aspects that are essential to the field performance of a chemical release program. In certain types of releases there are thermochemical considerations that are vital to a specific experiment. The theoretical analysis of these and other problems important to the total design of specific experiments has been performed in relative degrees for suggested experiments.

The chemical release program has input into several broad areas of geophysical research. The first general area is that of the physics of the atmosphere of the earth and other planets. The measurements from this program will help to elucidate such problems as nighttime density, upper atmosphere diffusion, the atomic oxygen transition region, wind structure, etc. Such data is important to the physics of the earth's atmosphere and consequently to the physics of the atmosphere of the other planets.

Cometary physics is another area to which atmospheric chemical release physics may contribute. Chemiluminescence is considered one of the important processes occurring in comets. Release experiments design-

ed during this program will contribute to knowledge of pertinent reaction rates, dynamics and optical phenomena.

While the program began as a theoretical and laboratory program, it was conceived as open-ended in terms of being a preparation for extension into a field program. To this end the exploratory laboratory chemiluminescent program has been carried on with existing GCA laboratory equipment. Also, new concepts have been explored which present broad opportunities. For instance, there have been investigated such new techniques as ozonospheric chemiluminescence, differential chemiluminescent spectra, etc. The purpose of this phase of the research has been to extend the potential and scope of chemical releases. Consequently the performance of selected rocket experiments has been recommended to NASA.

B. Outline of Program

This program has been divided into five basic parts. In the first phase a review has been made of the state-of-the-art of chemical releases. In the second part a series of innovative concepts for rocket chemical releases have been arrived at. Further they have been examined at reasonable depth to insure their feasibility.

In the third part, one of the concepts, in this case a chemical release experiment aimed at explicating the 6300Å night sky oxygen emission is examined in great depth. This includes the scientific evaluation of the operative mechanisms causing the glow, a mathematical evaluation of the associated set of non-linear differential equations, and the prototype engineering design.

The fourth phase and the one that has received the most emphasis in this study has been an extensive and systematic laboratory study of chemiluminescent compounds. This study has measured the reaction of many compounds with three reactive atmospheric species, atomic oxygen, atomic nitrogen and ozone. The spectra and intensity have been obtained at both high pressure and low pressure. Many interesting phenomena have been found. In particular there have been discovered:

(1) A compound TEB which gives far higher luminescent yields with atomic oxygen on a molar or weight basis. Comparison with TMA gives a weight equivalent of 1/20 for the same luminosity.

(2) A compound has been found, diethyl zinc which gives much higher luminescence with atomic nitrogen than compounds previously reported. At the same time its luminosity with atomic oxygen is very weak. Consequently this compound is the best compound found to date for titrating atomic nitrogen.

(3) It has been established that many compounds previously reported in the literature to luminescence with ozone do not do so. Further measurements have indicated that trimethyl aluminum is the most active chemiluminescent agent with ozone.

There is a fifth phase in which conclusions and recommendations are made.

Much of the work has been described in a series of five Technical Reports which together with this Final Report comprise the bulk of the work performed on this contract.

C. Reports

In addition to the Quarterly Reports and the Final Report, a series of GCA Technical Reports listed below have been written and are being published on this contract. In parenthesis, next to each title, is given the scientific journal for which the paper has either been accepted or to which it is being transmitted.

(1) "A Spectroscopic Study of the Chemiluminescent Reaction of Germane with Atomic Oxygen" (To be published in Journal of Chemical Physics).

(2) "A Study of the Chemiluminescent Reactions of some Organometallics with Atomic Oxygen" (To be published in J. Phys. Chem.)

(3) "A Study of the Chemiluminescent Reactions of CS_2 and COS and H_2S with Atomic Oxygen" (Published in Journal of Chemical Physics.)

(4) "The Chemiluminescent Reactions of Ozone" (To be submitted to Am. J. of Chem.)

(5) "Chemical Release Study of the Upper Atmosphere" (To be submitted to Ann. de Geophysique.)

D. Review of Chemical Release Studies of Upper Atmosphere

This phase of the work is reported on completely in Technical Report No. 5, "Chemical Release Study of the Upper Atmosphere," and to avoid repetition only a brief listing of its contents will be given here. It should be mentioned that the purpose of this review is to present the state-of-the-art of the use of chemical release experiments for obtaining information on the state-of-the-upper atmosphere. A listing of the Table of Contents is given below:

1. Introduction
2. Summary of previous release experiments
3. Theory of the interaction and dynamics of released chemical with ambient atmosphere
4. Winds and turbulence
5. Electronic and ionic properties of upper atmosphere
6. Chemical properties of upper atmosphere

7. Physical properties of upper atmosphere
8. Elucidation of upper atmospheric processes
9. Summary and conclusions

2. OUTLINE OF PROJECTED ROCKET SERIES AND PRIORITIES

In this section an extensive series of GCA-suggested rocket experiments is identified and analyzed as to feasibility. Further there are selected out of these and set up in a priority, five of the analyzed experiments. First below we list in order the priority experiments concisely. This is followed by a list of the suggested experiments and an analysis of these experiments.

A. List of Priority Experiments

The list of priority experiments given below is annotated only briefly. The motivation for the TEB experiment's primacy has been given in the introduction.

(1) Release of tri-ethyl boron (TEB). See Introduction

(2) Release of molecular oxygen to test hypothesis of 6300Å mechanism. See original proposal to which this report is an addendum for full discussion

(3) Simultaneous measurement of ratio of two minor constituents, e.g., O and O_3, through differential chemiluminescent spectra. This technique provides the ratio of two active atmospheric constituents without the need of knowing the dynamics of expansion.

(4) NO (or other compounds) measurements of atomic oxygen and simultaneous ground measurement of 5577Å. A check on theories of 5577Å emission.

(5) Release of atomic hydrogen into region of hydroxyl emission. A check on theory of the natural hydroxyl emission by perturbing the concentration of atomic hydrogen. See paragraph B below.

B. Suggested Rocket Experiments

In this phase a series of rocket chemical release experiments is suggested for probing at some of the as yet unsatisfactorily understood phases of atmospheric physics. The analysis of these experiments because of their large number is only carried out in sufficient detail to establish their reasonable validity with the exception of one experiment which has been analyzed in full in the original GCA proposal. The listing of experiments is given in the Table of Contents.

The stated purpose of the selected experiments is to improve our scientific understanding of the upper atmosphere. Consequently, not only upper atmospheric characteristics such as temperature and composition were suitable for rocket experimentation but also atmospheric processes. In particular, experiments have been designed for the purpose of elucidating the mechanisms for the emission of various airglow lines and bands. An effort has been made

to eschew types of experiments already performed unless a reasonable degree of improvement is expected.

The proposed experiments are divided into three types. They include experiments designed to test atmospheric mechanisms, experiments to test a variety of improved titration techniques, and those experiments designed to improve temperature measurements of the upper atmosphere. These experiments are discussed below.

Experiments to test atmospheric mechanisms. - This group of experiments is designed to provide some check on the causative mechanisms of various airglow emissions. They include the 6300Å atomic oxygen line, the 5577Å atomic oxygen line and the hydroxyl emission.

Release of molecular oxygen between 250 and 300 km to test the 6300Å mechanism. - This experiment was selected for detailed analysis in the original proposal. Consequently, here only a description of the concept will be given. For an evaluation of the concept see Section 3.

The purpose of this chemical release experiment is to further elucidate the mechanisms of the 6300Å atomic oxygen emission of the night airglow. As yet neither the basic mechanism or mechanisms nor the altitude distribution of the emission is well established. A brief review is given below.

The nocturnal intensity of the red line is between 50 R and 100 R. The daytime intensity is considerably higher, being of the order of 50 kilo-Rayleighs. Earlier calculations of the 6300Å airglow were based upon relatively simple schemes of reactions involving ion removal and were dependent upon the adopted values of the reaction rate constants. As yet, significant doubts exist as to the specific mechanisms. These are undoubtedly ion-atom interchanges leading to ionized molecules, probably either O_2^+ or NO^+. This is followed by dissociative recombination with an excited atom of oxygen.

Rocket experiments have not conclusively defined the region of emission; however, it is generally considered to be rather broad with maximum in the F_1 region. Consequently, it is proposed that a twofold experiment be performed in which substantial amounts of oxygen and nitrogen are deposited in the F_1 region (250 to 300 km). At 300 km O_2 and N_2 constitute approximately 0.1 percent and 0.8 percent of the total gas number, while at 250 km they constitute 0.3 percent and 15 percent respectively. Consequently, a release of 10^3 moles will substantially increase the oxygen and nitrogen concentration over hundred to thousands of cubic kilometers and may change the 6300Å emission. One thousand moles occupy 30 to 35 liters for liquid oxygen and nitrogen and allowing for efficiency of evaporation some 60 liters will be required. No significant change in electron density should occur because of the rapid movement of electrons.

Chemical release experiment to investigate the mechanism of the hydroxyl emission. - The OH vibration-rotation bands of the airglow extending from

5000Å to 2.3μ are the dominant feature of the airglow. A total emission rate of 5000 kR makes this extensive system the brightest night airglow emission.

Since the first measurements of the hydroxyl emission there have been considerable numbers of observations made of the hydroxyl airglow. There have been many studies of the rotational and vibrational structure of the hydroxyl emission in the field and in the laboratory. The equivalence of the ambient gas temperature and the rotational temperature is reasonably well established.

There remain major inconsistencies in the atomic hydrogen-ozone hypothesis. The total emission is accounted for on the basis of this hypothesis operating in a night-time model hydrogen-ozone atmosphere. However, the calculated maximum of emission is lower than that observed. The only way to account for this fact is to assume deactivation is operative. However, such deactivation would then lower the total rate of emission.

Consequently, any experiments which would significantly elucidate the mechanisms of emission of the hydroxyl emission would add to our knowledge of the upper atmosphere. It is with this viewpoint that the release of atomic hydrogen at an altitude of about 80 km seems worthwhile.

The basic concept is to release from a rocket at appropriate altitudes (circa 80 km) sufficient atomic hydrogen to increase significantly the ambient concentration of this species. This should perturb the emission mechanism of those systems linked with atomic hydrogen. Although the major emission involved is the hydroxyl emission several other emissions such as the sodium-D and hydrogen alpha have also been casually linked to atomic hydrogen. Consequently, these emissions will be monitored also by ground-based photometers both birefringent and interferometric. The catalytic activity of atomic hydrogen constitutes an asset.

The engineering considerations constitute a key factor in this proposed experiment since the basic problem is to manufacture and deliver approximately 1/10 of a mole to an altitude of 80 km within a volume of a few cubic kilometers. Unfortunately, while atomic hydrogen has been produced by many techniques, there have been no optimization studies of the kind necessary for this program. Techniques for generating atomic hydrogen are basically of the gaseous discharge, arc, furnace, and chemical technique and their output has been evaluated.

There are two techniques, the hydrogen arc and the furnace technique, which are presently under examination as possible techniques. They are discussed a little more fully below.

(1) Hydrogen Arc. The energy of dissociation of hydrogen is about 100 kilocalories per mole or approximately 400,000 joules. Consequently, with our 1.10 mole requirement the minimum energy needed is 40,000 joules. Since we desire to dissociate the hydrogen within about one second in order to ensure its localization within one cubic kilometer, the minimum requirement is

for 40 kilowatts. Consequently, "beefing up" the hydrogen torch by about a factor of 3 or utilizing 3 such devices in concert seems reasonably possible with a power source delivering 100 kilowatts for one second. It is noted that the total apparatus - power supply, arc, electrodes, etc., constitute a "one shot" device. A major factor is the energy storage. While batteries are capable of storing 10 watt hours per pound or 36,000 joules, their peak capability for time as short as a second goes down considerably. A reasonable estimate is 2000 joules for 2.3 pounds of batteries. Consequently, the energy storage weight would range from 100 to 150 pounds. This would constitute the major bulk of the apparatus.

(2) Thermal Technique of Generation. The technique to be used here circumvents the energy storage requirements of the in situ generation. Basically, the system is one in which, through an umbilical cord, power is piped into our furnace system, thus avoiding the above calculated weight of the power supply. There are two possible types of systems. In one the hydrogen is incorporated directly in the furnace. This system has the disadvantage that it has to retain a pressure of several atmospheres and operate at 3000°C. The alternate system consists of two parts, of which the first is a hydrogen reservoir in which the hydrogen is preheated to approximately 1500 to 2000°C. The second unit is the hot furnace at 3000°C. These units are carried aloft and at a prescribed time a diaphragm is broken and the hydrogen is flushed through the 3000°C furnace. The interior of the furnace will be fabricated of a combination of tungsten and refractory ceramic. Good heat transfer will have to be assured through the use of a pebble bed, network of wires, or other heat transfer mechanisms within the furnace.

Formation of atomic hydrogen under equilibrium conditions. - From equilibrium thermodynamic considerations one can calculate the percentage dissociation of hydrogen gas as a function of temperature and pressure. Figure 1 shows the results of such calculations for hydrogen at pressures ranging between 10^{-3} atm to 10^{5} and temperatures ranging between 1000 to 6000°K.

Again using equilibrium considerations one can calculate the heat content of a given distribution of the various hydrogen species. Figure 2 displays the values for the heat content of two grams of hydrogen as a function of temperature and pressure. If we combine Figures 1 and 2, we can derive Figure 3 which gives the heat content of a container holding one mole of hydrogen atoms.

The volume of these various equilibrium distributions of hydrogen can be obtained with the aid of the ideal gas law. Figure 4 shows the volumes of containers that will be required in order to hold one mole of hydrogen atoms at various temperatures and pressures. This shows that in order to contain 0.1 of a mole of hydrogen atoms in a 10-liter container, we would have to heat it to 3300°K if it were pressurized at 10^{5} atm. Considering the very large values of the diffusion coefficient of hydrogen at high temperatures, these considerations lead to the conclusion that we will be faced with a rather severe materials problem if we were to attempt to produce the hydrogen by this method.

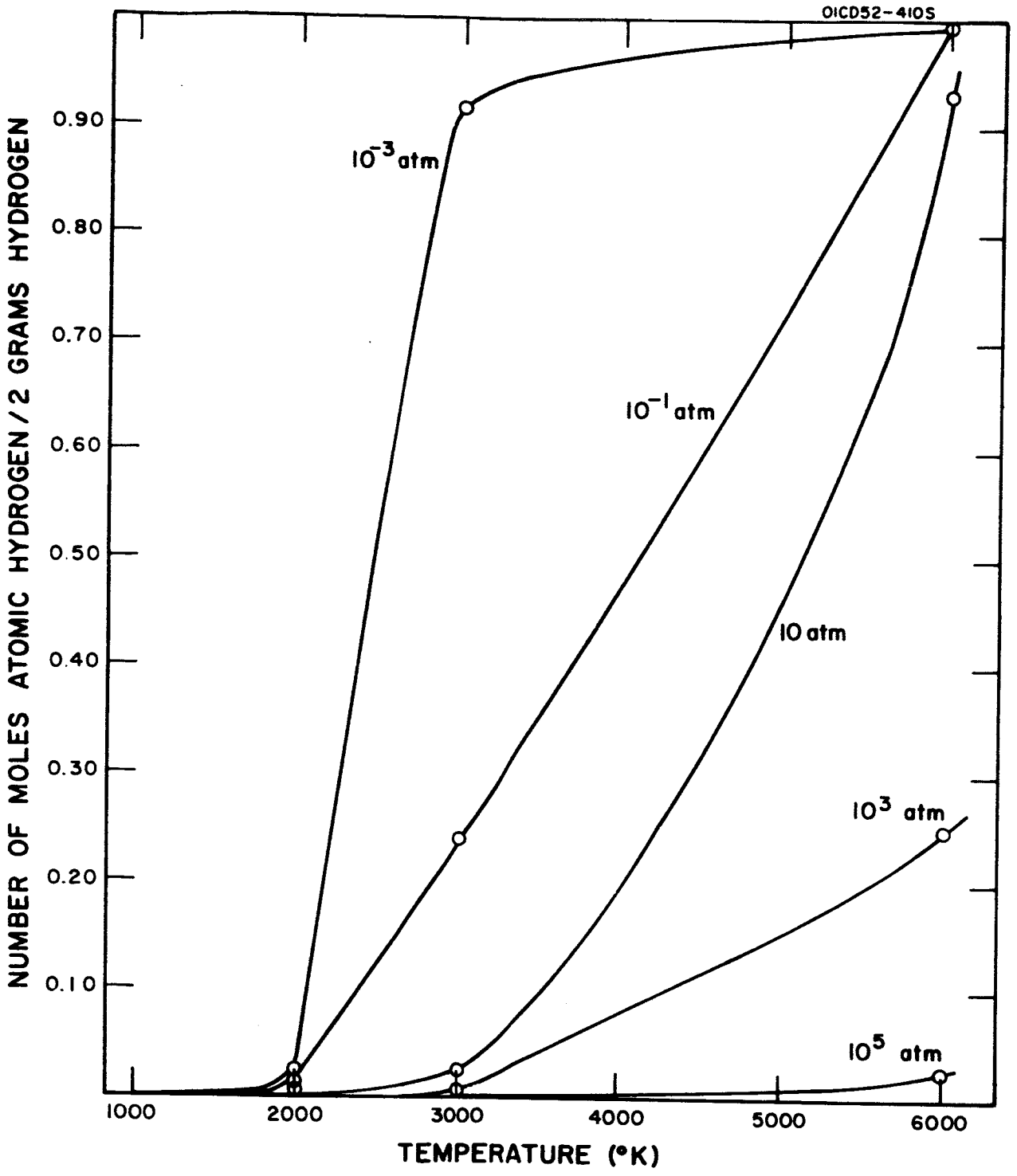

Figure 1. Fraction dissociated as function of temperature and pressure.

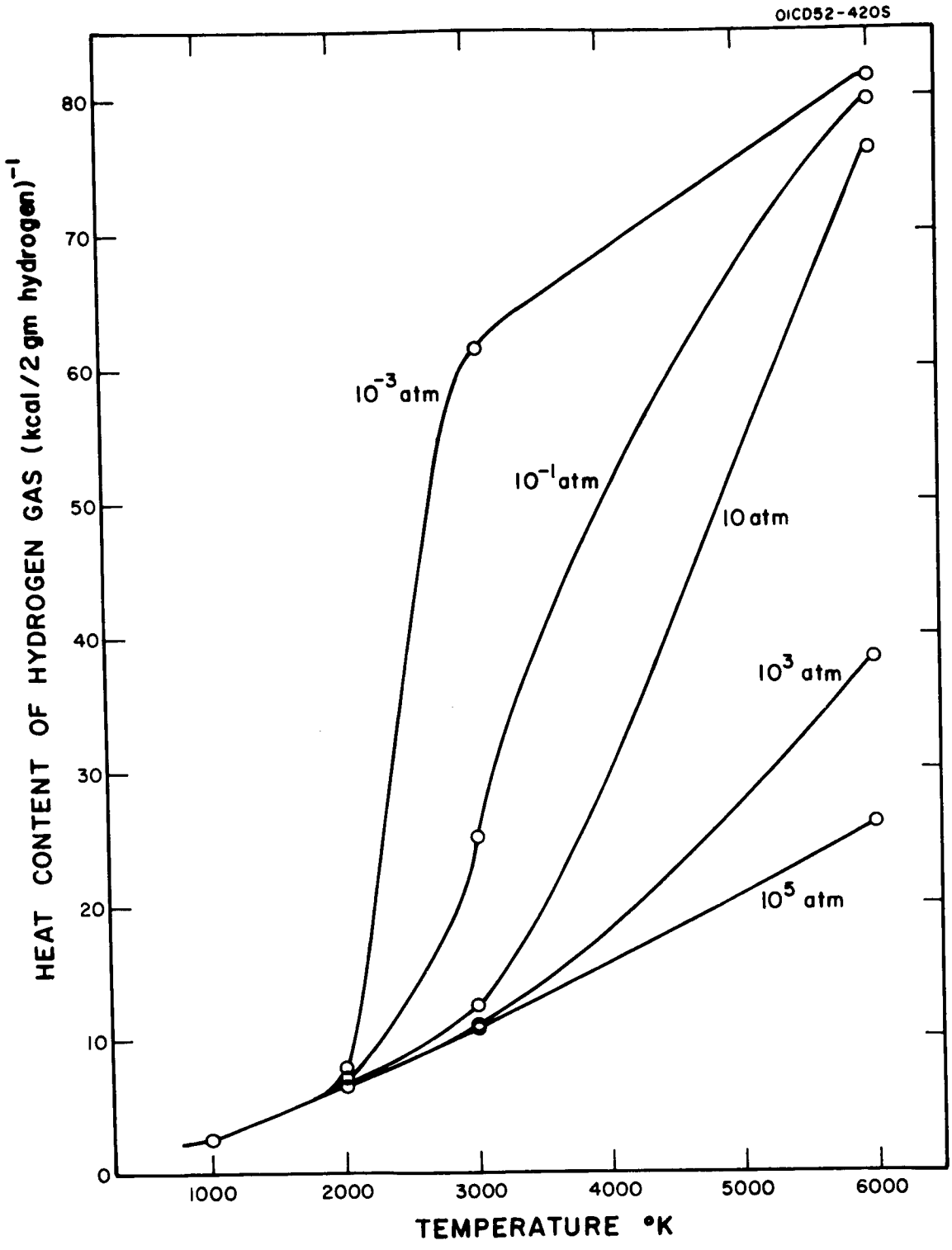

Figure 2. Heat content of 2 gm of hydrogen as a function of temperature and pressure.

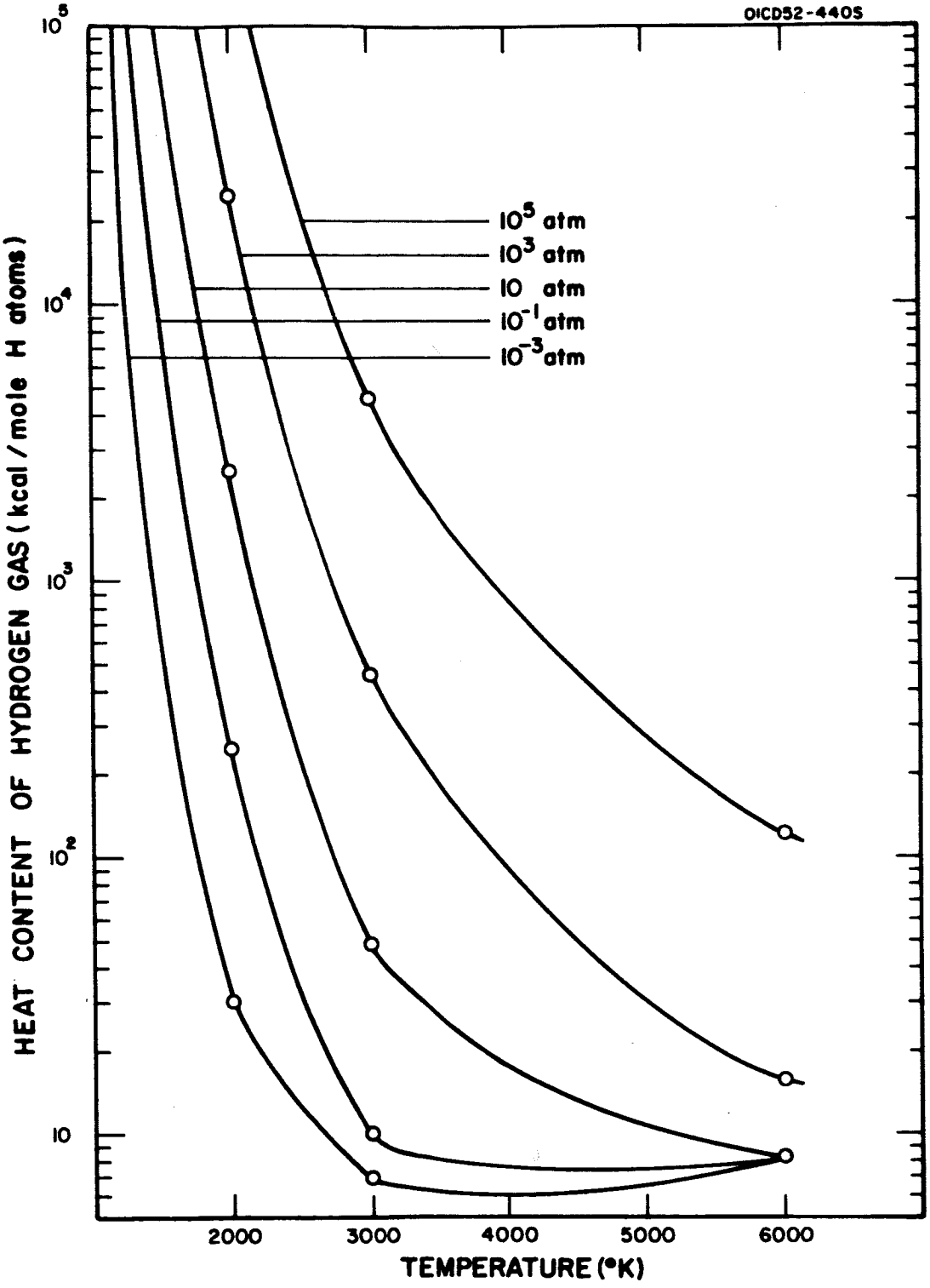

Figure 3. Heat content of hydrogen gas containing one mole of hydrogen atoms as a function of pressure and temperature.

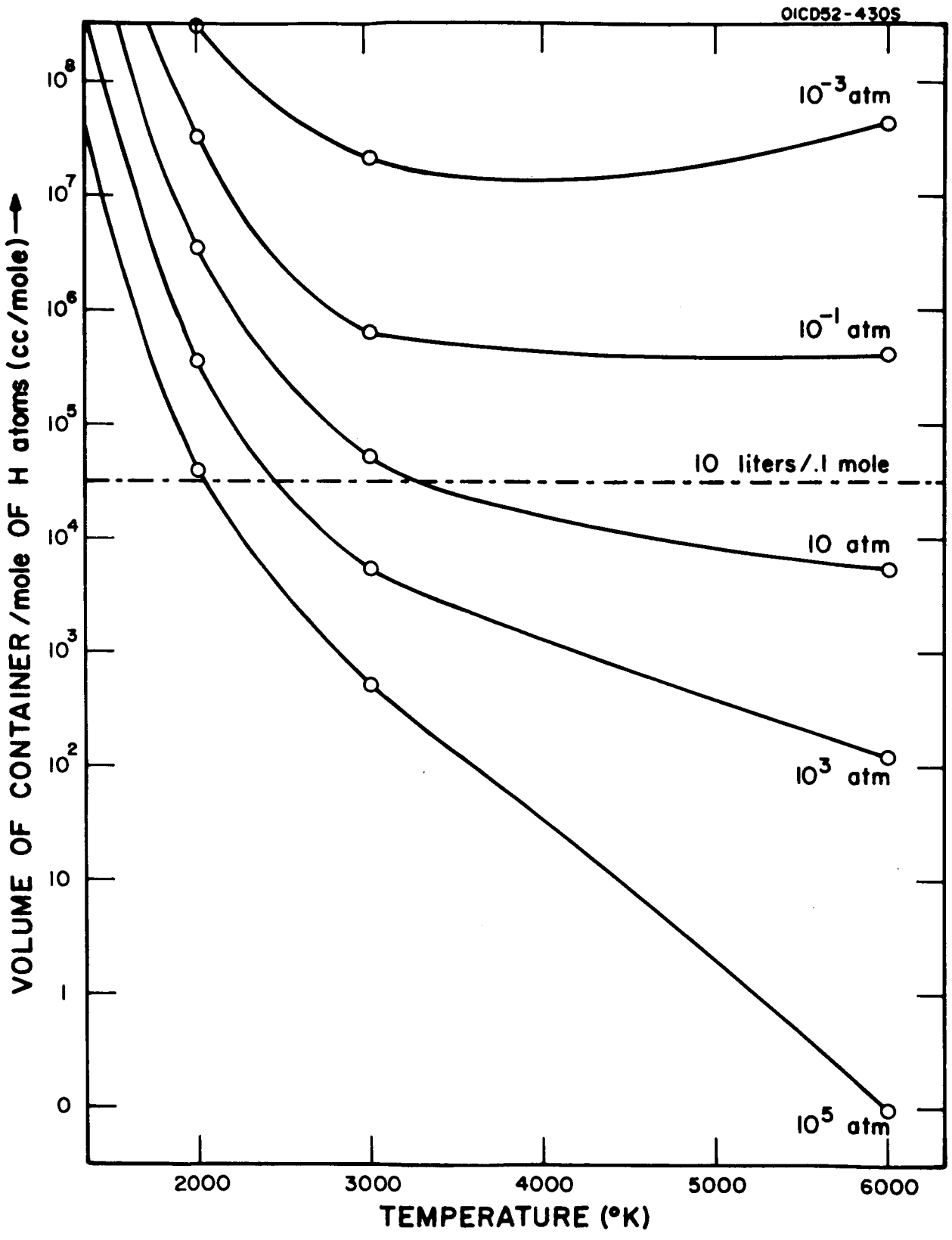

Figure 4. Container volume as a function of temperature and pressure.

These calculations also point out that the major energy dissipation mechanism in this system is the dissociation of molecular hydrogen. In line with this it appears from these calculations that an appreciable amount of energy can not be stored in these systems by preheating them before launch.

Considering the various factors involved in producing an equilibrium mixture containing 0.1 mole of atomic hydrogen (volume of system, weight of systems, weights of energy source, materials problems), it is felt that this is not the optimum method of producing the required atomic hydrogen.

However, it is evident from these graphs that, if the kinetics were favorable, the most efficient method of producing atomic hydrogen would be via some steady state process that can operate at a low pressure.

A plasma gun, to be described later, is such a device. If the gases from such a plasma device could be made to exit at 3000°K at a pressure of 0.1 atm, it would require only about 16 kW to produce the 0.1 mole. These values are well within the present state of the art.

Description of plasma gun. - This section outlines the hardware requirements which are needed to impart 40 kW of power for one second to 2 grams of hydrogen. The design philosophy is based upon the assembling of existing components each of which has been tested and proven. These components consist of a plasma generator silver zinc battery package, supply of pressurized molecular hydrogen and a high-frequency oscillator. The hydrogen, under a slight positive pressure, passes through the plasma generator arc, and is exposed to the enormous electric fields within the arc. The hydrogen emerges as a dissociated ionized gas at a high temperature. The arc can be started by means of a standard welding oscillator, that provides a high-frequency discharge across the anode-cathode gap, which creates momentarily a low resistance current path. The arc, once started by the oscillator, is sustained by a bank of silver zinc batteries which are packaged to produce the current at the required arc operating voltage.

The system requirements are as follows:

Emerging gas:	Atomic hydrogen
Quantity (min.):	0.2 grams
Operating time (min.):	1.0 second
Input power (min.):	40 kW
Flow rate (min.):	0.2 gram/sec

Experiments to test theory of 5577Å atomic oxygen emission. - The purpose of this group of experiments is to test in one fashion or another, by chemical release, significant theories of emission of the 5577Å atomic oxygen lines. The three suggested experiments are: (1) to actively change the concentration of atomic oxygen by dilution and measure the change in the 5577Å emission, (2) to simultaneously measure the atomic oxygen concentration and the 5577Å emission for correlation, and (3) to shield the 5577Å emitting region with an overlying gaseous patch absorbing Lyman-alpha checking the theory that nocturnal Lyman-alpha is inducing the green line.

Dilution of atomic oxygen region with helium. - The purpose of this experiment is to check the order of the reaction which emits the atomic oxygen green line. The concept here is to change in a prescribed volume, the concentration of atomic oxygen by diluting this volume with an inert gas. This change in concentration will alter the rate of emission. For example, suppose the mechanism is the Chapman mechanism

$$O + O + O \rightarrow O_2 + O^*$$

$$O^* \rightarrow O + h\nu$$

This implies that the emission is proportional to the third order of the atomic oxygen concentration. Consequently, a reduction of the concentration by one-half means a diminution of one-eighth, whereas, if the emission is first order, the diminution will be one-half. In Table 1 is calculated for a thousand moles of helium for varying degrees of dilution (100, 10 and 1 percent) at two different ambient concentrations of 10^{13} and $10^{12}/cm^3$ the diminution to be expected for the fact that the perturbed region may only be a portion of the total region. For instance, at $n_a = 10^{13}$ and $n_c = 10$ percent for a third-order reaction the intensity is 73 percent if the total emitting region is diluted.

In practice the time during which dilution would occur would be reasonably long. If we set h the gaussian half-width then

$$h^2 = r_o^2 + 4Dt$$

where r_o is the halfwidth at $t = 0$. For $D = 10^5$ cm^2 sec^{-1} t must be of the order of tens of minutes before the dilution falls by a factor of e. Consequently, there is a reasonable period for examining the time behavior of the diminution of intensity. If gaussian distribution for the diluent is assumed and the order of the reaction producing the 5577Å emission is n then I_d, the emission per cm^2 at a distance d from the center of the release is given by (to within a constant of proportionality)

$$I_d = 2 \int_d^\infty \left\{ f_{[0]}(r)\, n_a \left[1 - \frac{r_o^3}{h^3} \exp\left(- \frac{r^2}{h^2} \right) \right] \right\}^n \frac{r\, dr}{\sqrt{r^2 - d^2}}$$

where $h = [r_o^2 + 4Dt]^{1/2}$

$$r_o = \left(\frac{N}{\pi^{3/2} n_a} \right)^{1/3}$$

TABLE 1

DIMINUTION OF 5577Å EMISSION THROUGH DILUTION WITH 10^3 MOLES OF HELIUM ASSUMING THIRD ORDER AND FIRST ORDER REACTIONS

n_a	n_c		V	Size		3rd Order $\frac{I_p}{I_{oT}}$			1st Order $\frac{I_p}{I_{oP}}$		
(cm^{-3})	Percent n_a	cm^{-3}	cm^3	d_c (km)	θ (deg)	$\frac{I_{oP}}{I_{oT}} = 0.2$	$\frac{I_{oP}}{I_{oT}} = 0.5$	$\frac{I_{oP}}{I_{oT}} = 1.0$	$\frac{I_{oP}}{I_{oT}} = 0.2$	$\frac{I_{oP}}{I_{oT}} = 0.5$	$\frac{I_{oP}}{I_{oT}} = 1.0$
10^{13}	100	10^{13}	1.5×10^{15}	1.15	0.65	0.80	0.50	0.00	0.8	0.5	0.00
10^{13}	10	10^{12}	1.5×10^{16}	2.50	1.45	0.95	0.86	0.73	0.98	0.95	0.90
10^{13}	1	10^{11}	1.5×10^{17}	5.31	3.0	0.99	0.98	0.97	0.998	0.995	0.99
10^{12}	100	10^{12}	1.5×10^{16}	2.50	1.45	0.80	0.50	0.00	0.80	0.5	0.00
10^{12}	10	10^{11}	1.5×10^{17}	5.31	3.0	0.95	0.86	0.73	0.98	0.95	0.90
10^{12}	1	10^{10}	1.5×10^{18}	11.45	6.5	0.99	0.98	0.97	0.998	0.995	0.97

n_a = ambient concentration

n_c = concentration of diluent either in percentage of ambient or absolute concentration

V = volume occupied by diluent at concentration n_c

d_c = size of cube of volume V

θ = angle subtended by d_c at distance of 100 km

I_{oP} = emission from unperturbed region of depth d_c

I_{oT} = emission from total 5577Å emitting region

I_p = emission from perturbed region of depth d_c

N = total number of diluent molecules

n_a = ambient concentration

$f_{[O]}(r)$ = fractional concentration of atomic oxygen

D = coefficient of diffusion

With r_o determined from the mass of the release, and D and n_a from the height, the preceding formula integrated over the field of view provides a reasonable approximation to the expected intensity for the correct value of the exponent n. If the Chapman mechanism is correct a value of n = 3 should give the closest fit to the data.

Nitric oxide (or other compounds) measurements of atomic oxygen and simultaneous ground measurements of 5577Å. - The experiment suggested here provides for a direct correlation between the vertical distribution of atomic oxygen and the 5577Å atomic oxygen emission. The vertical distribution of atomic oxygen will be measured by a chemical release technique utilizing NO, TMA, or some alternate compound. The integrated emission of 5577Å will be measured by ground-based photometers. Measurements will be made on a series of days so as to ensure obtaining a reasonably wide range of intensity of 5577Å. Then comparisons will be made with parameters derived from the measured vertical distribution. Such parameters will be used as:

(a) The integrated vertical distribution

$$\int_{-\infty}^{\infty} [O]\, dz$$

(b) The integrated power distribution

$$\int_{-\infty}^{\infty} [O]^n\, da \quad n = 2,3,4 \cdots$$

Presumably, if the Chapman mechanism is correct n = 3 will give the best correlation.

(c) Truncated distributions - Here the concept is that at certain altitudes there are additional mechanisms (such as deactivation) which render the atomic oxygen in situ nonproductive. Our parameter then would be of the form

$$\int_{z_1}^{z_2} [O]^n\, dz$$

where as an example $z_1 = 90$, $z_2 = 110$ km

It is considered that a series of at least five flights yielding five points on the various correlation charts for each of the abstracted parameters would be required to give any meaningful pattern. Additionally, rocket flights which measure the flux of 5577Å as a function altitude would provide the opportunity for better correlation. In effect they perform a space correlation where the five flights proposed above in essence perform a time correlation.

A plasma generator which can satisfy the system requirements is commercially available. Its specifications are as follows:

Operating gases:	argon, nitrogen or hydrogen
Operating power:	40 kW (maximum operating power for sustained operation)
Operating voltage:	100V dc (H_2)
Weight:	less than 3 pounds
Mass flow rate (max.):	0.5 gram/sec (H_2)
Volume:	less than 0.1 ft^3
Cost:	$1750
Availability:	immediate
Cooling water required:	3 gallons per min**
Efficiency:	50 to 80 percent (with water cooling)
Operating time:	2 seconds (max)

**Cooling required to prevent cathode-anode erosion for sustained operation.

The plasma generator can operate at power levels exceeding 40 kW for only several seconds with subsequent erosion of the electrodes. Also, since water cooling decreases the plasma gun efficiency or actual energy imparted to the emerging gas, it is planned to operate the plasma gun without water cooling at 60 kW. Use of 60 kW would allow sufficient energy to be imparted to the atomic hydrogen in order to ensure dissociation.

A battery package which can produce 600 A dc at 100 volts dc for 2 seconds can be assembled from existing battery cells. The specifications of such a package are as follows:

Battery type:	silver zinc
Output voltage:	100V dc nominal
Output current:	600 amp dc nominal
Operating time:	2 seconds
Number of cells:	100
Package volume:	1.2 ft^3
Package weight:	170 pounds
Availability:	3 months
Package cost:	$8,700
Temperature range:	60 to 100°F

A large savings in battery size, weight and cost can be effected if the operating temperature of the battery package were maintained from 90°F to 120°F. Self-powered heaters immersed in the package and energized about one hour before the pulse is required can be used. The weight and volume reduction are 14 and 13 percent.

Shielding of 5577Å emitting region with overlying chemical patch to absorb Lyman-Alpha. - The purpose of this experiment is to test the hypothesis that the 5577Å nocturnal emission is induced by Lyman-alpha. The concept is to create by rocket release an overlying absorbing layer which would diminish the flux of Lyman-alpha into the active region producing the 5577Å emission. The compound used must have several distinct properties.

(a) It must have as large an absorbing cross section for Lyman-alpha as possible.

(b) It must not chemiluminesce or only minimally.

(c) It must not be consumed chemically or only minimally.

(d) It must have low molecular weight.

A search of the literature for gases having large cross sections at Lyman-alpha is given in Table 2. Unfortunately, the measurements are sporadic and have been centered on the hydrocarbons. The higher values are about 1000 to 2000 cm^{-1}. However, it is pointed out that these values are random and may represent nowhere near the maximum possible value of the absorption cross section. For example, N_2^+ has a value of 10,000 cm^{-1} for Lyman-alpha.

Of the compounds listed water vapor or propane is probably best on a weight basis. They do not have the maximum cross section; however, they are satisfactory on the three other counts. They have a reasonably low molecular weight. They do not chemiluminesce nor are they consumed rapidly by atomic oxygen. Consequently, the calculation below will be made on the basis of the use of propane.

However, it is noted that a necessary aspect of this proposed rocket experiment would be a preliminary program of laboratory measurements to optimize the selected compound and hence minimize the payload to be carried.

Assuming the use of 200 pounds of propane or roughly 2 to 3 x 10^3 moles with a k(cm^{-1}) of 10^3 or σ = 3 to 7 x 10^{-17}/molecule, a cloud one optical thickness deep (2 to 7 x 10^{16} particles/cm^2) will cover a circular area of 2 to 4 km diameter. At an altitude of 100 km this diluent cloud subtends an angle of 1° 22'. With presently available photometers such a spot size is experimentally susceptible. It should be noted that material with cross sections an order-of-magnitude greater per unit of weight seems within reach of laboratory determination. For such substances the diluent cloud would have a diameter of 5 to 32 km and would subtend an angle at 100 km of 3° 3' and would make the job of observation considerably easier.

TABLE 2

GASES WITH LARGE LYMAN-ALPHA CROSS SECTIONS

Compound	Absorption Coefficient (k), cm^{-1}	Molecular Weight
H_2O	387	18
Propylene ($CH_2CH\ CH_3$)	1000	42
Propane ($CH\ CH_2CH_3$)	1000	44
Toluene ($C_6H_5CH_3$)	1500	92
Benzene (C_6H_6)	1100	78
C_4H_2OH } Methyl, Ethyl n-propyl and n-butyl alcohols	1960	67
C_3H_7OH }	1560	60
Ethylene	700	28

The experiment then would consist of making measurements of the glow from a selected region of the sky which would be the target region. After suitable calibration of this region the rocket would release the Lyman-alpha absorbing compound above the observation area at an altitude sufficiently high so that there is no dilution or chemical interaction with the 5577Å emitting region - an altitude of 120 km seems reasonable. If Lyman-alpha is the causative factor then a substantial diminution of 5577Å should occur in the shielded region.

Improvement in atmospheric titration experiments. - The purpose of this phase of the program is to suggest possible concepts and compounds which will improve upon existing atmospheric titration experiments. These experiments include the simultaneous measurement of two reactive species, the measurement of previously unmeasured species, the use of more efficient compounds for measuring atomic oxygen and the extension of chemiluminescent techniques to lower portion of the atmosphere.

Simultaneous measurement of two minor constituents (e.g., O and O_3) through differential chemiluminescent spectra. - The aeronomy of the oxygen allotropes constitute one of the major problems of upper atmospheric physics. While a considerable advance has been made in recent years in the absolute measurement of the various oxygen allotropes and their ratios as yet many aspects of the oxygen problem remain in an unsatisfactory condition. The ozone concentration has been measured many times to altitudes of 30 km but only on one or two occasions has it been measured up to 60 km. The concentration of atomic oxygen has been measured with increasing accuracy from 90 km up. In particular the ratio of atomic oxygen to molecular oxygen has been measured mass-spectrometrically recently.

However, as yet here have been no simultaneous measurements of atomic oxygen and ozone above 30 km or at all. Such simultaneous measurement would be of value in determining the photochemistry of oxygen. At present the vertical distributions of atomic oxygen and ozone have not been cross correlated experimentally. Simultaneous measurements at one or more points can serve this function. In particular, a measurement at the crossover points at approximately 50 to 70 km would be of value. Such a measurement would not only have direct implications for the photochemistry of oxygen but contribute to our understanding of airglow phenomena and the mixing processes of the atmosphere.

The approach to the experimental design is to use a compound which chemiluminesces with both atomic oxygen and ozone and which yields a different spectrum for each reaction. Consequently, measurements with filters in different portions of the glow should yield knowledge of the relative concentrations of atomic oxygen and ozone. This technique has the remarkable advantage that it is independent of the hydrodynamic mixing since the ratio of atomic oxygen to ozone remains the same.

It is remarked that not only must there be a differential spectrum of chemiluminescence between atomic oxygen and ozone but the rates of reaction must be appropriate so that the released compound not be consumed by only

one species. A basic problem here is that studies of chemiluminescent ozone reactions in general have not been prosecuted in significant depth. There is lacking in general reaction rates, chemiluminescent rates, spectra and mechanisms. Consequently, it is proposed that appropriate compounds be determined in the experimental phase of this program. There is good reason to believe that suitable compounds can be found because of the literally hundreds of compounds which chemiluminesce with both atomic oxygen and ozone. In order to render the experimental design more precise, calculations were made for nitric oxide as an exemplar originally, because the overall chemiluminescence data for nitric oxide reactions with atomic oxygen and ozone are reasonably well established and a differential spectrum exists. It was one of the purposes of the experimental phase of select the optimal compound.

However, extensive studies made for many compounds (Section 4) have revealed that nitric oxide remains, to the best of our present knowledge, the optimal compound for this purpose.

In Table 3 is given the relative intensities for various wavelength region for the chemiluminescent reaction of NO with atomic oxygen and ozone. On the basis of this tabulation and also the spectrum of the NO + O reaction given in Figure 5, a preliminary selection of two wavelength regions, Region I - 4950 to 5700Å and Region II - 7200 to 7750Å, has been made. From these data a tabulation of percentage of total emission has been made in Table 4.

The chemiluminescent rate for NO + O is given as $k = 6.4 \times 10^{-17}$ cm^3 molecule^{-1} sec^{-1} in the equation

$$E = k\,[NO]\,[O]$$

For ozone according to Fontijn, et al., the rate of emission is given by

$$E_{O_3} = I_o \frac{[NO][O_3]}{[M]}$$

where [M] is the third body and $I_o = 120 \exp(-4180/RT)$. The ratio of emission due to the reaction with atomic oxygen to that with ozone is

$$\frac{E_O}{E_{O_3}} = \frac{k}{I_o} \frac{[O][M]}{[O_3]} \quad \text{for } T = 300^\circ K \text{ and } [O] = 10^{11}/cm^3,$$

$$[O_3] = 10^9/cm^3$$

$$[M] = 10^4/cm^3$$

at approximately 90 km

$$\frac{E_O}{E_{O_3}} = 5.6$$

TABLE 3

INTENSITY DISTRIBUTION OF NO_2 FLUORESCENCE AND CHEMILUMINESCENT SPECTRA IN THE RANGE 5000 TO 8000Å

Relative Intensities (quanta sec^{-1}) Observed in Various Wavelength Ranges, Å

	4950-5700	6150-6700	6700-7200	7200-7750
NO+ O emission (air afterglow)	0.37	1.00	0.83	0.62
NO_2 fluorescence (4358Å excitation)	0.36	1.00	0.82	0.46
NO_2 fluorescence (5461Å excitation)	--	1.00	1.01	0.53
NO+ O_3 emission	0.00	1.00	2.38	3.40

TABLE 4

PERCENTAGE (f) OF TOTAL SPECTRUM CONTAINED IN SPECIFIED WAVELENGTH REGIONS

Reaction	Region I (4950-5700Å)	Region II (7200-7750Å)
NO + O	10	20
NO + O_3	0	10

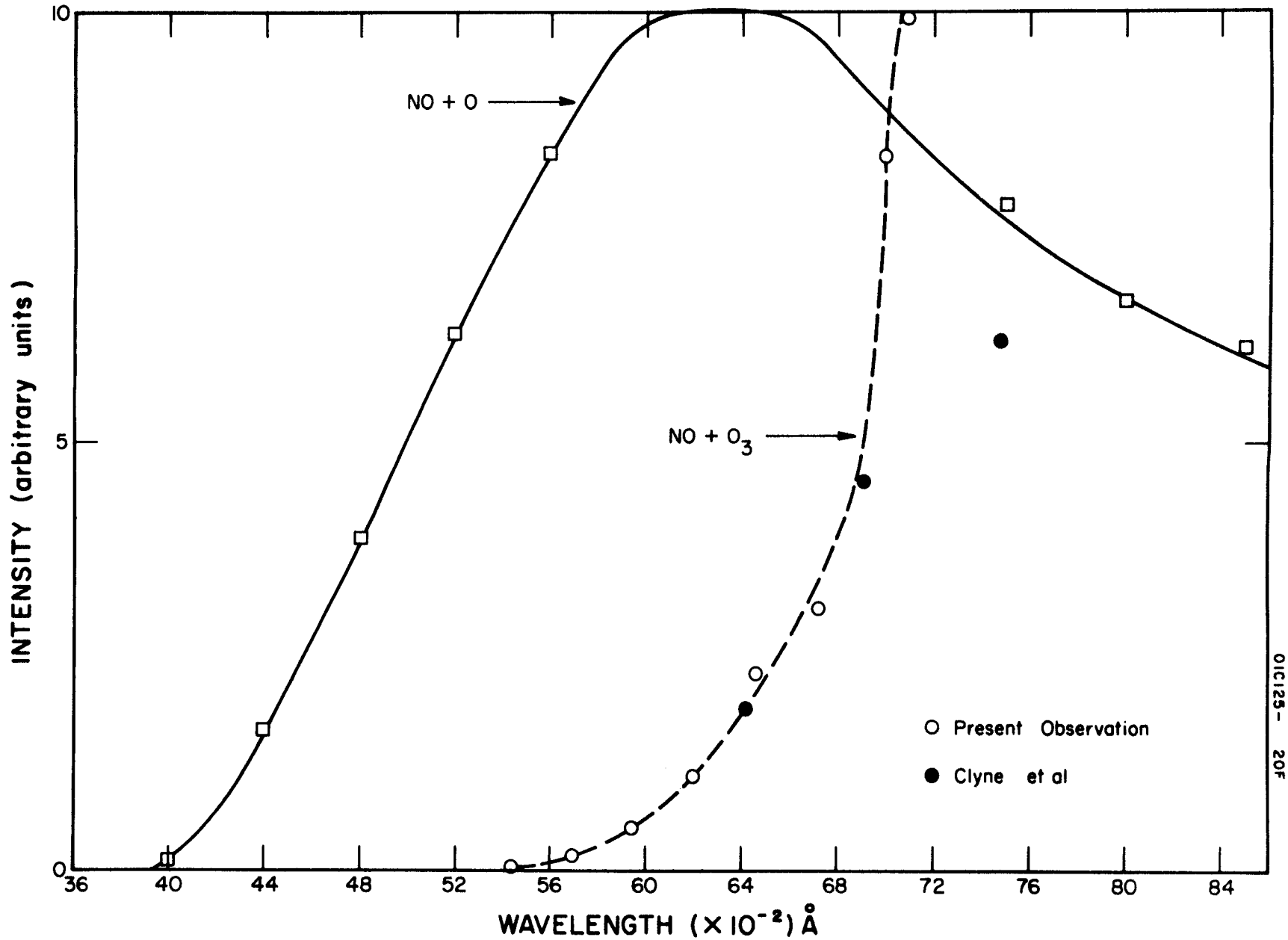

Figure 5. Visible spectrum of chemiluminescent reaction of nitric oxide with atomic oxygen and ozone.

Consequently, it can be seen that there is an altitude and a range of altitudes from which the total emission is apportioned reasonably to the interaction with both atmospheric species. There is calculated below the intensity in two wavelength regions I_I and I_{II} due to the atomic oxygen and ozone reactions. I_I is the intensity in the wavelength region 4950 to 5700Å and I_{II} in the region 7200 to 7750Å. The subscript O or O_3 indicates that the intensity is due to the species O or O_3. The symbol f suitably subscripted describes the percentage of chemiluminescence due to reaction with O or O_3 in Region I or II (see Table 4).

If I_0/M is set equal to k_3 then there may be written

$$I_I = k_1 f_{I_O} [NO][O]$$

$$I_{II} = k_1 f_{II_O} [NO][O] + k_3 f_{II_{O_3}} [NO][O_3]$$

Then

$$\frac{I_I}{I_{II}} = R = \frac{k_1 f_{I_O} [O]}{k_1 f_{II_O} [O] + f_{II_{O_3}} k_3 [O_3]}$$

and

$$\frac{[O_3]}{[O]} = \frac{k_1}{k_3} \frac{1}{f_{II_{O_3}}} \left[\frac{f_{I_O}}{R} - f_{II_O} \right]$$

It is noted that the ratio of $[O]/[O_3]$ is independent of the concentration of NO, consequently the degree of mixing or dynamics is irrelevant so long as the signal is strong enough to be measured. Further, only the relative strength of the bandpass signals, R, need be measured. Consequently, it is easier to measure the relative concentration than the absolute concentration. It is noted that the rate of consumption of the active species is so small that it is practically unperturbed.

By use of computation techniques already developed for the measurement of atomic oxygen with NO there may be computed the concentration of atomic oxygen and also NO using a prescribed diffusion model.

By using the equation for I_{II} the absolute concentration of O_3 may also be calculated. The ratio of the absolute values so obtained for $[O]$ and $[O_3]$ may then be checked against the relative values obtained directly. Consequently an internal check for consistency may be obtained.

Simultaneous measurement of ozone through chemiluminescent release and through spectrophotometric measurements in the Hertzberg region as cross checks. - The purpose of this experiment is to provide a check and cross correlation between spectrophotometric measurements in the Hertzberg region as already performed in a rocket experiment and chemiluminescent measurements of ozone. The rocket experiment of NASA Goddard has measured the vertical distribution of ozone in a broad region. The use of TMA as an ozone titrant is presently being checked out by GCA. Its luminosity is high. However, its rate of chemical consumption must be measured.

The program then envisions a rocket flight in which spectrophotometric measurements of ozone will be made on the upward leg and a chemiluminescent trail of TMA will be laid on the downward leg.

Use of NO_2 to titrate ozone. - The basic concept here is that for atmospheric altitudes in which there is an appropriate mixture of atomic oxygen and ozone it may be possible to measure the ozone more effectively through the use of nitrogen dioxide (NO_2) because of the rapidity with which atomic oxygen is consumed.

The primary interaction of NO_2 with the ambient ozone is through the following reactions:

$$NO_2 + O \rightarrow NO + O_2 + 46 \text{ kcal} \qquad (1)$$

with a rate coefficient of

$$k = 1.5 \times 10^{-12} \, T^{1/2} \exp(-500/T) \text{ cm}^3 \text{ sec}^{-1}$$

also

$$NO_2 + O_3 \rightarrow NO_3 + O_2 + 26 \text{ kcal} \qquad (2)$$

$$k = 5 \times 10^{-13} \, T^{1/2} \exp(-3600/T)$$

and considering atomic oxygen

$$O + NO_2 + M \rightarrow NO_3 + M + 50 \text{ kcal} \qquad (3)$$

$$k = 5 \times 10^{-31} \text{ cm}^6 \text{ sec}^{-1}$$

It may be concluded from Table 5 that the consumption of NO_2 by reaction 2 is negligible in comparison with 1 and 3 and hence can be neglected. Further, the effect of 3 is also negligible.

Using the table of composition given below (Table 6) there is calculated the relative efficiency of the chemiluminescence of nitric oxide (NO) with atomic oxygen (P_O^*) and ozone ($P_{O_3}^*$) respectively.

TABLE 5

RELATIVE RATE COEFFICIENTS OF THE ABOVE PROCESSES AT DIFFERENT ALTITUDES IS APPROXIMATELY GIVEN BY:

Z	k_1	k_2	k_3
20	2.2×10^{-12}	1.2×10^{-24}	9.2×10^{-13}
40	3.9×10^{-12}	1.9×10^{-24}	4.2×10^{-14}
60	3.9×10^{-12}	1.9×10^{-24}	3.6×10^{-15}
80	1.2×10^{-12}	6.0×10^{-25}	2.2×10^{-16}
100	2.1×10^{-12}	1.0×10^{-24}	3.9×10^{-18}
120	1.3×10^{-11}	6.5×10^{-24}	1.6×10^{-19}
140	3.4×10^{-11}	1.6×10^{-23}	3.2×10^{-20}

TABLE 6

Z	n(M)	n(O)	$n(O_3)$
20	1.85×10^{18}	9.8×10^{9}	8.1×10^{12}
40	8.32×10^{16}	4.2×10^{10}	6.6×10^{14}
60	7.26×10^{15}	1.6×10^{11}	4.7×10^{10}
80	4.42×10^{14}	1.4×10^{12}	1.4×10^{9}
100	7.80×10^{12}	2.1×10^{12}	2.3×10^{6}
120	3.10×10^{11}	5.0×10^{10}	---
140	6.40×10^{10}	8.1×10^{9}	---

Our conclusions then are that for the normal atmosphere:

(1) Probability of excitation by O_3 is less than chemical consumption

(2) Above 40 km the excitation by O is predominant over consumption

(3) Above 60 km the excitation by O is predominant over that due to O_3.

At 80 km Table 7 indicates that the glow in the normal atmosphere due to NO chemiluminescence with atomic oxygen is some four orders greater than that due to ozone. A release of nitrogen dioxide (NO_2) at 80 km is capable of mopping up the atomic oxygen substantially in a fraction of a second. We calculate

$$R_c = k_1 [NO_2][O]$$

R_c = rate of consumption of atomic oxygen, where if we assume the release NO_2 is at ambient concentration then the rate of consumption of atomic oxygen is

$$R_c = 12 \times 10^{-12} \times 4.4 \times 10^{12} \times 1.4 \times 10^{12} \simeq 5 \times 10^{14}$$

or the atomic oxygen is used up in 10^{-2} seconds. Of course, this is an exponential decay and

$$[O] = [O]_o \exp(- 10^{-2} t)$$

These numbers indicate that the consumption of atomic oxygen is a comparatively rapid process and consequently that even where atomic oxygen is in far greater abundance than ozone the latter can be probed chemiluminescently. This is true because in the process of consuming NO_2, atomic oxygen is depleted rapidly, and NO is created for chemiluminescence with the undiminished ozone.

Use of improved agents such as trimethyl antimony and tri-ethyl boron to titrate atomic oxygen. - Tri-ethyl boron has been selected as the initial substance. The motivation for this has already been given. Experimental details are given in the next section (Section 3).

Use of di-ethyl zinc to titrate atomic nitrogen. - Initial laboratory experiments have been performed indicating that di-ethyl zinc glows substantially more intensely with atomic nitrogen than with atomic oxygen. This is presently being checked out at lowered pressures (see Section 3).

Use of trimethyl aluminum to titrate ozone in the lower atmosphere. - Present measurements have indicated that TMA gives substantially larger chemiluminescence with ozone than nitric oxide (NO) or other compounds. Its use in titrating ozone in the lower atmosphere is indicated pending the determination of its rate of consumption by molecular oxygen.

TABLE 7

Z	P_{O_3}	$P^*_{O_3}$	P_O	P^*_O
20	2.6×10^{-3}	3.8×10^{-4}	5.3×10^{-7}	6.3×10^{-7}
40	5.3×10^{-3}	1.7×10^{-1}	2.3×10^{-7}	2.7×10^{-6}
60	2.9×10^{-4}	9.8×10^{-6}	6.7×10^{-8}	1.0×10^{-5}
80	6.4×10^{-7}	2.4×10^{-9}	5.3×10^{-8}	9.0×10^{-5}
100	3.8×10^{-9}	7.3×10^{-11}	3.2×10^{-10}	1.3×10^{-4}
120	---	---	3.3×10^{-12}	3.2×10^{-5}
140	---	---	4.8×10^{-13}	5.2×10^{-7}

P_{O_3} = Probability of chemical consumption of NO without chemiluminescence by ozone

$P^*_{O_3}$ = Probability of production of excited NO_2 which can produce chemiluminescence

P_O = Probability of chemical consumption of NO by atomic oxygen without producing chemiluminescence

P^*_O = Probability of production of excited NO_2 by atomic oxygen which can produce chemiluminescence

The calculated rates are obtained from:

$$P_{O_3} = k_{O_3}\, n(O_3);\quad P^*_{O_3} = k^*_{O_3}\, n(O_3);\quad P_O = k_O\, n(O)\, n(M);\quad P^*_O = k^*_O\, n(O)$$

Measurement of temperature in upper atmosphere. - The use of improved compounds over TMA such as tri-ethyl boron with higher oscillator strength and calibration in laboratory is suggested.

The spectra of the chemiluminescence produced during the reaction of TEB with atomic oxygen causes BO_2 bands; the presence of some BO bands is also suspected. There is a strong possibility of the presence of BO molecules as an intermediate during the reaction of atomic oxygen and tri-ethyl boron. Therefore, the observation of BO bands in the spectra of fluorescence excited by solar radiation during twilight release of tri-ethyl boron can reveal the temperature of the emitting regions. It may, however, be noted that the v_e for BO molecules is (1.7803 cm^{-1}), three times as large as that of AlO molecules (0.64118 cm^{-1}), which indicates that BO bands may be more suitable for the measurement of temperature. Hence, the spectra of the luminescence produced during the twilight release of tri-ethyl boron should be studied.

3. ANALYSIS IN DEPTH OF ROCKET EXPERIMENT RELEASING OXYGEN

A. Introduction

This section analyzes in depth a rocket chemical release experiment to investigate the mechanism of the 6300Å air-glow emission of atomic oxygen. It is suggested that a payload of approximately one hundred pounds of oxygen be released during the night between 250 and 300 kilometers and that the ensuing glow be observed by suitable rocket and ground photometers. The present most favorably held theory is that the 6300Å glow is due to charge transfer between O^+ and O_2 followed by recombination of O_2^+ and an electron followed by dissociation and excitation of atomic oxygen and the emission of the 6300Å emission.

The key fact that makes this experiment feasible is that in the altitude concerned molecular oxygen has become a minor constituent (at 300 km the concentration of O_2 is 0.1 percent of the total concentration) and consequently its concentration can be increased by several orders of magnitude. This proposed rocket increase of molecular oxygen should accelerate the excitation mechanism causing an increased emission observable by ground or rocket photometers.

The mechanism of the 6300Å emission has been a fundamental problem of atmospheric physics for the last 36 years, since the first recording of this radiation by Slipher [1].* Even at present the causative mechanism is not understood despite the fact that there have been literally hundreds of papers, observational and theoretical, devoted to this problem.

The proposed simple rocket experiment offers a unique opportunity to test almost unequivocally the presumed mechanism and should add substantially to our knowledge of upper atmospheric physics. It is an experiment simply conceived which can afford an almost direct yes or no answer and is well within the GCA capability.

B. Short History of the 6300Å Emission Line Research

As pointed out above the history of research into the 6300Å night airglow line dates back to 1929 and as yet there is no clear understanding of the basic mechanism. It has been determined experimentally through rocket photometer measurements that the altitude of emission of 6300Å is relatively high in the upper atmosphere, > 160 km [2,3,4]. Also, correlation studies of the 5577Å emission indicate no relationship with this emission. Further the intensity of the 6300Å emission correlates well with the plasma frequency of the F-region [5-9].

---

*Numbers in [ ] throughout the text represent reference numbers.

The general consensus considers that the emission comes primarily from the F-region maximum between 250 to 300 km and that it is due to the dissociative recombination of molecular oxygen following charge transfer. The mechanism postulated is

$$O^+ + O_2 \rightarrow O_2^+ + O \qquad (4)$$

$$O_2^+ + e \rightarrow O^* + O^* \quad \text{(possibly 2 } O^*\text{)} \qquad (5)$$

$$O^* \rightarrow O + h\nu \ (6300\text{Å})$$

An alternative reaction is as noted:

$$NO^+ \ (X^1\Sigma^+) + e \rightarrow N \ (^4S) + O \ (^1O)$$

C. Theoretical Discussion of Possible Mechanisms

The mechanism for the night emission of 6300Å from the upper atmosphere is not well understood because the rates and cross sections of the various mechanisms postulated are poorly measured quantities. Additionally the rocket experiments to date have not been successful in characterizing the altitude distribution of this emission. It must be stated that even in those cases where the altitude distribution is well characterized such as the 5577Å green line or the 5890Å sodium line the mechanisms still remain unresolved.

There seems little doubt, however, that the emission is tied into ionic mechanisms and that the active region is relatively high up in the atmosphere (above the 5577Å region at 100 km) and at least above 160 km. In particular, the recent rocket measurement by Gulledge and Packer [9] indicates a maximum at about 240 to 260 km.

The question as to whether the pertinent mechanism is

$$O^+ + O_2 \rightarrow O_2^+ + O \qquad (4)$$

$$O_2^+ + e \rightarrow O^* + O^* \ (^1D) \quad \text{or} \qquad (7)$$

$$O^+ + N_2 \rightarrow NO^+ + O \qquad (8)$$

$$NO^+ + e \rightarrow N + O^+ \ (^1D) \qquad (9)$$

remains a puzzling one. The complications arise from the fact that the charge-transfer reactions (4) and (8) lie within to the best of present knowledge an order of magnitude or so. Also the concentrations as given below indicate larger concentrations for molecular nitrogen than molecular oxygen. While it is not possible to be certain it would seem that charge transfer to molecular nitrogen would be faster than to molecular oxygen. In general, mass spectrometric measurements of ions indicate that the NO^+ concentration is greater than that of O_2^+ up to at least 250 km. The indication although not conclusive is that at 300 km the concentrations of the two ions would be approximately the same.

At the next step, that of dissociative recombination combined with excitation, again the coefficients are not established within an order of magnitude. However, here we see that in Equation (9) for NO^+ the excited $O(^1D)$ is spin forbidden as pointed out by Dalgarno. This fact in itself would suggest that it is the O_2^+ which is the important molecular ion. Consequently, it is the release of O_2 which should rate higher priority over that of nitrogen.

In the next subsection will be presented some approximate estimates of the perturbation of 6300Å by the release of molecular oxygen. This is followed by a more quantitative section in which the differential equations of the system are treated.

D. Approximate Calculations

There is calculated below in this subsection two types of approximations. One calculation solves the differential equations directly (with no diffusion) using initial values constant over all space but with an oxygen concentration which is equivalent to the total particle concentration. This is graphed in Figure 6.

The second type of calculation represented in Table 8 is a direct numerical approach calculating rates for the pertinent reactions. In this calculation allowance is made for the diffusion of molecular oxygen but not for other species.

In paragraph E still more realistic models are examined.

A representative model of the ionosphere and upper atmosphere is given in Table 8.

Ionic composition of the ionosphere has been obtained from the percentage composition obtained from rocket observations and after assuming

$$n(e) = n(O_2^+) + N(NO^+) + n(O^+)$$

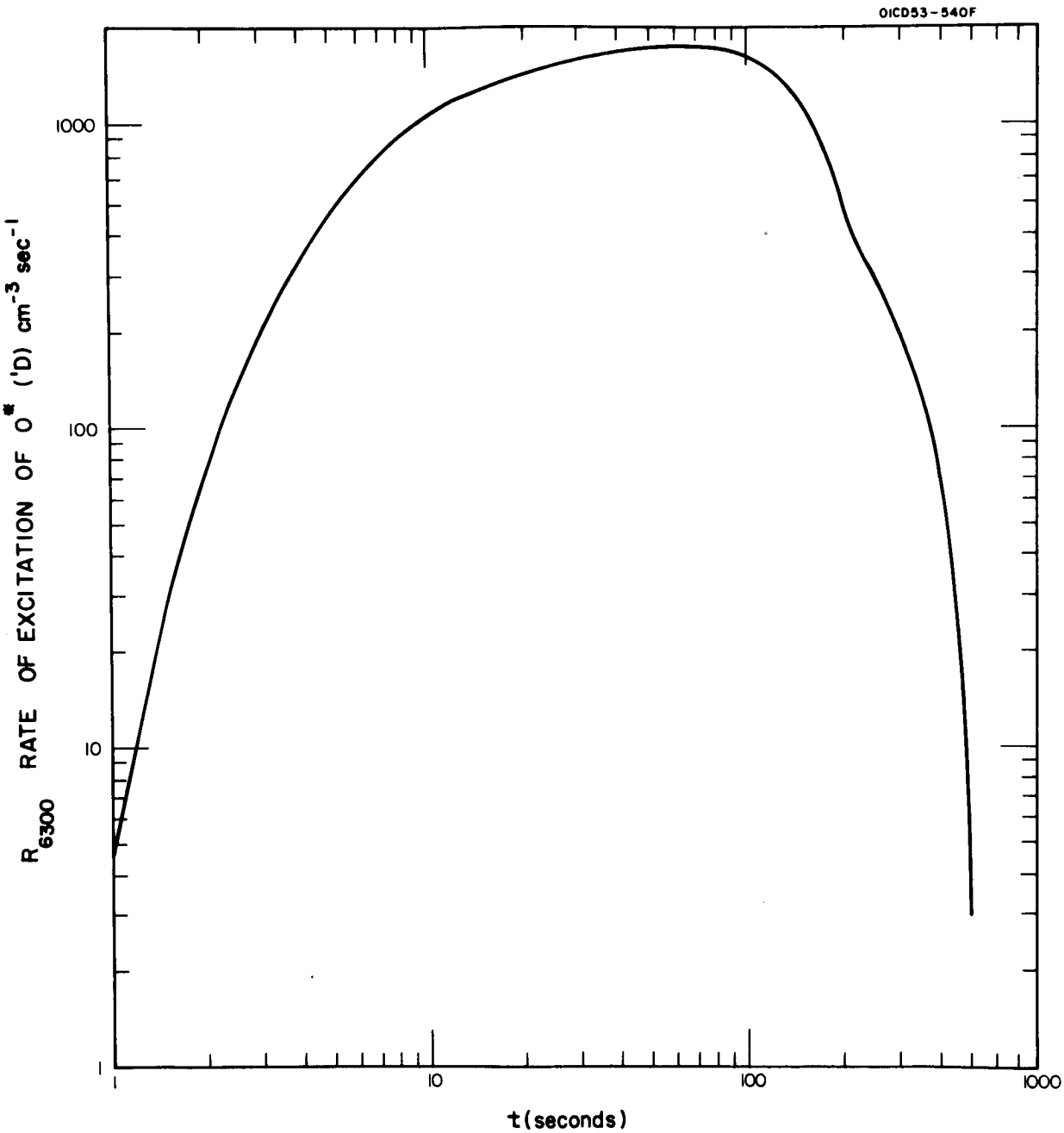

Figure 6. Rate of excitation, $O^*(^1D) = \alpha\ [e]\ [O_2^+]$ as a function of time.

TABLE 8

Altitude km	$n(N_2)$	$n(O_2)$	n(N)	n(O)	n(M)
100	1×10^{13}	1×10^{12}	2.1×10^{10}	3.4×10^{12}	1.4×10^{13}
150	5×10^{10}	8×10^{8}	1×10^{9}	1.6×10^{10}	6.6×10^{10}
200	1.6×10^{9}	2.5×10^{7}	2.4×10^{8}	1×10^{9}	2.8×10^{9}
250	4×10^{8}	2.5×10^{6}	7.5×10^{7}	2.8×10^{8}	3.9×10^{8}
300	4×10^{7}	4.1×10^{5}	3×10^{7}	1×10^{8}	1.7×10^{8}

Altitude km	n(e)	$n(O_2^+)$	$n(NO^+)$	$n(O^+)$
100	6×10^{3}	2×10^{2}	5.8×10^{3}	
150	8×10^{3}	3×10^{3}	4×10^{3}	1×10^{3}
200	5.5×10^{4}	2×10^{3}	3×10^{3}	5×10^{4}
250	3×10^{5}	2×10^{3}	1.2×10^{4}	2.9×10^{5}
300	4×10^{5}			4×10^{5}

The reactions controlling the ion equilibrium at night are:

		Best Estimates
4	$O^+ + O_2 \rightarrow O + O_2^+$	$k = 5 \times 10^{-11}$ cm^3/sec
5	$O^+ + N_2 \rightarrow NO^+ + N$	$k = 1 \times 10^{-12}$ cm^3/sec
6	$O_2^+ + N_2 \rightarrow NO^+ + NO$	$k = 3 \times 10^{-17}$ or 5×10^{-14} cm^3/sec
7	$O_2^+ + N \rightarrow NO^+ + O$	$k = 5 \times 10^{-12}$ cm^3/sec
8	$\rightarrow O^+ + NO$	$= 5 \times 10^{-12}$ cm^3/sec
9	$O_2^+ + e \rightarrow O + O^+$	$k = 1 \times 10^{-7}$ cm^3/sec, α
10	$NO^+ + e + N + O^+$	$k = 1 \times 10^{-8}$ cm^3/sec, α

The variation of the rate of dissociative recombination of O_2^+ in the ionosphere is given by $v = n(O_2^+)\ n(e) \times 10^{-7}$

100 km	$2 \times 10^2 \times 6 \times 10^3 \times 10^{-7}$	$= 12 \times 10^{-2}$	$= 0.12/\text{cm}^3$ sec
150 km	$8 \times 10^3 \times 3 \times 10^3 \times 10^{-7}$	$= 24 \times 10^{-1}$	$= 2.4/\text{cm}^3$ sec
200 km	$5.5 \times 10^5 \times 2 \times 10^{-7}$	$= 11.0$	$= 11.0/\text{cm}^3$ sec
250 km	$3 \times 10^5 \times 2 \times 10^3 \times 10^{-7}$	$= 60$	$= 60/\text{cm}^3$ sec
300 km	$4 \times 10^5 \times 2 \times 10^3 \times 10^{-7}$	$= 80$	cm/2 sec

The above calculation shows that the assumed concentration of O^+ ions and electrons is reasonable to give the observed altitude variation of the λ6300 line.

Perturbation of the 6300Å through the increased concentration of O_2 uniformly through space.— Introduction of O_2 mainly accelerates the conversion of O^+ ions into O_2^+ ion and consequently the recombination. If we assume that the concentration of O_2 molecules after introduction is equal to the total particle concentration then for the charge transfer reaction

$$O^+ + O_2 \rightarrow O_2^+ + O$$

the following table is constructed:

Rate/cm^3/sec

Altitude	Unperturbed $n(O^+)$ $n(O_2)$ k	$n(O^+)$	$n(O_2^+)$	After Introducing O_2 $n(O_2) = n(M); n(O^+)n(M)$ k
200	6.25×10^1	5×10^4	2×10^3	7×10^3
250	3.62×10^1	2.9×10^5	2.1×10^3	5.6×10^3
300	8.20	4×10^5		3.4×10^3

After one sec of introduction of O_2 above 200 km, there will occur changes in O_2^+ concentration. These changes considering the above table may continue for about 10 sec at 200 km and about 100 sec at 250 and 300 km. The conversion of O^+ to O_2^+ is followed by the dissociative recombination of O_2^+ with electrons.

The time variation of λ6300 line is now analyzed.

Above 200 km we can assume

$$n(O^+) = n(e)$$

The ionization decays as

$$O^+ + O_2 \xrightarrow{k} O_2^+ + O$$

$$O_2^+ + e \xrightarrow{\alpha} O + O \quad ,$$

and setting

$$n(O^+) = n(e) = x \qquad n(O_2^+) = y \qquad n(O_2) = a$$

we have

$$\frac{dn(O^+)}{dt} = -k\, n(O^+)\, n(O_2)$$

$$\frac{dn(O_2^+)}{dt} = \frac{dn(e)}{dt} = -\alpha\, n(O_2^+)\, n(e) + kn(O^+)\, n(O_2)$$

$$\frac{dx}{dt} = -k \cdot x \cdot a;\ \frac{dy}{dt} = -\alpha \cdot y \cdot x + k \cdot a \cdot x = x[ka - \alpha y]$$

Since atmospheric ionic processes only create minor changes the concentration of O_2 will not change substantially; therefore, the concentration of O_2 molecule is treated as constant.

Assuming at $\tau = 0$ $x = x_o$ $y = y_o$

$$\int_{x_o}^{x} \frac{dx}{x} = -\int_{o}^{\tau} ka\, dt$$

and

$$x = (x_o\, e^{-ka\tau})$$

Substituting in second equation, we have

$$\frac{dy}{dt} = ka\, x_o\, e^{-ka\tau} - \alpha\, y\, x$$

$$= ka\, e^{-ka\tau} - y\alpha \cdot e^{-ka\tau}$$

$$= x_o\, e^{-ka\tau}\, [k \cdot a - y \cdot \alpha]$$

$$\int_o^y \frac{dy}{ka - y\alpha} = x_o \int_o^\tau e^{-ka\tau}\, dt$$

$$\left[-\frac{1}{\alpha}\log(ka - y\alpha)\right]_o^y = -x_o \times \frac{1}{ka}\left[e^{-ka\tau}\right]_o^\tau$$

$$y = \frac{k \cdot a}{\alpha}\left\{1 - (1 - \frac{yo\alpha}{ka})\, e^{\frac{x_o\alpha}{ka}} \exp[(-ka\tau) - 1]\right\}$$

The time rate of variation of the λ6300 line is given by

$$q = R6300 = \alpha\, y\, x = ka\, x_o\, e^{-ka\tau}\left[1 - \left(1 - \frac{y_o\alpha}{ka}\right) e^{\frac{x_o\alpha}{ka}} \left\{\exp(-ka\tau) - 1\right\}\right]$$

A plot of this equation is given in Figure 6. Similar calculation for the N_2 system may be made.

Calculations allowing for the diffusion of released molecular oxygen.— There is calculated in the table below the effect of the release of 10^3 moles of oxygen at 300 km. The symbols are self-evident except for $r_g = \sqrt{h^2 + 4Dt}$ which represents the Gaussian halfwidth which varies with time due to diffusion and q which is the flux of 6300Å photons. q is calculated on the basis of a probability of de-excitation of 10^{-2}.

It is noted from the table that the time scale of buildup is of the order of hundreds of seconds. Further the generation of O_2^+ increases by a thousandfold and the generation of $O(^1D)$ by several hundredfold.

The steady state concentration of $O^*(^1D)$ is obtained by setting

$$\frac{dO^*}{dt} = q - k_D\, O^*$$

equal to zero. Here

$$O^*(^1D) = \frac{q}{k_D}$$

300 km

$n(M) = 2 \times 10^{8}$, $k = 5 \times 10^{-11}$, $\alpha = 10^{-7}$ cm^3/sec

Unperturbed		0 sec	1 sec	2 sec	4 sec	10 sec	100 sec	200 sec
$n(O_2)$	4×10^{5}	2×10^{8}	1.5×10^{8}	1.2×10^{8}	1×10^{8}	6×10^{7}	3×10^{6}	1×10^{6}
$n(e)$	4×10^{5}	4×10^{5}	4×10^{5}	4×10^{5}	4×10^{5}	4×10^{5}	3×10^{5}	1×10^{5}
$n(O_2^+)$	2×10^{2}	2×10^{2}	4.2×10^{3}	7.1×10^{3}	1.13×10^{4}	2.1×10^{4}	7×10^{4}	1.2×10^{5}
$n(O^+)$	4×10^{5}	4×10^{5}	4×10^{5}	4×10^{5}	3.9×10^{5}	3.7×10^{5}	3.6×10^{5}	3.1×10^{5}
$k(O^+)$ (O_2)	8	4×10^{3}	3×10^{3}	2.4×10^{3}	2.0×10^{3}	1.32×10^{3}	5.4×10^{2}	3.4×10^{2}
$q = \alpha(O_2^+)$ (e)	8	8	1.68×10^{2}	2.8×10^{2}	4.4×10^{2}	8.4×10^{2}	2.1×10^{3}	1.2×10^{3}
r_g (km)		8.1	8.6	9.2	10.10	12.5	31.38	44

If we take the value of q at about 100 seconds

$$q = 2.1 \times 10^{3} \quad \text{and} \quad k_D = 10^{-2},$$

then at steady state

$$O^*(^1D) = 2.1 \times 10^{5} \quad \text{and} \quad R_{6300} = 2.1 \times 10^{3}$$

or the rate of decay equals the rate of excitation. The buildup time is 1/k or approximately 100 seconds. Since the generation q operates at the level of approximately $10^3/cm^3/sec$ for several hundred seconds this level of decay should be attained. This is roughly 100 times the normal flux per cm^3.

Of course, here interpenetration has been assumed, the calculations are for the centerpoint, no depletion of electrons are assumed and consequently this number is on the high side. Rather than further analyze this model we will proceed to the next stage which assumes a more accurate mathematical model.

E. More Accurate Calculations from Full Differential Equations

In the earlier portions of this section rather crude estimates have been made of the perturbation to be obtained through the release of molecular oxygen (nitrogen). It is our purpose in this section of the Final Report to present a more accurate evaluation of the perturbation. To this end the full-scale differential equations are solved in a reasonable order of approximation as described below. It should be stated that as part of the projected program an even higher order of approximation will be utilized. A direct numerical evaluation may be performed rather than the iterative scheme described herein.

The analysis performed was of a progressive nature attempting to evaluate the various segments of the problem since a full-scale analytical solution was intractable. Consequently, as described below some of the results obtained were for the purpose of seeing how fast the inverted Gaussian concentration fills in, others to obtain a measure of the effectiveness of the background $O^*(^1D)$, while others attempt to measure the strength of the generative term producing $O^*(^1D)$.

It is cautioned that the results calculated are specifically for 300 km and a release of 1000 moles of molecular oxygen. This calculation, while not parameterized over altitude or for molecular nitrogen, presents the basic information as to the feasibility of the proposed rocket experiment.

Summary of problems analyzed.— The principal scope of this section is a mathematical study of two proposed physical models to account for the production

of excited oxygen 6300Å (red line) airglow due to the nighttime rocket chemical release of molecular oxygen between 250 to 300 kilometers. The specific mathematical details are relegated to Appendix A. Only the setting up of the problem and some of the results are given here so as not to break the continuity of the argument.

The injected molecular oxygen particles are assumed to have an initial Gaussian distribution with the initial concentration configuration $[O_2(P,+0)]$ defined by the exponential rule:

$$[O_2(P,+0)] = [O_2(0)]\left[1 - \exp\left(-\frac{r^2}{h^2}\right)\right]$$

where $[O_2(0)]$ signifies the concentration of the molecular oxygen particles at the origin, $r = 0$, at the instant $t = +0$, and where h is a suitable Gaussian halfwidth.

The monitor point $P:(x,y,z)$ is defined by the spherical radial distance coordinate r, $r = \sqrt{x^2 + y^2 + z^2}$.

The ambient atmospheric region, between 250 and 300 kilometers, in which the molecular oxygen is released (after being dispersed from a point-source canister sent aloft by a high-altitude rocket) contains species of particles in a steady-state configuration.

In the process of attaining the initial Gaussian configuration

$$[O_2(P,+0)] = [O_2(0)][1 - \exp(-r^2/h^2)],$$

the molecular oxygen particles (contained inside the point-source canister prior to their release) are considered to have either one of two dispersion routes: (1) the molecular oxygen particles have a "snowplow" action (of sorts) on the steady state ambient particles, or (2) the molecular oxygen particles simply interpenetrate the ambient particles without disturbing their steady-state configuration at the time $t = +0$.

That is to say, in the "snowplow" model it is assumed that the concentration fields $[e(P,t)]$, $[O_2^+(P,t)]$, $[O^+(P,t)]$, and $[O^*(P,t)]$, of the electrons, molecular oxygen ions, atomic oxygen ions, and excited oxygen atoms, respectively, at the time $t > 0$ after release at time $t = +0$, have initial inverted Gaussian configurations:

$$[e(P,+0)] = [e(\infty)]\,[1 - \exp(-r^2/h^2)],\quad [e(\infty)] \equiv [e(P,t)]_{r\to\infty},$$

$$[O_2^+(P,+0)] = [O_2^+(\infty)]\,[1 - \exp(-r^2/h^2)],\quad [O_2^+(\infty)] \equiv [O_2^+(P,t)]_{r\to\infty},$$

$$[O^+(P,+0)] = [O^+(\infty)]\,[1 - \exp(-r^2/h^2)],\ [O^+(\infty)] \equiv [O^+(P,t)]_{r\to\infty},$$

and

$$[O^*(P,+0)] = \epsilon \cdot [O^*(\infty)]\,[1 - \exp(-r^2/h^2)],\ [O^*(\infty)] \equiv [O^*(P,t)]_{r\to\infty},$$

where ϵ is an off-on factor, $\epsilon = 0, 1$, depending on whether or not it is assumed that excited oxygen atoms are present in the nighttime atmosphere at the time $t < 0$.

The concentrations $[e(\infty)]$, $[O^+(\infty)]$, and $[O^*(\infty)]$ designate the steady state values of the $[e([,t)]$, $[O_2^+(P,t)]$, $[O^+(P,t)]$, and $[O^*(P,t)]$ concentration fields; that is to say, the concentrations of e, O_2^+, O^+, and O^* prior to the release at $t = +0$ and for very long times, t, after release at $t = 0$.

In the "snowplow" model it is assumed that there is a negligible amount of molecular oxygen, O_2, in the ambient region prior to the release at $t = +0$. The same assumption applies to the excited oxygen atoms O^* if the on-off factor ϵ is defined as zero, $\epsilon = 0$, in the specification of $[O^*(P,+0)]$. For a basis of comparison both cases, $\epsilon = 0$ and $\epsilon = 1$, are studied in this report.

In the "interpenetrability" model, it is assumed that initially the [e], $[O_2^+]$, $[O^+]$, and $[O^*]$ concentration fields are constant throughout all space with the assigned values $[e(\infty)]$, $[O_2^+(\infty)]$, $[O^+(\infty)]$, and $[O^*(\infty)]$, respectively, at the instant $t = +0$. Further, it is assumed that the initial Gaussian release configuration of O_2 particles is superimposed on the steady state value $[O_2(\infty)]$ at the instant $t = +0$.

The distinction between the two physical models, the "snowplow" and the "interpenetrability" models, described above are based on initial configuration assumptions.

Further assumptions are incorporated in the investigation of these models, relative to the equations of continuity, as will be pointed out subsequently.

The production of 6300Å airglow in the nighttime can be accounted for, from a physico-chemical reaction standpoint, by a consideration of the following set of reaction equations:

$$O_2 + O^+ \xrightarrow{k_1} O_2^+ + O\,, \tag{10}$$

$$O_2^+ + e \xrightarrow{k_2} O^* + O\,, \tag{11}$$

$$O^* \xrightarrow{k_3} h\nu + O\,. \tag{12}$$

In reaction (10) there is an ion-atom exchange, the injected molecular oxygen particle attaining a positive charge through the oxygen ion-atom exchange.

In reaction (11) the electron is lost through dissociative recombination with the production of excited atomic oxygen O^*.

In reaction (12) the excited oxygen atom O^* loses energy through the production of photons which appear as the 6300Å airglow, red line excitation.*

These physico-chemical processes, occurring at the point $P:(x,y,z)$ in space and at the instant $t > 0$, evidently give rise to sources and sinks of the individual species of particles, at $P:(x,y,z)$ and t, and account for non-homogeneous additions to the equations of continuity associated with the several transient concentration fields established by the injected molecular oxygen particles.

In the "snowplow" model the system of equations of continuity, which define the space-time variations of the concentration fields at the point $P:(x,y,z)$ in (P): $-\infty < x < \infty$, $-\infty < y < \infty$, $-\infty < z < \infty$, at the time $t > 0$, is assumed to be defined by the following array:

$$\frac{\partial}{\partial t}[O_2] = D\nabla^2[O_2] - k_1[O_2][O^+] ,$$

$$\frac{\partial}{\partial t}[O^+] = D\frac{\partial^2}{\partial z^2}[O^+] - k_1[O_2][O^+] ,$$

$$\frac{\partial}{\partial t}[O_2^+] = D\frac{\partial^2}{\partial z^2}[O_2^+] + k_1[O_2][O^+] - k_2[O_2^+][e] ,$$

$$\frac{\partial}{\partial t}[e] = D\frac{\partial^2}{\partial z^2}[e] - k_2[O_2^+][e] ,$$

$$\frac{\partial}{\partial t}[O^*] = D\nabla^2[O^*] + k_2[O_2^+][e] - k_3[O^*] ,$$

---

*Reference is made to Physics of the Aurora and Airglow by J. W. Chamberlain, Academic Press, New York City, 1961, pp.521-532.

where

$$\nabla^2( ) \equiv \frac{1}{\xi}\frac{\partial}{\partial\xi}\left[\xi\frac{\partial}{\partial\xi}( )\right] + \frac{\partial^2}{\partial z^2}( ) \ .$$

In the "interpenetrability" model the system, required to define the excited oxygen field $[O^*(P,t)]$, is reduced to the pair

$$\frac{\partial}{\partial t}[O^*] = \qquad\qquad + k_2[O_2^+][e] - k_3[O^*] \ ,$$

$$\frac{\partial}{\partial t}[O_2^+] = D\frac{\partial^2}{\partial z^2}[O_2^+] + k_1[O_2][O^+] - k_2[O_2^+][e]$$

wherein

$$[O_2] \equiv O_2(0)\left(\frac{h}{T_1}\right)^3 \exp\left(-\frac{r^2}{T_1^2}\right) + [O_2(\infty)] \ ,$$

$$[e] \equiv [e(\infty)], \ [O^+] \equiv [O^+(\infty)], \ T_1^2 = h^2 + 4Dt \ .$$

In order to construct a formal solution of the "snowplow" boundary value problem in the concentration field functions $[O_2]$, $[O^+]$, $[O_2^+]$, $[e]$, and $[O^*]$, an iterative scheme is introduced in which the concentration functions are approximated by the functions $[O_2^{(i)}]$, $[O^{+(i)}]$, $[O_2^{+(i)}]$, $[e(i)]$ and $O^{*(i)}]$ at the i-th approximation, with $i = 0$ corresponding to the initial configurations.

Vital to this scheme is the feasibility of solving the partial differential equation of the form

$$\frac{\partial U}{\partial t} = D\frac{\partial^2}{\partial z^2}U + u$$

with

$$U = U(P,t), \quad u = u(P,t), \quad U]_{t=0} = U(P,+0) = F_1(P)$$

and the equation

$$\frac{\partial V}{\partial t} = D \nabla^2 V + v$$

with

$$V = V(P,t), \quad v = v(P,t), \quad V]_{t=0} = V(P,+0) = F_3(P)$$

This need is met by the use of Green's functions, ($G_1(z,z';t,\tau)$ and $G_3(P,P';t,\tau)$), and the integral formulas:

$$U = \int_{-\infty}^{\infty} F_1(z')G_1(z,z';t,o)dz' + \int_{o}^{t} d\tau \int_{-\infty}^{\infty} u(z',\tau)G_1(z,z';t,\tau)dz'$$

$$V = \iiint_{-\infty}^{+\infty} F_3(P')G_3(P,P';t,o)dV(P') + \int_{o}^{t} d\tau \iiint_{-\infty}^{+\infty} v(P',\tau)G_3(P,P';t,\tau)dV(P') .$$

In this report the Green's function technique is used to obtain first approximation representations of the several concentration fields associated with the "snowplow" model and a formal solution is presented by the second approximation representations. This study is carried out for both $\epsilon = 0$ and $\epsilon = 1$.

The simplicity of the "interpenetrability" model system of equations makes it possible to obtain exact formulas for the O_2^+ and O^* concentration field functions (without recourse to iterative procedures).

The concentration field of the excited oxygen atoms, O^*, is analyzed for its time variation at the center point, $r = 0$, and for its integrated particle count, $S_{[O^*]}(t,h)$, along a line-of-sight coincident with the axis of symmetry, the z axis, from $\xi = 0$, $z = 0$ to $\xi = 0$, $z = h$ where $\xi = \sqrt{x^2 + y2}$, $r^2 = \xi^2 + z^2$. Numerical values for $[O^*(o,t)]$ and $S_{[O^*]}(t,h)$ are obtained for both models when the parameters involved are assigned typical values corresponding to the 250 to 300 kilometer region in the Earth's atmosphere.

Results of perturbation analysis.— In this section there are presented some of the results of the mathematical analysis with the mathematical details relegated as noted before to the Appendix A.

Snowplow analysis.— In Table 9 and Figure 7 are given the results of a center-point calculation and in Table 10 and Figure 8 the integrated density over a Gaussian halfwidth for a quasi-snowplow-type analysis performed under the first order of the iterative scheme. Here all the constituents are swept out. There is also assumed a zero background value of O^* (or e = u). Further, the first-order iterate of O^* works on the zero order of O_2^+. Consequently, the generating effect of the released O_2 is not felt. Therefore, the change in O^* calculated is due to the generation of O^* by the background concentrations of O^+, O_2, O_2^+ and the diffusion of all species.

It is further noted that uncharged species diffuse isotropically in all three dimensions while the charged species move only along the magnetic field lines. In summary this calculation gives us information on the effect of snowplowing by an inert substance which does not increase O_2^+. The second interaction outlined in Appendix A in effect turns on the generative term by allowing for the increase in O_2^+ through charge transfer of O^+ with O_2. But this effect— the basic one — has not been calculated in this approximation.

The calculation reported above is significant in that it gives us a time constant for the regeneration of O^* when flushed out of a region at 300 km and allowing for its regeneration through the postulated charge transfer and recombination processes of the natural ambient. This time constant is of the order of 100 seconds.

Interpenetrability model calculation.— The next calculation presented in Figure 9 is for a different type of model described by the phrase interpenetrability model and allows for increased generation of O_2^+ through the released oxygen. The basic assumption here is that while the oxygen distribution is described by a Gaussian curve, still the pertinent minor constituents such as the electrons and ions are mixed through so that their initial distribution is constant through all space. Further, the integrated line density for one Gaussian halfwidth has been calculated since fundamentally the photometers measure the integrated radiation. In this calculation because of mathematical intractability the diffusion of $O^*(^1D)$ has been omitted. This is not a serious omission because the integrated line density in effect cancels out the diffusion. Basically, the photometer does not care where the excited atomic oxygen is located along its line-of-sight. Since the diffusion is three-dimensional the integration along the line-of-sight only makes up in part for the diffusion of O^* and the calculated values are an upper limit. However, the increase in O^* due to the increased molecular oxygen concentration beyond Gaussian halfwidth has not been allowed for since attention has been riveted in the region close into the center. This will increase the integrated line density and compensate to some extent for the losses due to diffusion.

Although even at this phase the approximation is still a gross one as pointed out above, nevertheless, it includes the major aspects of the perturbation. An important question is that relevant to the initial conditions expressed by the interpenetrability assumption vis-a-vis the snowplow-type of model. It is difficult *a priori* to establish the degree of mixing in the

TABLE 9

CENTER-POINT CONCENTRATION COMPUTED BY USE OF FIRST APPROXIMATION FORMULAS

t (sec)	$n(e)$ $\left(\frac{\text{particle}}{\text{cm}^3}\right)$	$n(O^+)$ $\left(\frac{\text{particle}}{\text{cm}^3}\right)$	$n(O_2^+)$ $\left(\frac{\text{particle}}{\text{cm}^3}\right)$	$n(O_2)$ $\left(\frac{\text{particle}}{\text{cm}^3}\right)$	$n(O^*)$ $\left(\frac{\text{particle}}{\text{cm}^3}\right)$
0.1	2.80×10^3	2.80×10^3	0	1.96×10^8	0
0.2	5.52×10^3	5.49×10^3	3.0×10^1	1.92×10^8	0
0.4	1.09×10^4	1.08×10^4	3.0×10^1	1.84×10^8	0
0.8	2.05×10^4	2.04×10^4	5.0×10^1	1.71×10^8	1.4×10^{-1}
1	2.55×10^4	2.53×10^4	1.4×10^2	1.64×10^8	5.2×10^{-2}
2	4.63×10^4	4.59×10^4	3.8×10^2	1.38×10^8	8.98×10^{-1}
4	7.98×10^4	7.86×10^4	1.2×10^3	1.03×10^3	4.22×10^0
8	1.25×10^5	1.22×10^5	3.0×10^3	6.05×10^7	1.67×10^1
10	1.42×10^5	1.37×10^5	5.0×10^3	5.38×10^7	2.47×10^1
20	1.95×10^5	1.85×10^5	1.0×10^4	2.70×10^7	7.14×10^1
40	2.44×10^5	2.26×10^5	1.8×10^4	1.18×10^7	1.64×10^2
80	2.85×10^5	2.53×10^5	3.2×10^4	4.66×10^6	3.04×10^2
100	2.96×10^5	2.58×10^5	3.8×10^4	3.41×10^6	3.52×10^2
200	3.25×10^5	2.62×10^5	6.3×10^4	1.25×10^6	4.71×10^2
300	3.37×10^5	2.56×10^5	8.1×10^4	6.81×10^5	5.04×10^2
400	3.45×10^5	2.48×10^5	9.7×10^4	4.36×10^5	5.10×10^2
500	3.50×10^5	2.39×10^5	1.11×10^5	3.06×10^5	5.16×10^2

TABLE 9 (continued)

t (sec)	n(e) $\left(\frac{\text{particle}}{\text{cm}^3}\right)$	$n(O^+)$ $\left(\frac{\text{particle}}{\text{cm}^3}\right)$	$n(O_2^+)$ $\left(\frac{\text{particle}}{\text{cm}^3}\right)$	$n(O_2)$ $\left(\frac{\text{particle}}{\text{cm}^3}\right)$	$n(O^*)$ $\left(\frac{\text{particle}}{\text{cm}^3}\right)$
600	3.53×10^5	2.30×10^5	1.23×10^5	2.27×10^5	5.17×10^2
700	3.55×10^5	2.21×10^5	1.34×10^5	1.74×10^5	5.17×10^2
800	3.57×10^5	2.12×10^5	1.45×10^5	1.48×10^5	5.17×10^2
900	3.59×10^5	2.04×10^5	1.45×10^5	1.11×10^5	5.17×10^2
1000	3.60×10^5	1.95×10^5	1.65×10^5	9.10×10^4	5.17×10^2
1200	3.61×10^5	1.79×10^5	1.82×10^5	6.24×10^4	5.17×10^2
1400	3.62×10^5	1.65×10^5	1.97×10^5	4.38×10^4	5.17×10^2
1600	3.63×10^5	1.50×10^5	2.13×10^5	3.07×10^4	5.17×10^2
1800	3.62×10^5	1.37×10^5	2.25×10^5	2.12×10^4	5.17×10^2
2000	3.62×10^5	1.24×10^5	2.38×10^5	1.41×10^4	5.17×10^2

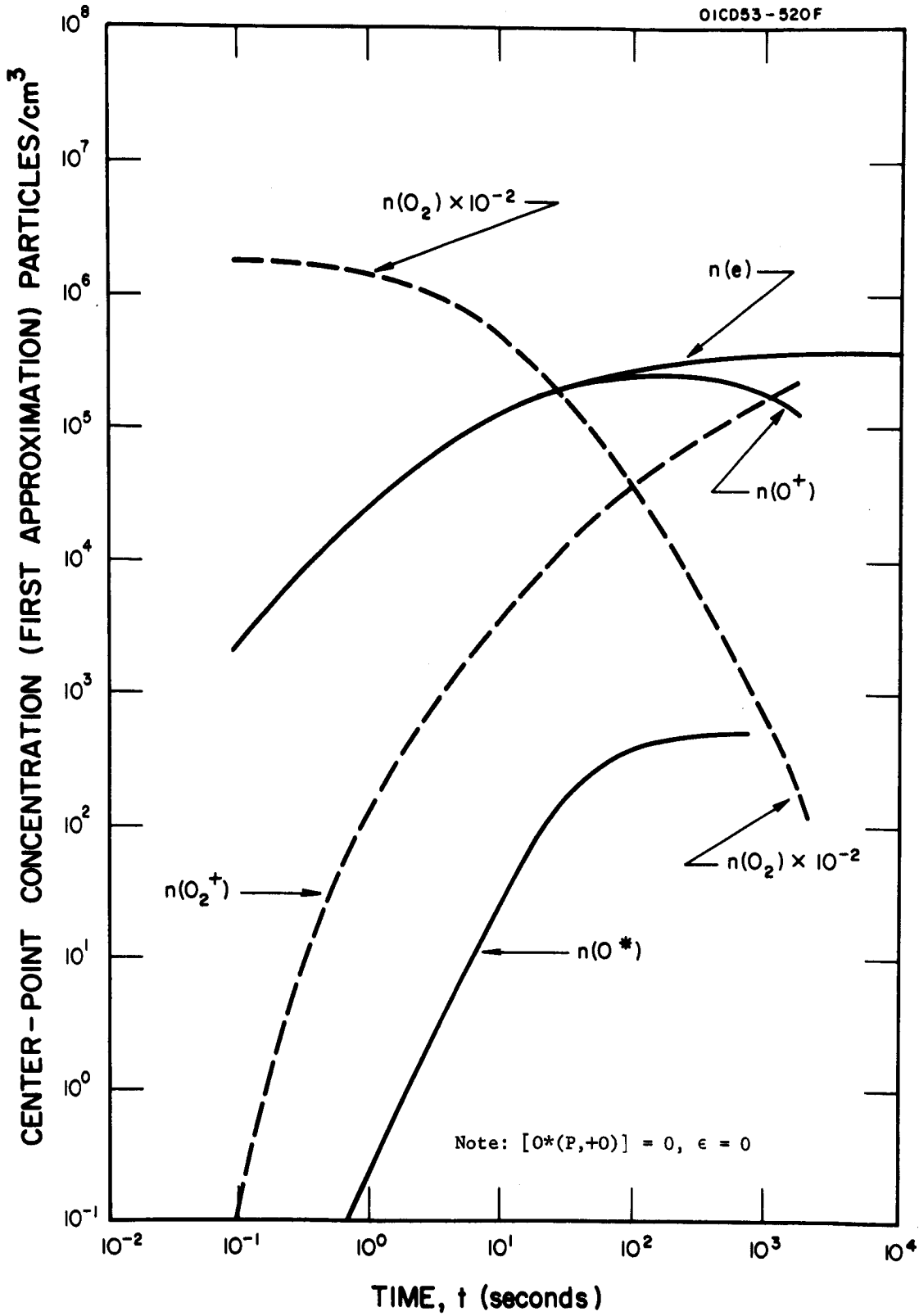

Figure 7. Center-point values of concentration fields of several species for Snowplow model.

TABLE 10

CONTRIBUTIONS TO VALUE OF INTEGRATED LINE DENSITY FUNCTION

$S^{(1)}_{[O^*]}(t,h)$ WHEN $[O^*(P,+O)] = \epsilon\, O^*(\infty)\left[1 - \exp\left(-\frac{r^2}{h^2}\right)\right]$

t (sec)	Initial Distribution Contribution $S^{(1)}_{[O^*]}(t,h)$ Particles/cm^2	Generation Term Contribution $S^{(1)}_{[O^*]}(t,h)$ Particles/cm^2	Sum of Both Contributions $S^{(1)}_{[O^*]}(t,h)$ Particles/cm^2
.0000	1.262×10^8	.0000	1.262×10^8
.01	1.269×10^8	6.770×10^3	1.269×10^8
.05	1.293×10^8	3.385×10^4	1.294×10^8
.10	1.324×10^8	6.770×10^4	1.325×10^8
.2806	1.432×10^8	1.900×10^5	1.434×10^8
.5	1.555×10^8	3.385×10^5	1.558×10^8
.973	1.792×10^8	8.800×10^5	1.801×10^8
1.973	2.196×10^8	2.29×10^6	2.219×10^8
2.742	2.437×10^8	3.70×10^6	2.474×10^8
3.565	2.644×10^8	5.53×10^6	2.700×10^8
5.281	2.956×10^8	8.123×10^6	3.038×10^8
7.972	3.249×10^8	1.883×10^7	3.437×10^8
11.819	3.398×10^8	3.282×10^7	3.727×10^8
14	3.423×10^8	3.099×10^7	3.733×10^8
15	3.424×10^8	3.644×10^7	3.788×10^8

TABLE 10 (continued)

t (sec)	Initial Distribution Contribution $S^{(1)}_{[O^*]}(t,h)$ Particles/cm^2	Generation Term Contribution $S^{(1)}_{[O^*]}(t,h)$ Particles/cm^2	Sum of Both Contributions $S^{(1)}_{[O^*]}(t,h)$ Particles/cm^2
16	3.426×10^8	4.045×10^7	3.831×10^8
18	3.400×10^8	4.851×10^7	3.885×10^8
22	3.325×10^8	6.467×10^7	3.972×10^8
27.203	3.190×10^8	8.536×10^7	4.043×10^8
57.972	2.263×10^8	1.904×10^8	4.167×10^8
73.357	1.891×10^8	2.309×10^8	4.180×10^8
111.819	1.148×10^8	3.041×10^8	4.189×10^8
227.203	2.586×10^7	3.932×10^8	4.190×10^8
300	1.005×10^7	4.168×10^8	4.268×10^8
400	2.743×10^6	4.242×10^8	4.269×10^8
500	7.487×10^5	4.262×10^8	4.269×10^8

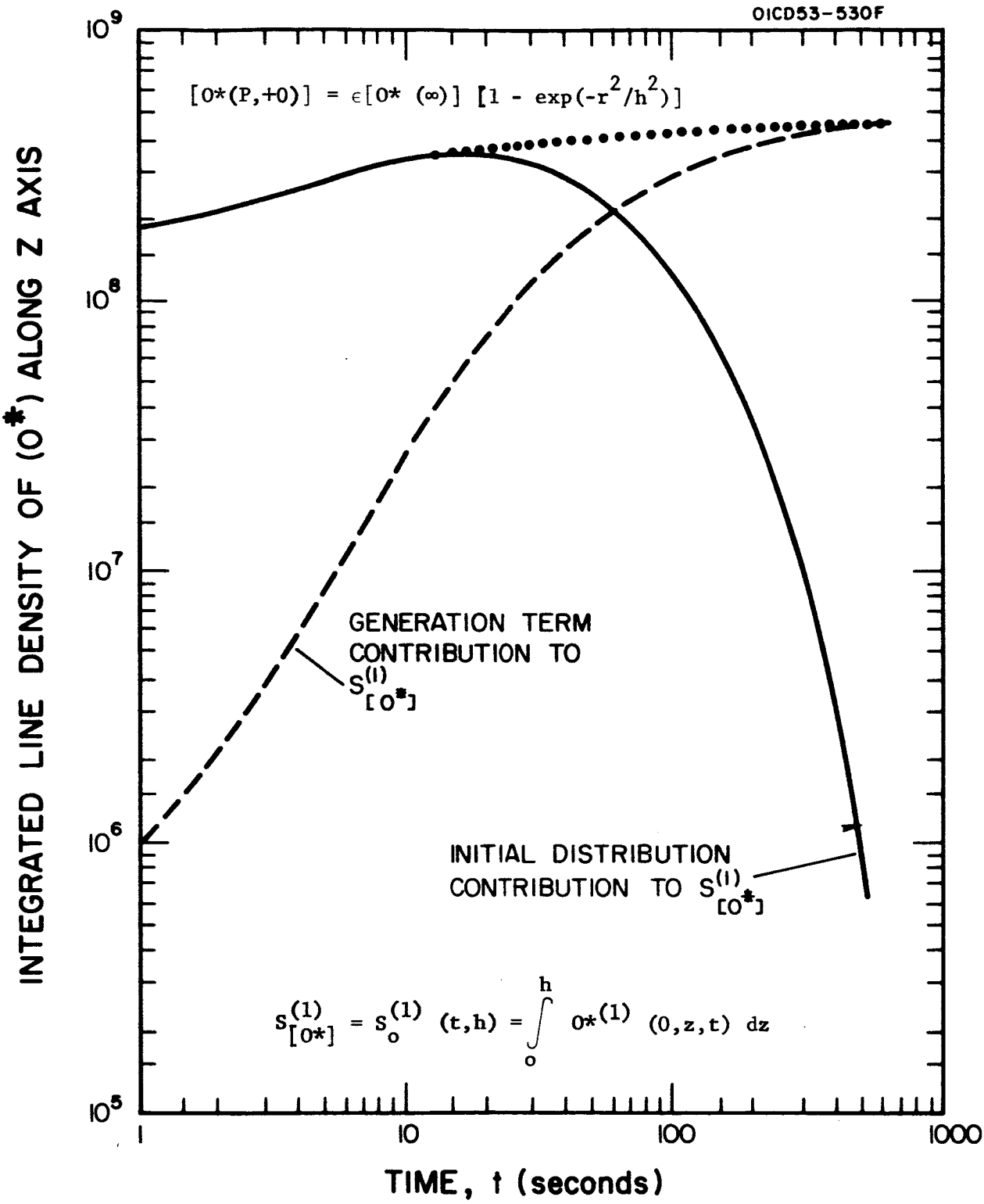

Figure 8. Integrated line density $S^{(1)}_{[O^*]}$ of O* for Snowplow model, $\epsilon = 0$, and $\epsilon = 1$.

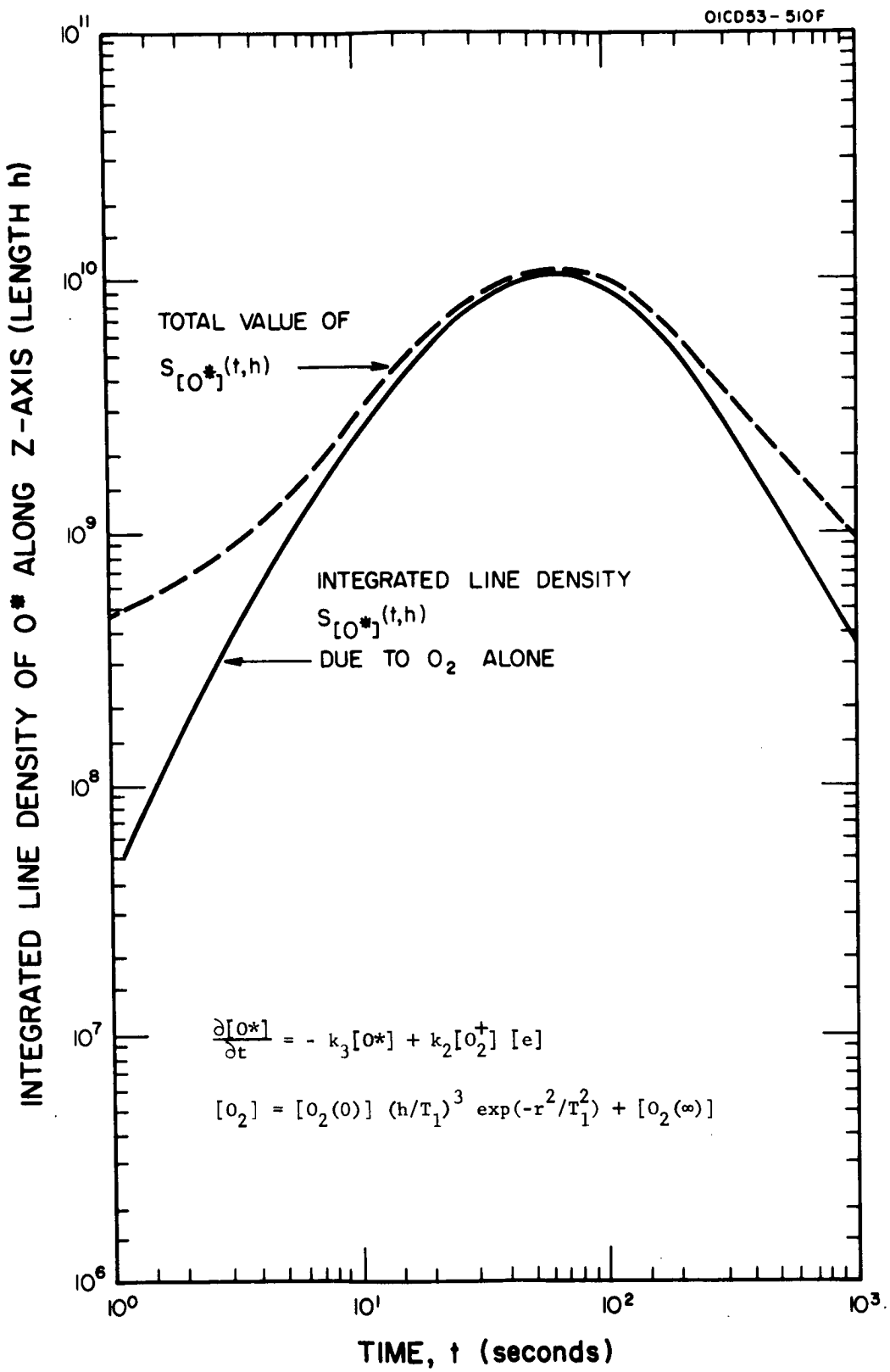

Figure 9. Integrated line density $S_{[O^*]}(t,h)$ of O* for Inter-penetrability model.

initial release. Certainly because of hydrodynamic Taylor-type instabilities, jetting and entrainment will occur ensuring some degree of mixing. Further, because of the relatively large mean free path in the ambient of the order of a kilometer once the released oxygen (nitrogen) spreads out to the order of several kilometers, the mean free path in the contaminant begins to approach that in the ambient and some degree of interpenetrability occurs. Consequently, the interpenetrability model constitutes a reasonable picutre of what may actually transpire.

Summary of calculations.— The initial calculations in this section which allowed for no diffusion (Figure 6) gave proportional increases in flux (R_{6300}) per cm^3 over background by approximately a factor of 100. The numerical calculation in Table 9 gave increases similarly of a factor of 1000, again for the center point but allowing for diffusion of molecular oxygen.

The more realistic calculations integrating over a Gaussian halfwidth and allowing for diffusion of all species but $O(^1D)$ give a factor of increase over background by a factor of twenty. It was pointed out that this calculation does not allow for the diffusion of $O(^1D)$. However, this omission is balanced to some extent by the integration over the Gaussian halfwidth and also the increased generation of $O(^1D)$ outside the Gaussian halfwidth.

Consequently, while the above has not been an exact solution of the problem the indications are good for the possibility of increasing severalfold the intensity of the emission of 6300Å over a region of some 40 km.

4. LABORATORY STUDIES

A. Introduction

It is noted that a significant portion of the laboratory studies is incorporated in four technical reports (see Section 1, Paragraph C). These, together with this section, describes the GCA laboratory studies in a complimentary fashion. The chemical release studies of the upper atmosphere have been pursued for obtaining information regarding wind, diffusion, temperature, ionic processes and chemical composition of the upper atmosphere. In order to obtain information about wind, diffusion and chemical composition of the upper atmosphere a chemical is released in the upper atmosphere, which during its reaction with atmospheric constituents produces a chemiluminous glow. A selection of a suitable compound for the chemical release study has been handicapped due to the lack of a general survey of the gas phase chemiluminescent reactions of several compounds with atmospheric constituents. We have therefore undertaken and completed a general survey of the chemiluminous gas phase reactions of different types of compounds (saturated, unsaturated and halogenated hydrocarbons; sulfur, boron and germanium compounds and some organometallic compounds) with chemically reactive atmospheric constituents, namely atomic nitrogen, atomic oxygen and ozone. The chemiluminous reactions of the above atmospheric constituents have been separately studied [10-16], by previous workers. For example the gas phase chemiluminescent reactions of atomic oxygen have been investigated in this laboratory and have been reported by Pressman [10] and Jonathan, et al. [11,12]. The chemiluminous reactions of atomic nitrogen have been surveyed by Kiess, et al. [13], and Jennings, et al. [14]. The information regarding the kinetics of atomic oxygen and nitrogen reactions has been collected by Barnes, et al. [15]. Bernanose [16] has summarized the chemiluminous reactions of ozone with several compounds. On the basis of information available in the literature, one can not estimate the relative intensity of the chemiluminescent reactions of different compounds with one atmospheric constituent or the intensity of the chemiluminous reactions of the same compound with different atmospheric constituents. Some indication of the relative intensity of chemiluminescence observed in different reactions can be obtained from the present observations.

Table 11 presents the salient features of the present study of the gas phase chemiluminous reactions of several compounds with atomic oxygen, atomic nitrogen and ozone at a pressure of about 1 mm and room temperature. It is generally found that organometallic compounds produce strong chemiluminescence during their reactions with upper atmospheric constituents. However, the compounds showing strong chemiluminescence with each of the studied constituent of the upper atmosphere are listed in Table 12.

The intercomparison of the chemiluminous efficiencies of some compounds during their reactions with atomic oxygen at low pressure under simulating upper atmospheric conditions have also been undertaken.

TABLE 11

CHEMILUMINESCENT REACTIONS OF SEVERAL SUBSTANCES
WITH ATMOSPHERIC CONSTITUENTS
(Spectral Features)

Titrant	Atmospheric Constituent		
	Atomic Oxygen	Atomic Nitrogen	Ozone
Nitric oxide	Continuum (4100Å - 6500Å) λ_{max} 5200Å		Continuum
Nitrosyl chloride	Continuum (4100Å - 6500Å) λ_{max} 5200Å		
Boron trichloride	BO_2 bands	BO bands	
Carbonyl chloride	Chemiluminescence doubtful	CN red and violet systems	
Carbon disulfide	Continuum (2700Å - 5200Å) λ_{max} 3450 ± 100Å	Faint glow	
Carbonyl sulfide	Continuum (2700Å - 5200Å) λ_{max} 3450± 100Å		
Hydrogen sulfide	Continuum (2700Å - 5200Å) λ_{max} 3450± 100Å		
Hydrazene	NH_2, NH and OH bands		Faint Glow
Acetylene	C_2, CH, OH bands & Continuum	CN red and violet system	
Ethylene	C_2, CH, OH bands & Continuum	CN red and violet system	Faint Glow OH Bands
Methyl acetylene	C_2, CH, OH bands & Continuum	CN red and violet system	

TABLE 11 (continued)

CHEMILUMINESCENT REACTIONS OF SEVERAL SUBSTANCES
WITH ATMOSPHERIC CONSTITUENTS
(Spectral Features)

Titrant	Atmospheric Constituent		
	Atomic Oxygen	Atomic Nitrogen	Ozone
Allene	C_2, CH, OH bands & Continuum	CN red and violet system	
Hexyne	C_2, CH, OH bands & Continuum	CN red and violet system	
Hexene	CH, OH bands & Continuum	CN red and violet system	Faint glow
Carbon tetrachloride		CN red and violet system	
Trichloroethylene		CN red and violet system	
Ethyl alcohol	OH and CH bands	CN red and violet system	
Benzene	OH and CH bands		
Nitromethane	OH and NO_2 Continuum		
Germane	GeO and Unknown bands	Continuum	
Diborane	BO and BO_2 bands	Continuum	Faint glow
Triethyl Boron	BO and BO_2 bands	CN red and violet system NH, CH	BO_2 bands
Trimethyl Aluminium	Continuum	CN red and violet system NH, CH, OH	Faint glow (Continuum)
Germanium tetrachloride		One band at 3850Å	
Diethyl Zinc	Continuum	CN red and violet system	Faint glow
Trimethyl Antimony	SbO bands α and β systems	CN red and violet system	
Sulfur Dioxide	——	——	——
Trimethyl Boron	BO_2 bands		

TABLE 12

COMPOUNDS SHOWING STRONG CHEMILUMINESCENCE

Atomic Oxygen	Atomic Nitrogen	Ozone
Nitric Oxide	Hexene and Hexyne	Nitric Oxide
Acetylene	Trichloroethylene	Trimethyl Aluminum
Carbon Disulfide	Diethyl Zinc	Triethyl Boron
Triethyl Boron	Trimethyl Antimony	
Trimethyl Antimony	Triethyl Boron	
Trimethyl Aluminum	Trimethyl Aluminum	

B. Experimental

The present study of the gas phase chemiluminous reactions has been carried out in two steps: (1) preliminary observations in a medium pressure fast flow system and (2) the study of the chemiluminous reactions of some selected compounds under simulated upper atmospheric conditions.

The preliminary observations were carried out in a medium pressure flow tube apparatus which can handle a pressure up to 1 mm Hg., and is shown in block diagram form in Figure 10. The initial investigation included the determination of the optimum conditions for obtaining maximum intensity of the chemiluminescence and the observation of the spectrum of the chemiluminescence. The spectrometer used for the observation of the spectrum was a Perkin-Elmer (Model 99) monochromator equipped with a 600 lines/mm grating and an EMI 9558Q photomultiplier tube. This was a single beam, double-pass instrument and covers the wide spectral range by interchanging the grating and the detectors. We have also designed a housing for the photomultiplier so that it can be cooled down to liquid nitrogen temperature.

Since the sensitivity of the spectral recording system drops considerably at shorter wavelength, the spectra of some chemiluminescent reactions were photographed with a Hilger small quartz spectrograph. The dispersion and the resolution of the above spectroscopic equipments were not sufficient for definite identification of some spectra and therefore a 1.5 m Jarrel-Ash grating spectrograph with a grating blazed at 3000Å and reciprocal dispersion of about 11Å/mm was also used.

To obtain definite information regarding the true relative intensity of the different spectral features recorded by the spectrometer, the spectral response of the recording system employed was calibrated with a standard light source (GE quartz iodine tungsten filament lamp, Model 6.6A/T4Q/1CL-200W). The absolute irradiance of the lamp was obtained from Stair, et al. [17].

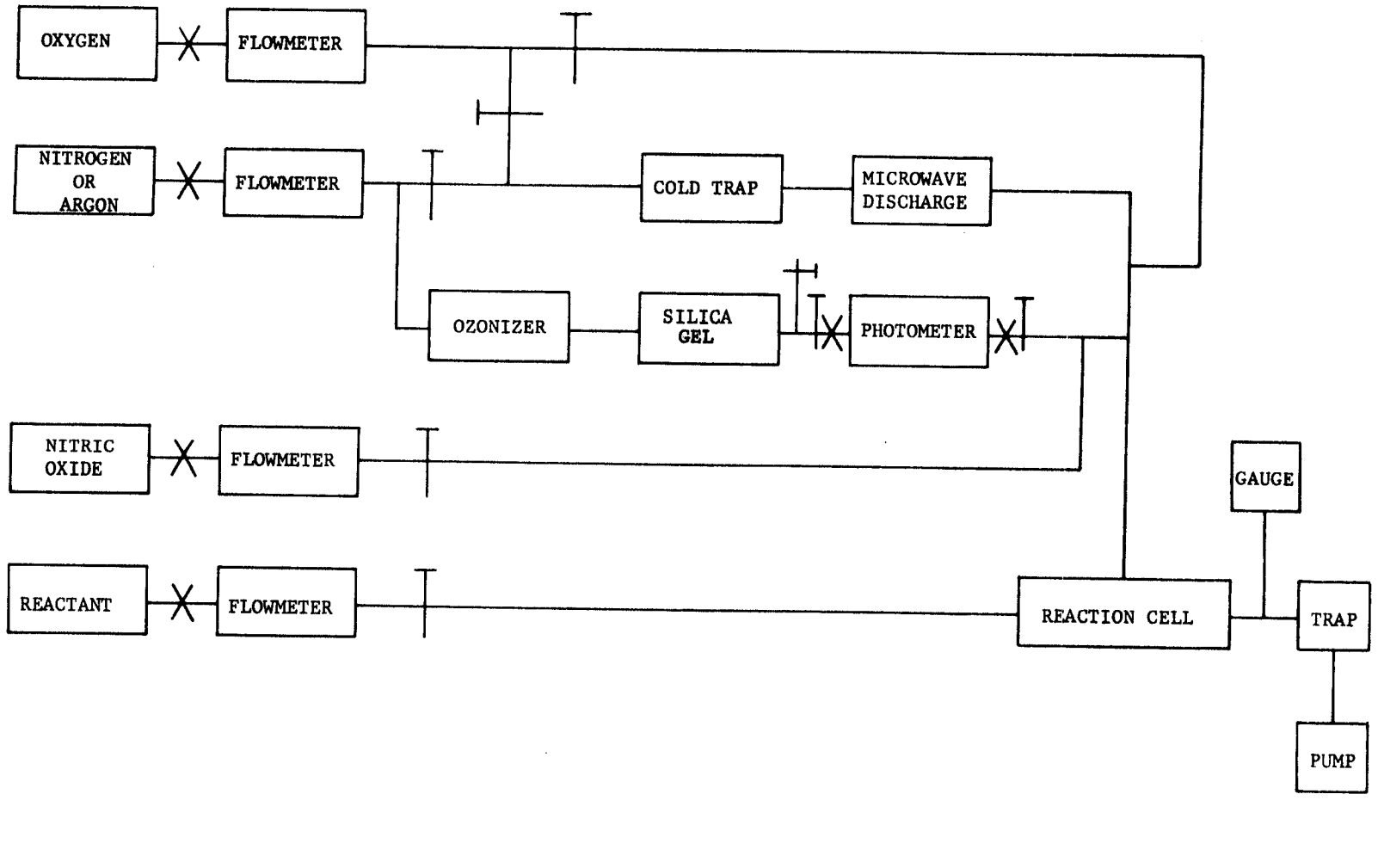

Figure 10. Medium pressure reaction system

In order to obtain information regarding the chemiluminous reactions for the upper atmospheric chemical release studies, the chemiluminous reactions of some compounds were studied at low pressures, which were of the order of tens of microns. The reaction cell simulating the upper atmospheric condition was a 50 liter, 3-necked pyrex flask (Figure 11). The gases were let into the cell through the two side arms of the flask. The center neck is connected to an oil booster pump backed by a Welsh mechanical pump which working together are capable of keeping the cell pressure at 10μ of Hg when the flow rates of gases were up to 70 standard cc/minute. The overall intensity was measured with RCA 1P28 photomultiplier, which was placed in front of a small aperture sealed with a quartz window. The pressure within the cell was measured with a calibrated McLeod gauge. The photoelectric current was measured by an Electrometer Model VTE 1 (of the Victoreen Instrument Co.). Figure 12 shows the complete apparatus in schematic form.

Using the above (with minor modifications) we could have atomic oxygen in the presence of molecular oxygen by passing a microwave discharge through molecular oxygen only. The atomic oxygen with very little molecular oxygen could be produced by microwave discharge through a 99:1 mixture of argon and oxygen. Finally, the atomic oxygen in the absence of molecular oxygen could be produced by dissociating nitrogen by microwave discharge and then titrating the nitrogen atoms with nitric oxide.

A technique, as that described by Cook, et al. [18] was used for the preparation and handling of ozone. This technique utilizes the sorption process for the separation of ozone from oxygen. The ozone production and handling system is shown in Figure 13. The oxygen from the cylinder is passed through a silent electric discharge at atmospheric pressure and then through a U-tube containing silica gel at the dry ice-acetone temperature of about -80°C. When enough ozone is adsorbed by the silica gel the oxygen flow and discharge is stopped and finally the ozone is desorbed by replacing the dry ice-acetone trap by the ethylene glycol trap maintained at -30°C. The details of the handling procedure are given by Sharma and Padur [19].

Since the organometallic compounds studied by us are highly pyrophoric, an arrangement shown in Figure 14 was used for transferring the organometallic liquid from its container to the reaction system under the inert atmosphere of nitrogen. The details of the necessary precautions are described by Sharma and Padur [20].

C. Results of Survey Experiments

The results of our extensive survey of the gas phase chemiluminous reactions of atomic oxygen, atomic nitrogen and ozone are described in this section. The present study of the chemiluminous reaction was conducted at a pressure of about 1 mm Hg and room temperature. The present results are only applicable under the above conditions. The spectral features observed in the spectra of chemiluminescence produced during the reaction of several reactants with the above atmospheric constituents are summarized in Table 11. We shall now describe the results of our study for each reactant separately.

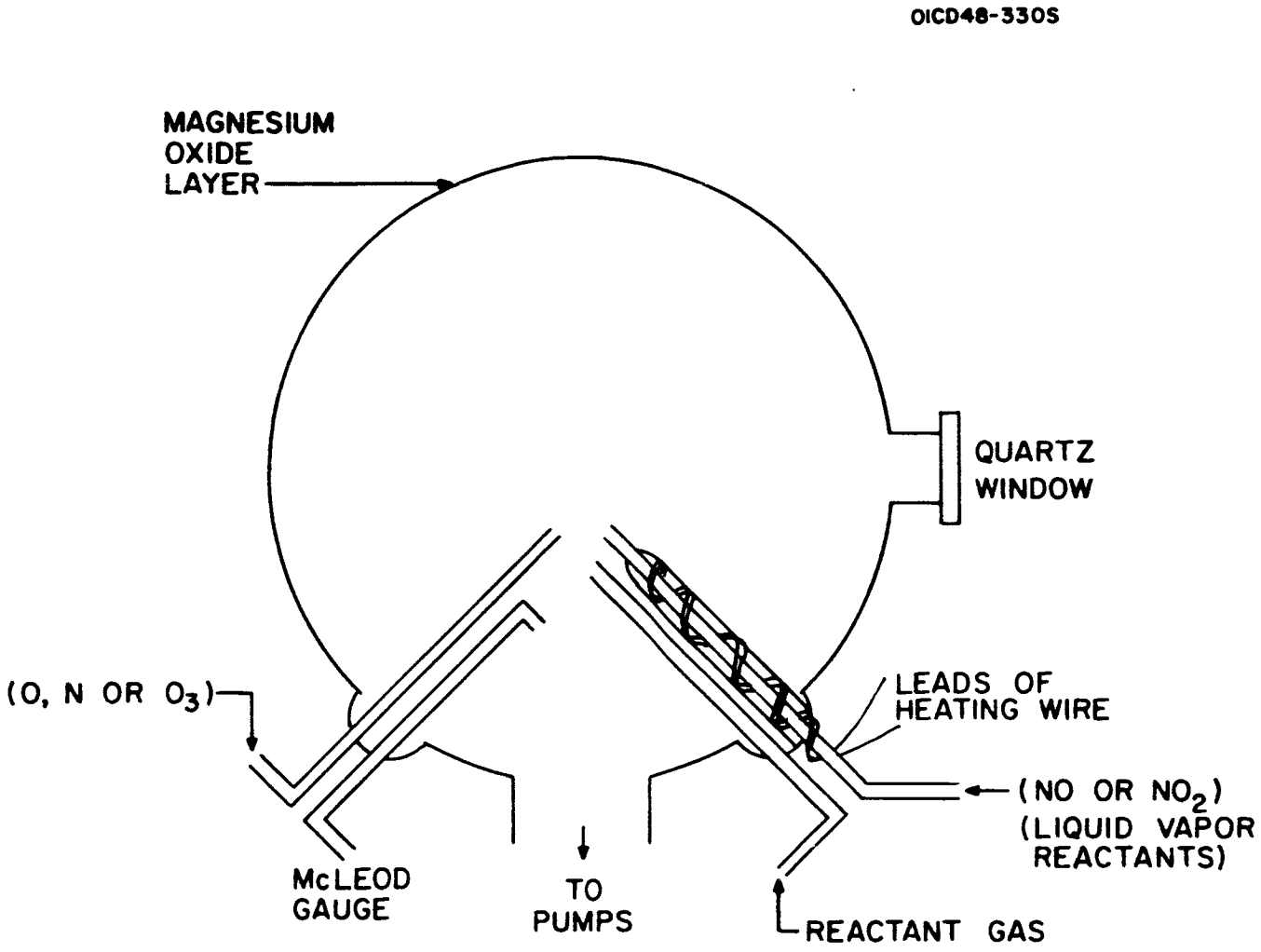

Figure 11. Low pressure reaction chamber

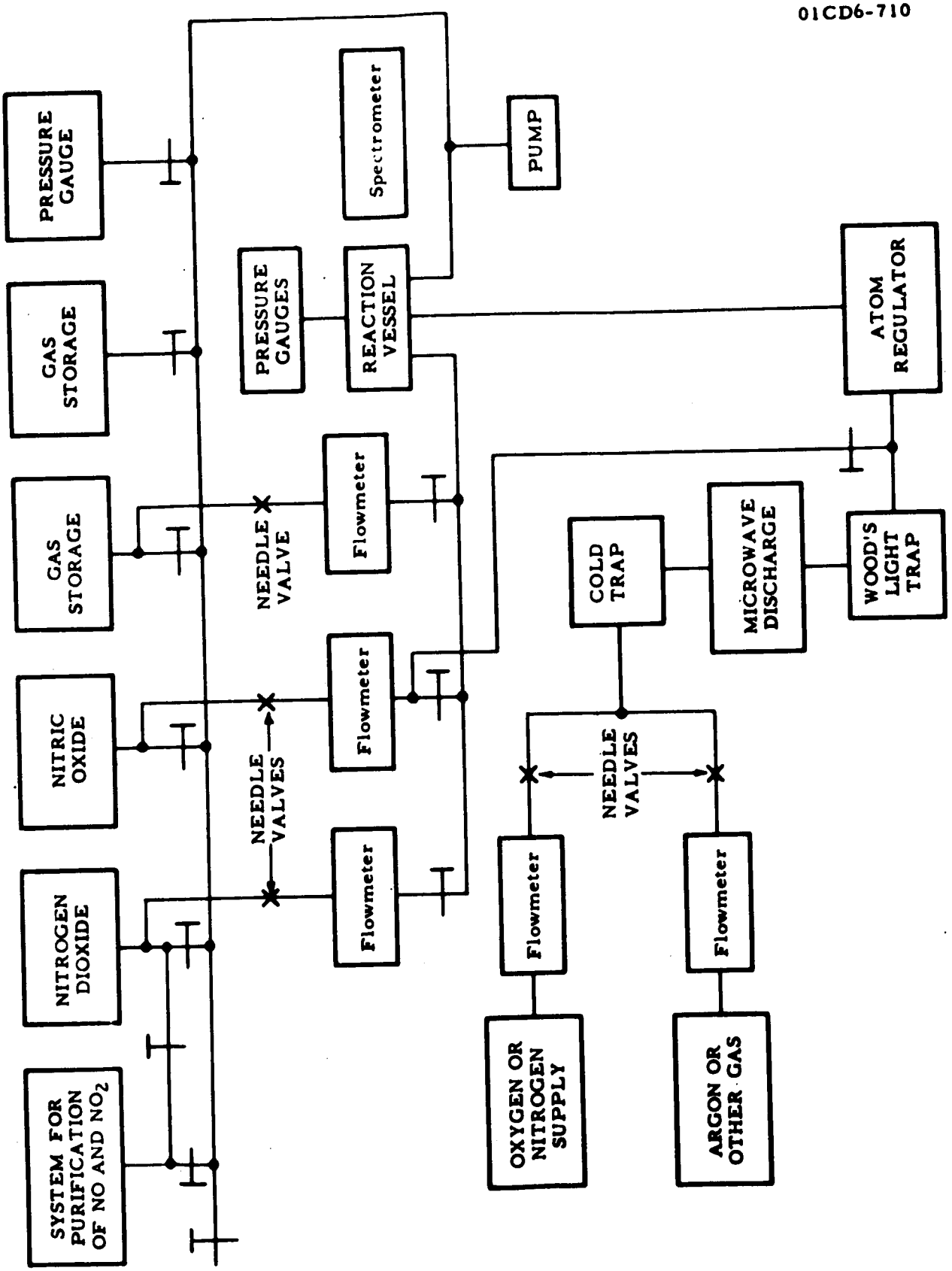

Figure 12. Block diagram of apparatus for observation of chemiluminescence.

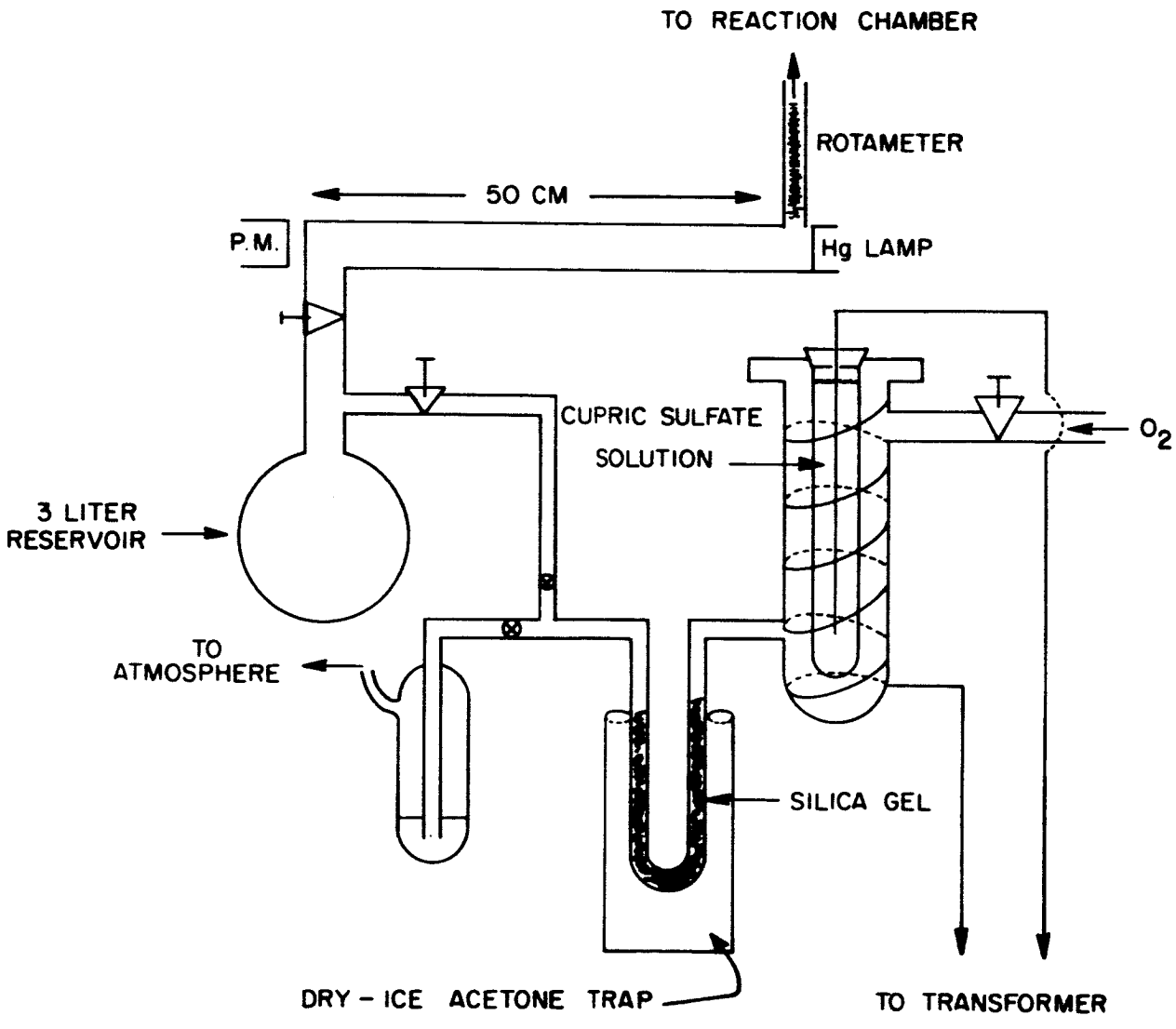

Figure 13. Ozone-handling system.

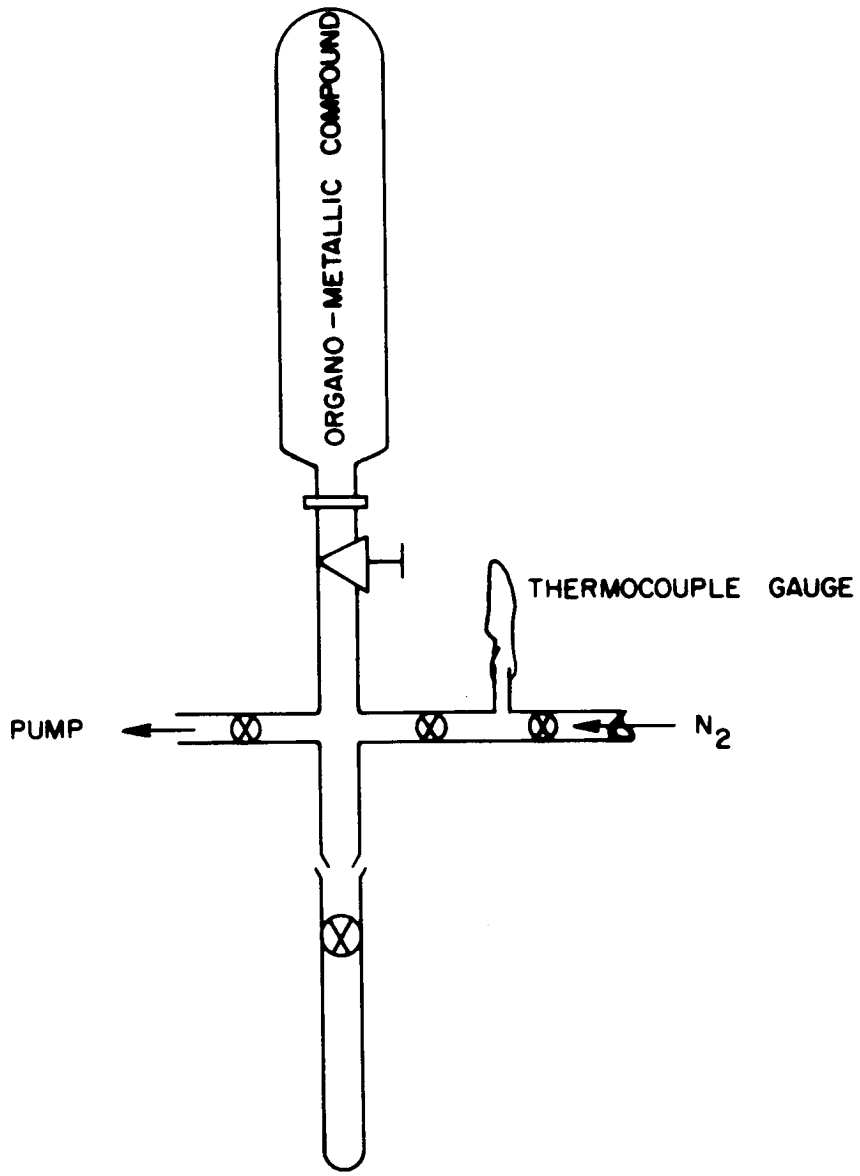

Figure 14. An arrangement for transferring organometallic liquid.

Atomic oxygen. - The relative intensities and spectral features of the chemiluminescent reactions involving oxygen atoms are given in Table 13. A capillary flow meter with a U-tube manometer was used for monitoring the flow rate of the reactant gases. Column two of the above table indicates the flow-meter reading. The overall intensity of the chemiluminescence produced during the reaction was obtained from the gain factor of the amplifier required for the recording of the spectrum. The numbers in the subsequent column indicates the relative intensity of the different spectral features in the spectrum. The wavelengths in the last column indicate the lower and upper wavelength limits of the continua observed in each spectrum together with the wavelength of the maximum intensity. It has been found that nitric oxide, carbon disulfide, acetylene, triethyl boron, trimethyl antimony and trimethyl aluminum produce strong chemiluminescence during their reactions with atomic oxygen.

Hydrocarbons. - The chemiluminous reactions of atomic oxygen with several hydrocarbons have been studied [10-12] in this laboratory. In agreement with previous observations we have found that the unsaturated hydrocarbons produce strong chemiluminescence during their reactions with atomic oxygen. The main features of the spectrum of the chemiluminescence produced during the reactions of unsaturated hydrocarbons are the OH ($^2\Sigma \rightarrow {}^2\Pi$) band system at 3064Å, the C_2 Swan band system in the red and green region, the CH bands at 4300Å ($^2\Delta \rightarrow {}^2\Pi$), 3900Å ($^2\Sigma \rightarrow {}^2\Pi$) and 3143Å ($^2\Sigma \rightarrow {}^2\Pi$). The swan bands arise from the $^3\Pi \rightarrow {}^3\Pi$ transitions and are degraded towards the violet. Figure 15 shows the spectra of chemiluminescence produced during the reactions of acetylene and ethylene with atomic oxygen. The OH band is observed in the spectra of chemiluminescence produced by almost all hydrocarbons with atomic oxygen. C_2 bands are not observed in the spectrum of the chemiluminescence produced during the reactions of ethyl alcohol, benzene and nitromethane, etc. No visible chemiluminescence was observed during the reaction of atomic oxygen and carbon tetrachloride. From Table 13, it can be concluded that acetylene is the most efficient hydrocarbon in producing chemiluminescence during the reaction with atomic oxygen. Moreover, the other organic compounds like halogen substituted hydrocarbons, ethyl alcohol, benzene and nitromethane do not show marked chemiluminous efficiency.

Sulfur compounds. - The chemiluminous reactions of carbon disulfide, carbonyl sulfide and hydrogen sulfide were studied. Among these compounds, carbon disulfide showed comparatively stronger chemiluminescence. It was found that all the above three substances show a similar continuous spectrum (Figure 16). It was further observed that the spectrum of the chemiluminescence produced during the reactions of above sulfur compounds with atomic oxygen is similar to that of sulfur dioxide afterglow (Figure 16). On the basis of the above observation and other kinetic information, Sharma, et al. [21], have concluded that the reaction responsible for the production of chemiluminescence during the above reaction is:

$$SO + O \rightarrow SO_2 + h\nu \qquad (13)$$

TABLE 13

REACTIONS WITH ATOMIC OXYGEN

Reactant	Flow Meter Reading	Spectral Feature & Intensity* Intensity	(C_2 bands) 4700-5000	CH band 3143,3900 4300	OH band 3064	Other Bands	Continua
Nitric Oxide		60					4100Å-6500Å λ_{max} 5150
Nitrocyl chloride	30 cm	1					4100Å-6500Å λ_{max} 5150(6)
Boron trichloride	14 cm	9				BO_2(8)	Probably continuum
Carbonyl chloride							Continuum(to be checked)
Carbon disulfide	7 cm	80					2700Å-5200Å λ_{max} 3200Å(5)
Carbonyl sulfide	20 cm	15					2700Å-5200Å λ_{max} 3200Å(8)
Hydrogen sulfide	19 cm	32					2700Å-5200Å λ_{max} 3200Å(5)
Hydrazene	9 cm	4			(4.5)	NH(0.5) NH_2(7)	6200Å-6500Å λ_{max} 5600(6)
Acetylene	18	80	(7.5)	(>>10)	(0.4)		3800Å-6000Å λ_{max} 5000Å(3)

TABLE 13 (continued)

REACTIONS WITH ATOMIC OXYGEN

Reactant	Flow Meter Reading	Intensity	Spectral Feature & Intensity* (2 bands) 4700-5000	CH band 3143,3900 4300	OH band 3064	Other Bands	Continua
Ethylene	8 cm	1	(1.0)	(7,6)	(11)		Possibly continuum
Methyl acetylene	3 cm	1	(3)	(>>10)	(6)		3800Å-6000Å λ_{max} 5000Å(2)
Allene	4 cm	15	(1.5)	(>>10)	(9)		Possibly continuum
Hexyne	3 cm	9	7	(>10)	(>>10)		Continuum possible
Hexene	3 cm	1		(4.5)	(>>10)		Continuum as above possible (3) (3800 - 6000Å)
Ethyl alcohol	12 cm	1		(1.5)	(3.6)		
Benzene	16 cm	1		(>10)	(4.5)		
Nitromethane	7 cm	4			(8.7)		NO_2 Continuum 4100-6500Å λ_{max} 6500(3.8)
Trichloroethylene	8 cm	1	4.5	11	8.7		3800-6000Å λ_{max} 5000Å(4)
Germane	7 cm	14				GeO	
Diborane	3 cm	6				$BO;BO_2$	
Triethyl Boron	6 cm	32				BO_2	

TABLE 13 (continued)

REACTIONS WITH ATOMIC OXYGEN

Reactant	Flow Meter Reading	Intensity	Spectral Feature & Intensity* (2 bands) 4700-500	CH band 3143,3900 4300	OH band 3064	Other Bands	Continua
Trimethyl Aluminum	2.5 cm	6			(0.9)		Continuum λ_{max} 4750Å (λ3600-λ6500)
Diethyl Zinc	5 cm	1				ZnO bands	Continuum in the visible
Trimethyl Antimony	5 cm	80				SbO bands	

* The figure in the bracket indicates the peak relative intensity of the strongest observed spectral feature indicated by the recorder.

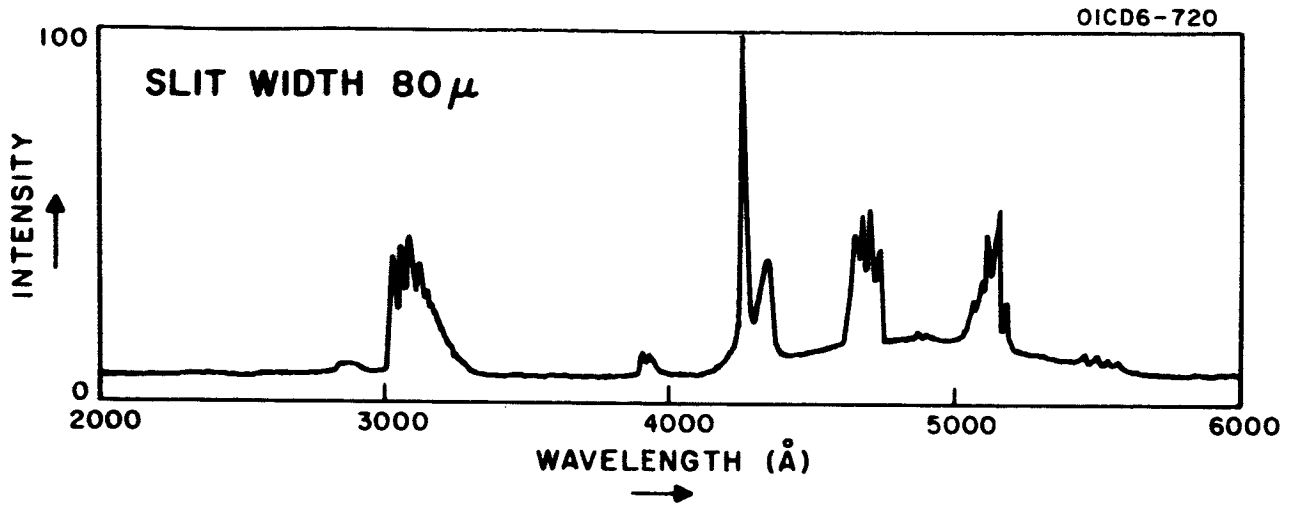

(a) Chemiluminescence spectrum of acetylene and atomic oxygen.

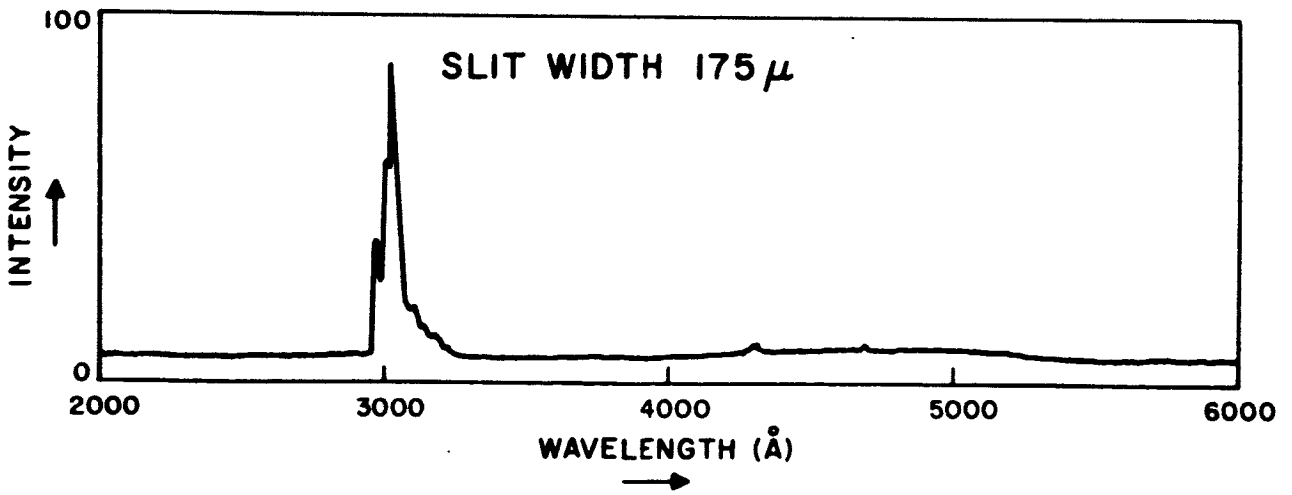

(b) Chemiluminescence spectrum of ethylene and atomic oxygen.

Figure 15.

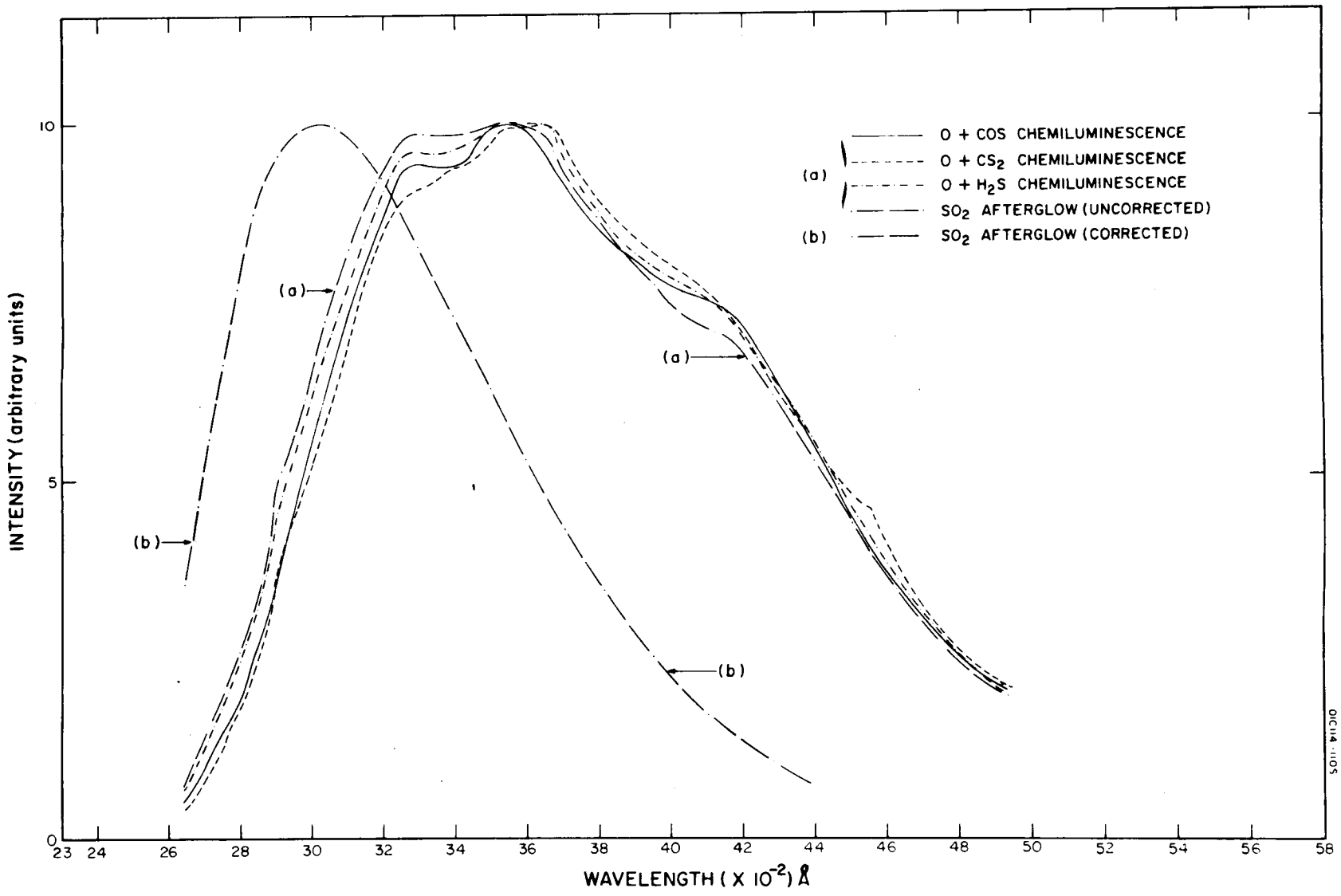

Figure 16. Chemiluminescent spectrum of carbon disulfide, carbonyl sulfide and hydrogen sulfide reaction with atomic oxygen and comparison with sulfur dioxide afterglow.

This is analogous to the recombination of NO and CO with atomic oxygen, which have been already studied [11] in this laboratory. The details of the above study are given by Sharma, et al. [21].

Nitrogen compounds. - The chemiluminous reactions of nitric oxide, nitrosyl chloride and nitromethane were studied. All of the nitrogen compounds show similar spectra, with a continuum starting from 4100Å and extending into the infrared region. The similarity of the spectra indicates that the following reaction is responsible for the production of chemiluminescence:

$$NO + O + M \rightarrow NO_2^* + M \qquad (14)$$

$$NO_2^* \rightarrow NO_2 + h\nu$$

Among the above studied compounds, nitric oxide is the substance which produces the strongest chemiluminescence during its reaction with atomic oxygen.

Boron compounds. - The boron compounds investigated during the present study are: boron trichloride, diborane, triethyl boron and trimethyl boron. The spectrum of the chemiluminescence produced during the reactions of boron trichloride, triethyl boron and trimethyl boron mainly consists of BO_2 bands in the region between 4000Å and 5000Å. Some indication of the presence of the BO α system ($A^2\Pi - X^2\Sigma$) is also obtained. However the intensity of the BO bands as compared to the BO_2 bands is low. On the other hand the spectrum of the chemiluminescence produced during the reaction of diborane consists of BO_2 bands as well as BO bands of the α system ($A^2\Pi - X^2\Sigma$) and β system ($B^2\Sigma - X^2\Sigma$). Here the relative intensity of the BO is larger than that of the BO_2 bands. Triethyl boron shows the strongest chemiluminescence during its reaction with atomic oxygen as compared with the other boron compounds. The corrected recorded spectrum of the chemiluminescent reaction between boron trichloride and atomic oxygen is shown in Figure 17. The details of the chemiluminescent reaction of triethyl and trimethyl boron with atomic oxygen are given by Sharma and Padur [20].

Germanium compounds. - The chemiluminous reactions of germanium tetrahydride or germane and germanium tetrachloride with atomic oxygen were investigated. It was found that the reaction between germane and atomic oxygen produced chemiluminescence, whereas no chemiluminescence was observed when germanium tetrachloride was mixed with atomic oxygen. This observation is similar to our previous observation with hydrocarbons. We have reported earlier that analogous to germanium tetrachloride, carbon tetrachloride also does not produce any chemiluminescence during its reaction with atomic oxygen. However, the chemiluminescence of carbon hydride with atomic oxygen is well known. This is understandable because both carbon and germanium belong to the same period of elements in the periodic table.

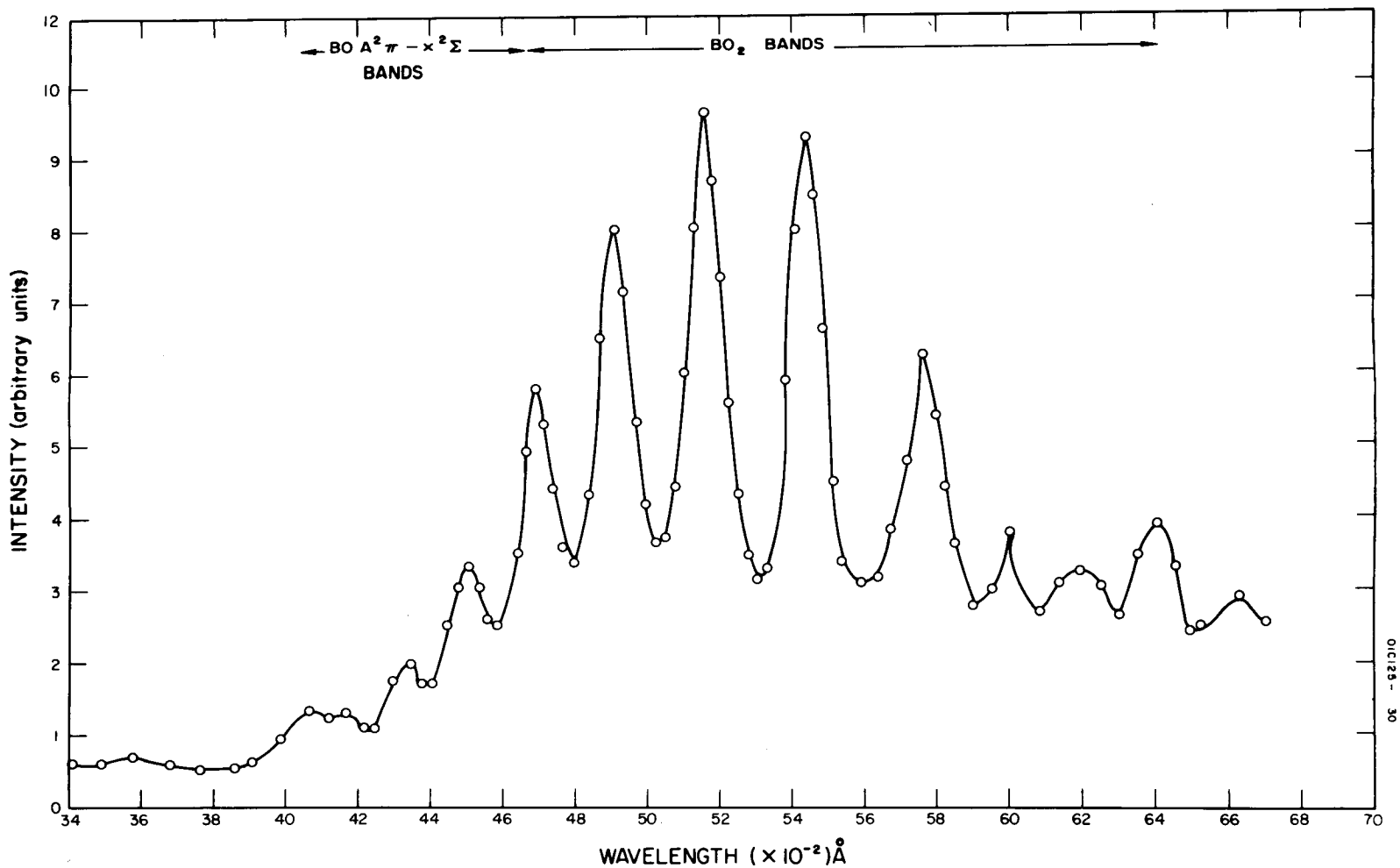

Figure 17. Corrected spectrum of the chemiluminescence produced during the reaction of boron trichloride and atomic oxygen.

The spectrum of the chemiluminescence produced during the reaction of germane with atomic oxygen consists of GeO bands. The corrected and recorded spectrum is shown in Figure 18. A number of new bands belonging to the D-X system of GeO have been observed. Moreover, an indication of the existence of a new band system on the longer wavelength side of the D-X system has been obtained. The details are described by Sharma and Padur [22].

Organometallic compounds. - The gas phase chemiluminous reactions of trimethyl aluminum, triethyl boron, trimethyl boron, trimethyl antimony and diethyl zinc with atomic oxygen were investigated. It was found that trimethyl aluminum is not the only organometallic compound to produce strong chemiluminescence with atomic oxygen. Stronger chemiluminescence is observed during the reaction of triethyl and trimethyl boron, and trimethyl antimony with atomic oxygen (Figure 19). The corrected spectra of the chemiluminescent reactions of the studied organometallic compounds are shown in Figures 20 to 23. The details of the study of the reactions of the above organometallics with atomic oxygen are given by Sharma and Padur [20].

Hydrazene. - The chemiluminous reaction of hydrazene with atomic oxygen was studied. The intensity of the above reaction was not very large. The spectrum of the chemiluminescence produced during its reaction with atomic oxygen consists essentially of OH, NH and NH_2 bands.

Atomic nitrogen. - Table 14 shows the relative intensity and spectral features of the chemiluminous reactions of several compounds with atomic nitrogen. The red and violet systems of CN are present in the spectrum of almost all the chemiluminous reactions of atomic nitrogen and carbon containing compounds. The presence of the CH band is also indicated. Kiess, et al. [13] have extensively studied the reactions of several hydrocarbons with atomic nitrogen. Figure 24 shows the corrected spectra of the chemiluminescence produced during the reaction of atomic nitrogen and the hydrocarbons. The chemiluminous reactions of atomic nitrogen were also studied with some organometallic compounds. Strongest chemiluminescence was observed during the reaction of diethyl zinc and trimethyl aluminum followed by the reaction of trimethyl antimony. Among other hydrocarbons, trichloroethylene produced strongest chemiluminescence during its reaction with atomic nitrogen.

Pannetier, et al. [23] have observed the presence of NS bands in the spectrum of chemiluminescence produced during the reaction of H_2S and atomic nitrogen at several mm Hg of pressure. However, we did not find strong chemiluminescence during the above reaction at submillimeter pressure. The spectrum of the chemiluminescence produced during the reaction of boron trichloride and atomic nitrogen is shown in Figure 25, and mainly consists of BO bands.

Ozone. - Bernanose, et al. [16] have collected a list of compounds which are supposed to produce chemiluminescence during their reaction with ozone. In this number of previously reported chemiluminous reactions of ozone, the conditions under which the chemiluminescence is observed are not clearly specified.

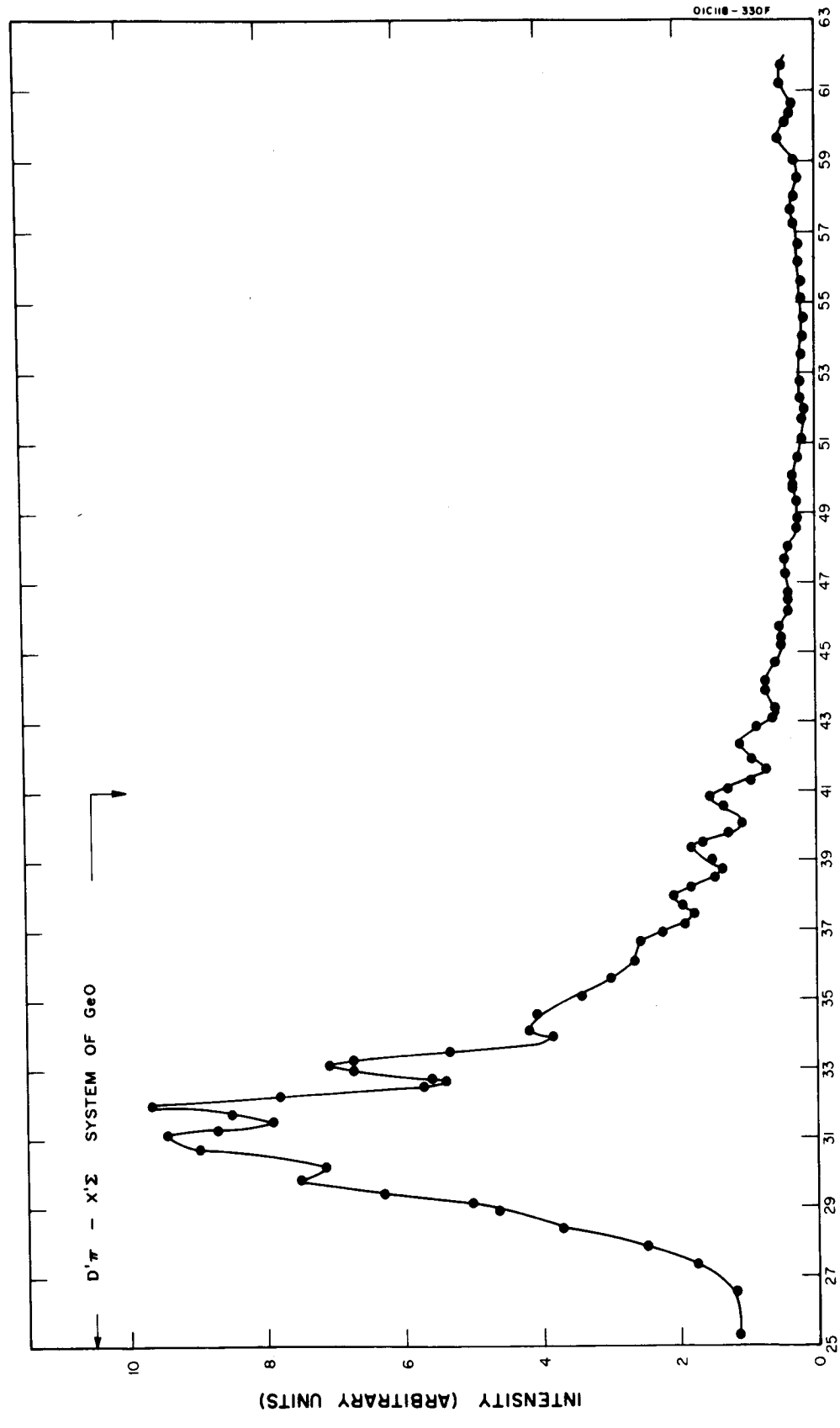

Figure 18. The spectrum of the chemiluminescent reaction of germane with atomic oxygen.

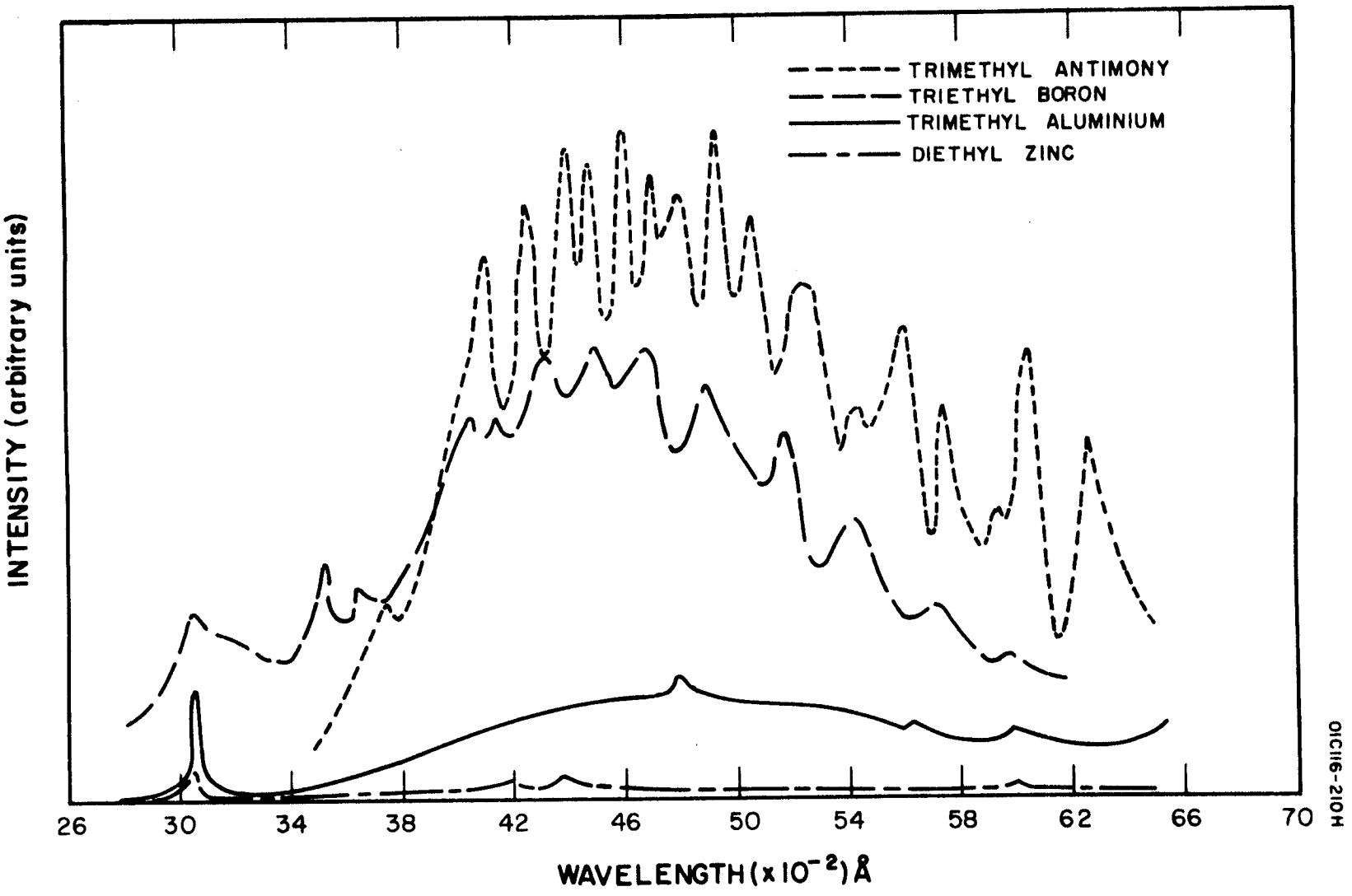

Figure 19. The spectra of the chemiluminous reactions of some organometallic compounds with atomic oxygen: the relative intensity of the different chemiluminous reactions is shown.

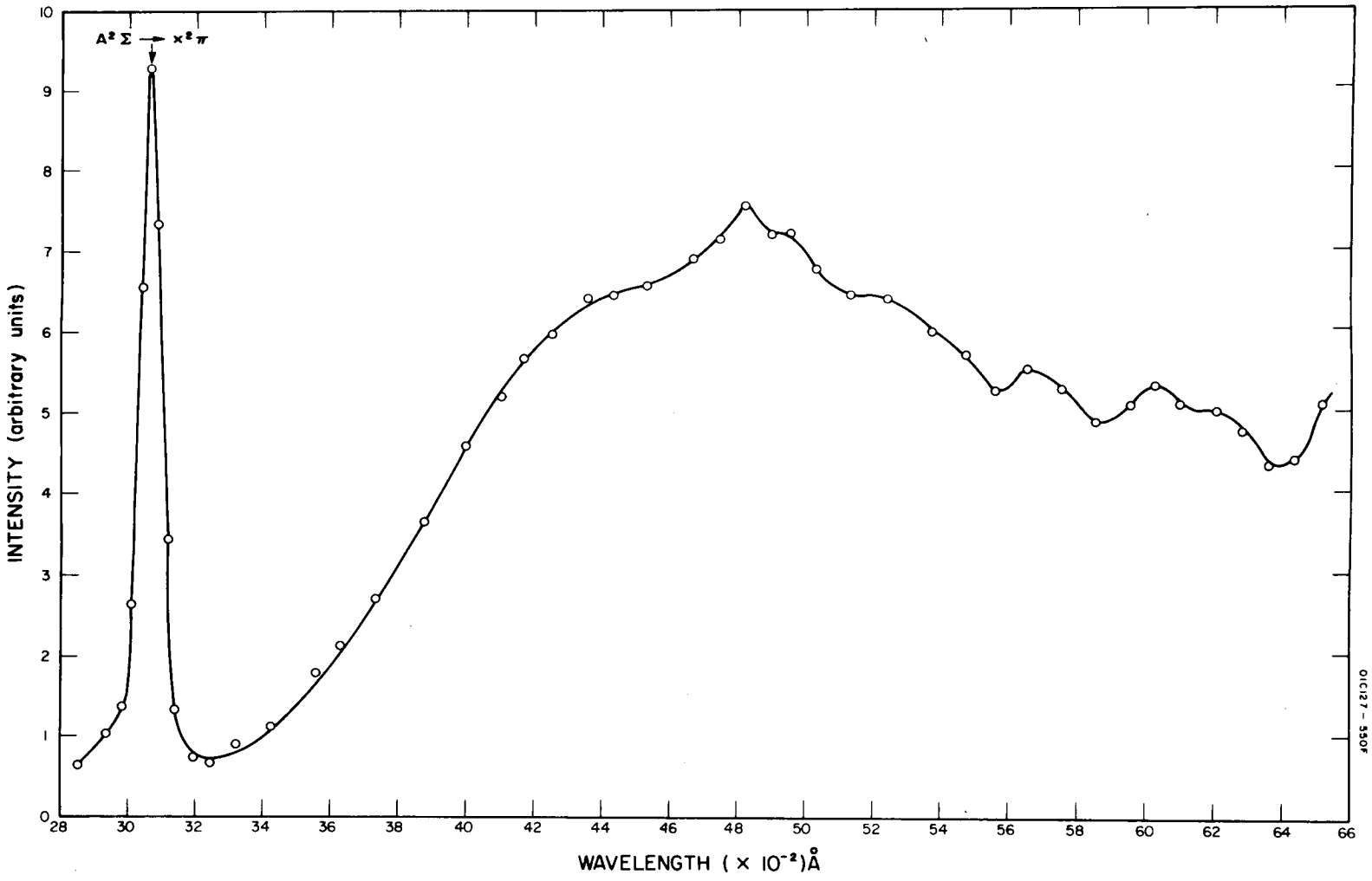

Figure 20. The spectrum of the chemiluminescence produced during the reaction of trimethyl aluminum and atomic oxygen.

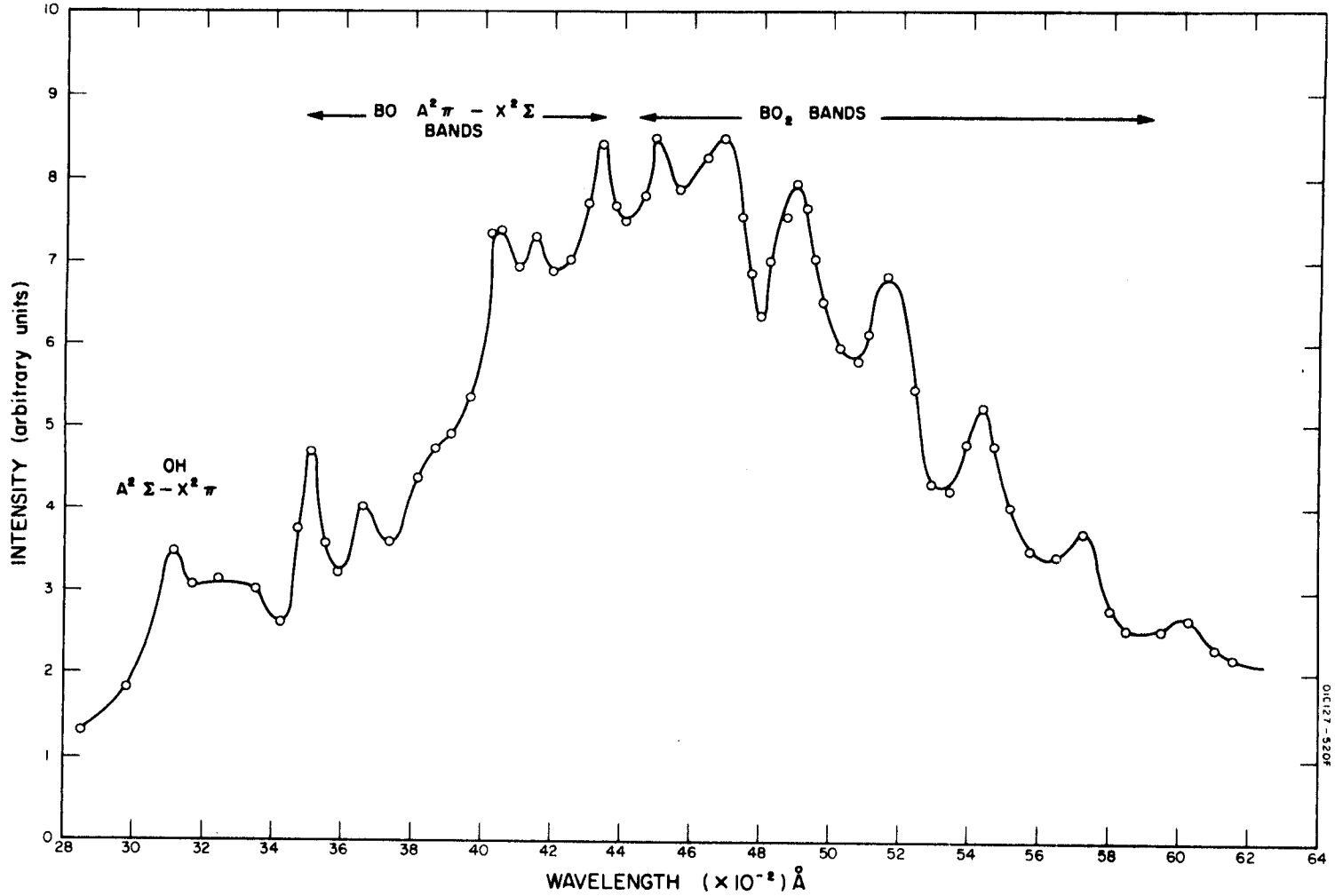

Figure 21. The spectrum of the chemiluminous reactions of triethyl boron and atomic oxygen

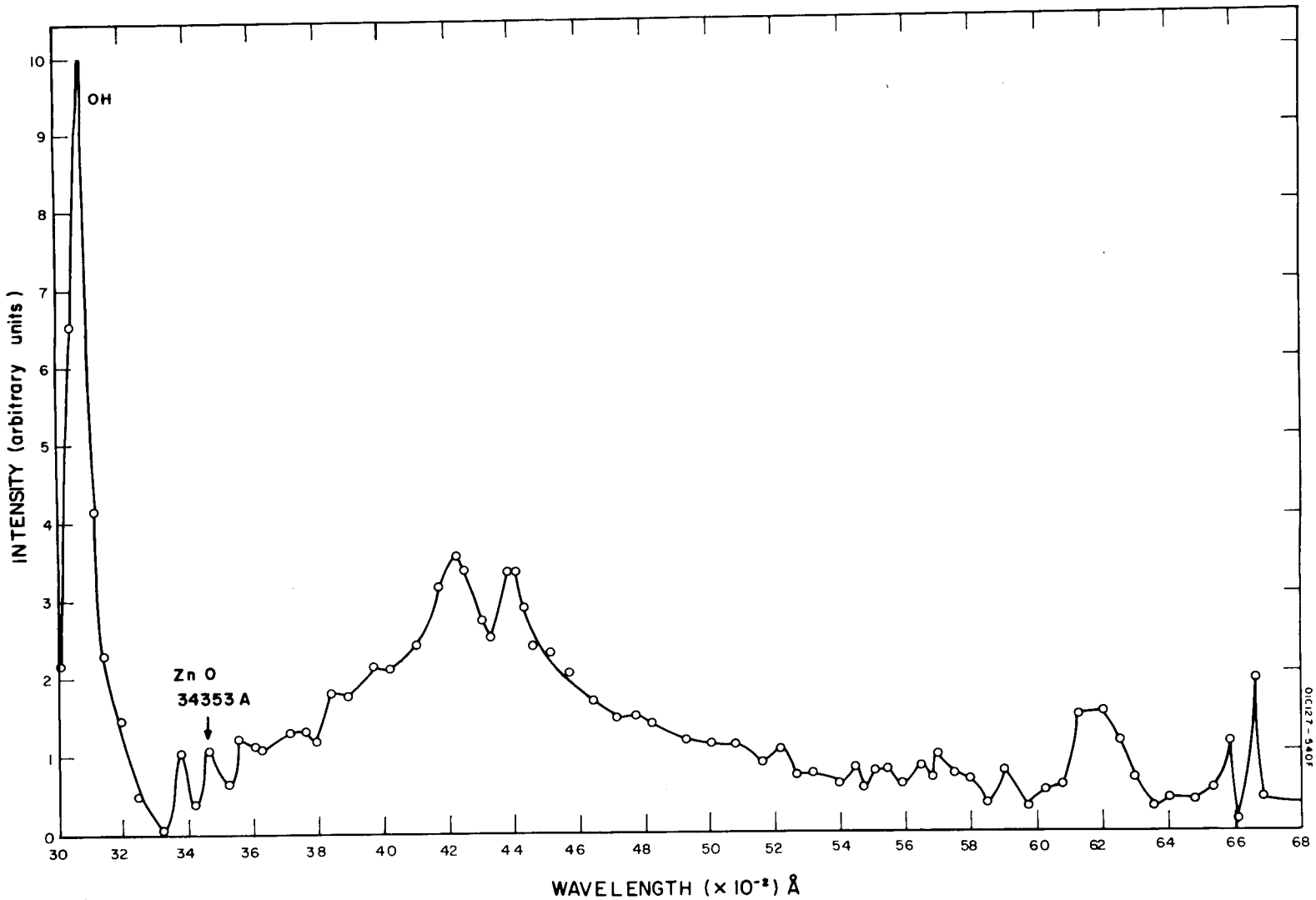

Figure 22. The spectrum of the chemiluminous reaction of diethyl zinc and atomic oxygen.

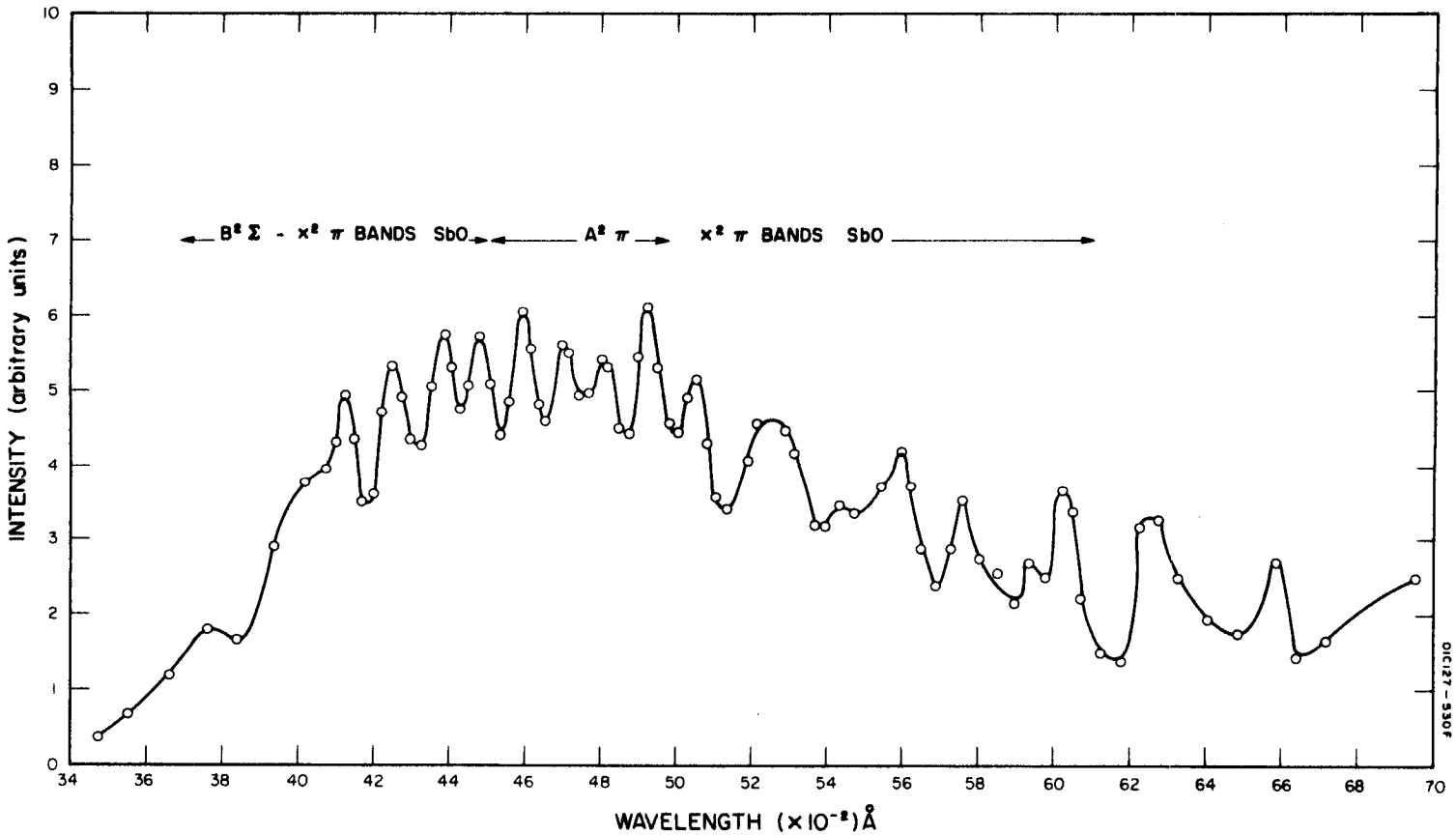

Figure 23. The spectrum of the chemiluminous reaction of trimethyl antimony and atomic oxygen.

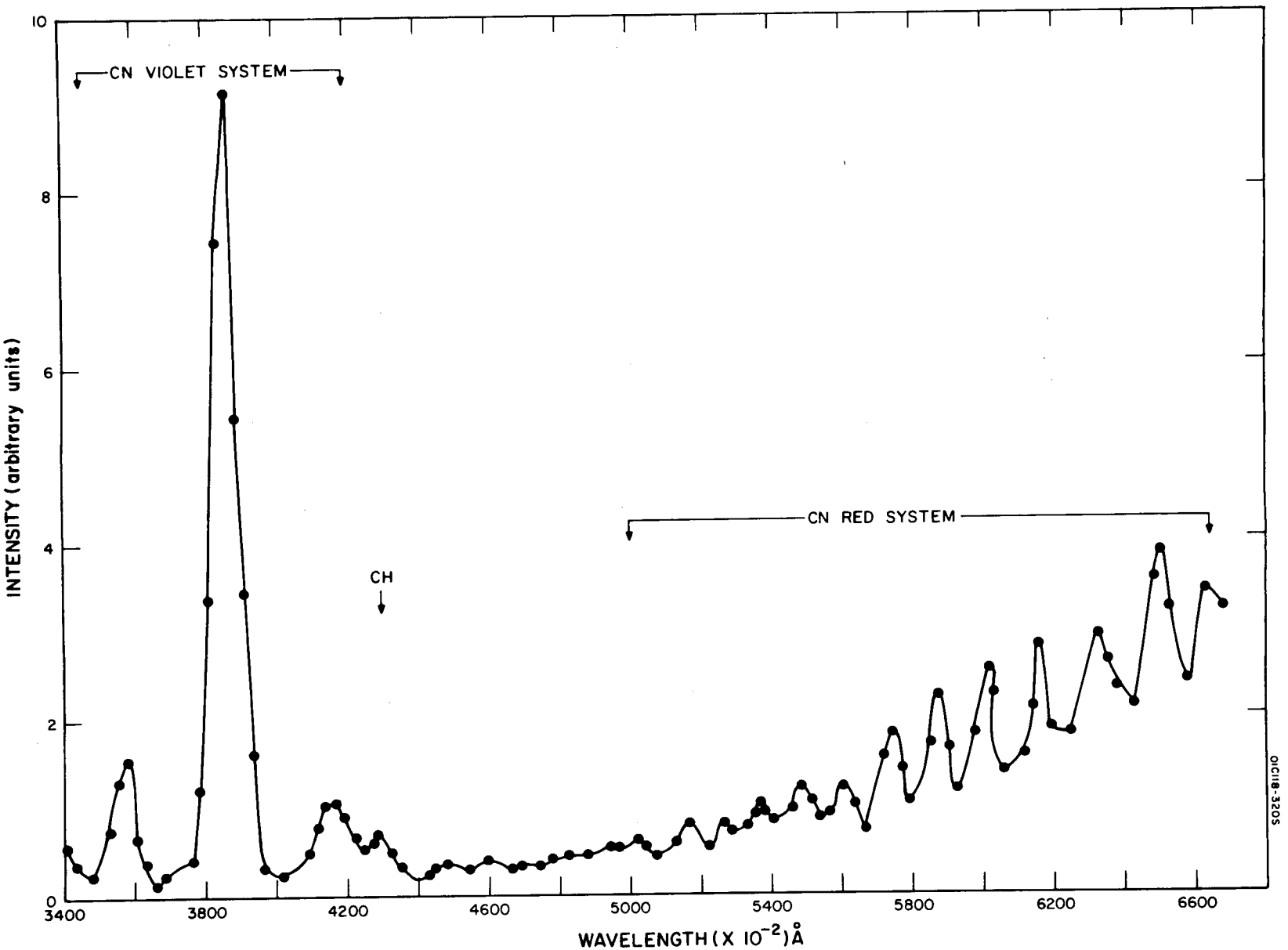

Figure 24. The spectrum of the chemiluminous reaction between hydrocarbon and atomic nitrogen.

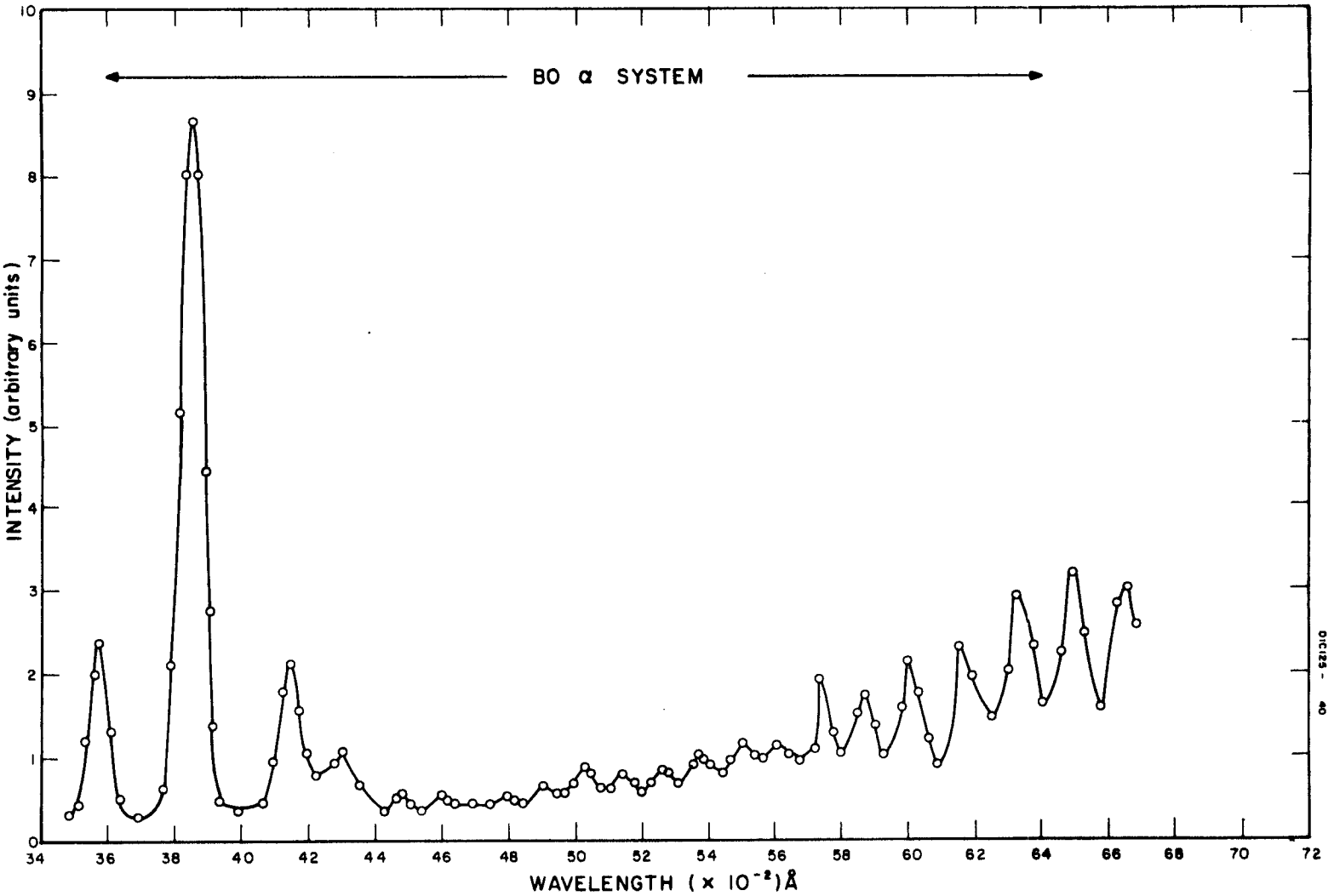

Figure 25. The spectrum of the chemiluminescence produced during the reaction of boron trichloride and atomic nitrogen.

TABLE 14

CHEMILUMINOUS REACTIONS OF ATOMIC NITROGEN

Reactant	Flow Meter Reading	Intensity	Spectral Feature and Intensity		
			CN Violet Band	CN Red Bands	Other Bands
Acetylene	~	9	(10)	(1.5)	
Ethylene	17	6	(11)	(1.5)	
Methyl Acetylene	17	9	(11)	(1)	
Allene	17	9	(12)	(1)	
Hexyne	7	21	(7)	(1)	
Hexene	3	14	(9)	(1.5)	
Ethyl Alcohol	19	1	(9)	(1.5)	
Benzene		1			
Nitromethane	>30	1			
Carbon Tetrachloride	23	1	(4)	(2)	
Trichloro ethylene	22	120	(6.5)	(1.8)	
Carbonyl chloride	24	1	(11)	(4)	
Germane	7 cm	14	-	-	Continuum (λ3400-6000Å)

TABLE 14 (continued)

CHEMILUMINOUS REACTIONS OF ATOMIC NITROGEN

Reactant	Flow Meter Reading	Intensity	Spectral Feature and Intensity		
			CN Violet Band	CN Red Bands	Other Bands
Di-borane	3 cm	1.5			Continuum(λ4000-6000Å)
Tri-ethyl Boron	8 cm	80	(6.8)	(1.5)	CH, NH
Tri-methyl Aluminum	2 cm	670	(5.5)	(1)	CH, OH, NH
Germanium Tetrachloride	-	-	-	-	-
Di-ethyl Zinc	5 cm	670	(6)	(3)	-
Tri-methyl Antimony	3.5 cm	180	(7)	(4)	-

A number of compounds (see Table 11) were investigated for the possible gas phase (at submillimeter pressure and room temperature) chemiluminous reactions of ozone. Only a few of them produced visible chemiluminescence. The results of the visual observation of the chemiluminescence produced during the gas phase reaction of several compounds with ozone are summarized in Table 15. The second column of the above table indicates the total pressure in the reaction tube, which was predominantly due to argon and ozone. The partial pressure of ozone given in column three was that measured in the absorption cell at its maximum flow rate. However, the pressure of ozone in the reaction tube was somewhat lower than the given. The characteristics of the chemiluminous reactions of ozone are summarized in Table 16, which shows that trimethyl aluminum produces the strongest chemiluminescence during its reaction with ozone.

It was found that the spectra of the chemiluminescence produced during the reaction of trimethyl aluminum and triethyl boron with ozone were similar to the spectra of the chemiluminous reaction of respective compounds with atomic oxygen. The characteristics of these spectra have been discussed previously.

The details of the chemiluminous reactions of ozone have been discussed by Sharma and Padur [19]. They have concluded that the similarity in the spectra of the chemiluminous reactions of ozone and atomic oxygen can not be explained by the thermal decomposition of ozone. However, a large concentration of atomic oxygen may be produced as an intermediate product during the reaction of the above reactant and ozone, which then can subsequently react with the organometallic compound and produce the similar chemiluminescence. Benson [24] has indicated that the thermal decomposition of ozone is extremely sensitive to the presence of metals, metallic oxide, organic matter, peroxides and oxides of nitrogen.

The effect of molecular oxygen on the chemiluminous reaction of trimethyl aluminum was studied by replacing argon with molecular oxygen. It was found that the intensity of chemiluminescence produced during the presence of molecular oxygen (the concentration of molecular oxygen was of the same order of magnitude as that of ozone) was about 10 percent less than that during its absence. The above observation indicates that the effect of oxygen on the chemiluminous reaction of trimethyl aluminum is not drastic.

D. Low Pressure Study

In order to apply the results of our present studies to chemical release studies of the upper atmosphere, the chemiluminescent reactions of a few compounds were studied at low pressure under simulating upper atmospheric conditions. Low pressure studies of the chemiluminescent reactions are furthermore important because the complex chemical reactions are in some cases found to be pressure dependent. Therefore the extrapolation of the observations of the chemiluminescent reactions from a pressure of about 1 mm Hg. to the upper atmospheric conditions may not be correct. Since some informating regarding

TABLE 15

A SURVEY OF THE GAS PHASE CHEMILUMINOUS REACTIONS OF OZONE

Reactants	Total Pressure in Reaction Vessel (microns)	Partial Pressure of Ozone in Absorption Cell (max.) (microns)	Remarks
Acetylene	280 to 700	160	No visible glow
Allene	280 to 1000	230	No visible glow
Benzene	340 to 700	83	No visible glow
Boron Trichloride	280 to 700	175	No visible glow
Carbon Disulfide	320 to 460	200	No visible glow
Carbon Tetrachloride	260 to 340	175	No visible glow
Caronyl Chloride	360 to 480	230	No visible glow
Carbonyl Sulfide	280 to 1000	230	No visible glow
Diborane	310 to 340	175	Faint white glow
Diethyl Zinc	280 to 330	140	Faint white glow-continuum and OH bands
Ethyl Alcohol	320 to 1800	115	No visible glow
Ethylene	280 to 310	125	Faint white glow - OH bands
Germanium Tetrahydride	170 to 360	230	No visible glow
Hexene	360 to 700	230	Faint white glow
Hexyne	280 to 570	200	No visible glow
Hydrazine	180 to 320	200	Faint glow
Hydrogen Sulfide	340 to 440	200	No visible glow
Methyl Acetylene	280 to 880	160	No visible glow
Nitric Oxide	280 to 620	140	Faint red glow - continuum and NO_2 bands
Nitromethane	320 to 550	230	No visible glow
Nitrosyl Chloride	280 to 700	230	No visible glow
Sulfur Dioxide	340 to 550	200	No visible glow

TABLE 15 (continued)

A SURVEY OF THE GAS PHASE CHEMILUMINOUS REACTIONS OF OZONE

Reactants	Total Pressure in Reaction Vessel (microns)	Partial Pressure of Ozone in Absorption Cell (max.) (microns)	Remarks
Trichloroethylene	240 to 340	230	No visible glow
Triethyl Boron	280 to 310	110	Greenish glow - BO_2 bands
Trimethyl Aluminum	260 to 310	125	Whitish glow - continuum and OH bands
Trimethyl Antimony	260 to 310	200	No visible glow

TABLE 16

CHEMILUMINOUS REACTIONS OF OZONE

Reactant	Flow Meter Reading	Intensity	Spectral Feature
Nitric Oxide	20 cm	< 1	Continuum, probably NO_2 bands
Ethylene	28 cm	1	OH band
Trimethyl Aluminum	4 cm	20	Continuum
Triethyl Boron	4 cm	1	BO_2 bands
Diethyl Zinc	6 cm	< 1	OH band and continuum

the mechanism of the chemiluminescent reactions of the sulfur compounds is available, we have studied the variation of the intensity of chemiluminescence (produced during the reaction of COS and H_2S with atomic oxygen) with the variation of their flow rates at 30μ and 100μ pressures. Under similar conditions the intensity variation of the chemiluminescent reactions of NO and C_2H_2 was also recorded. One set of observations taken at 100μ and about 6 seconds resident time is shown in Figure 26. It was found that the relative intensity of chemiluminescence produced in the low pressure system depends on the pressure, flow rate, and the resident time of the gases in the reactor. The observed variation of intensity of chemiluminescence with the flow rate of reactants can be understood if the reaction mechanism is known. However, the reaction mechanisms of the above studied chemiluminescent reactions are still not known. It may be noted that Harteck, et al. [25] have also reported a similar variation of the intensity of chemiluminescence with the flow rate of COS during the low pressure study of its reaction with atomic oxygen.

The chemiluminescent reactions between some organometallic compounds with atomic oxygen were also observed at 100μ and 30μ pressure. Keeping the oxygen and argon flow constant, the intensity variation of the chemiluminescent glow with the flow rate of trimethyl aluminum was observed. It was found that the intensity of the glow at first, rose very rapidly and then attained a maximum, after which a further increase in the flow rate of trimethyl aluminum slowly quenched the chemiluminescence. After an observation of a few minutes it was found that the inlet tubes were coated with a white metallic oxide and the subsequent observations showed decreasing maximum intensity of chemiluminescence. This is probably due to the catalytic recombination of atomic oxygen at the surface coated with metallic oxide. Due to rapid contamination of the low pressure system quantitative information about the chemiluminous efficiencies of different compounds could not be obtained. However, it was found that the chemiluminescent glow produced during the reaction of organometallic compounds with atomic oxygen can be observed to a pressure even as low as 30 microns. Some indication regarding the relative chemiluminous efficiency of the reaction of organometallic compounds can be obtained from Figure 19.

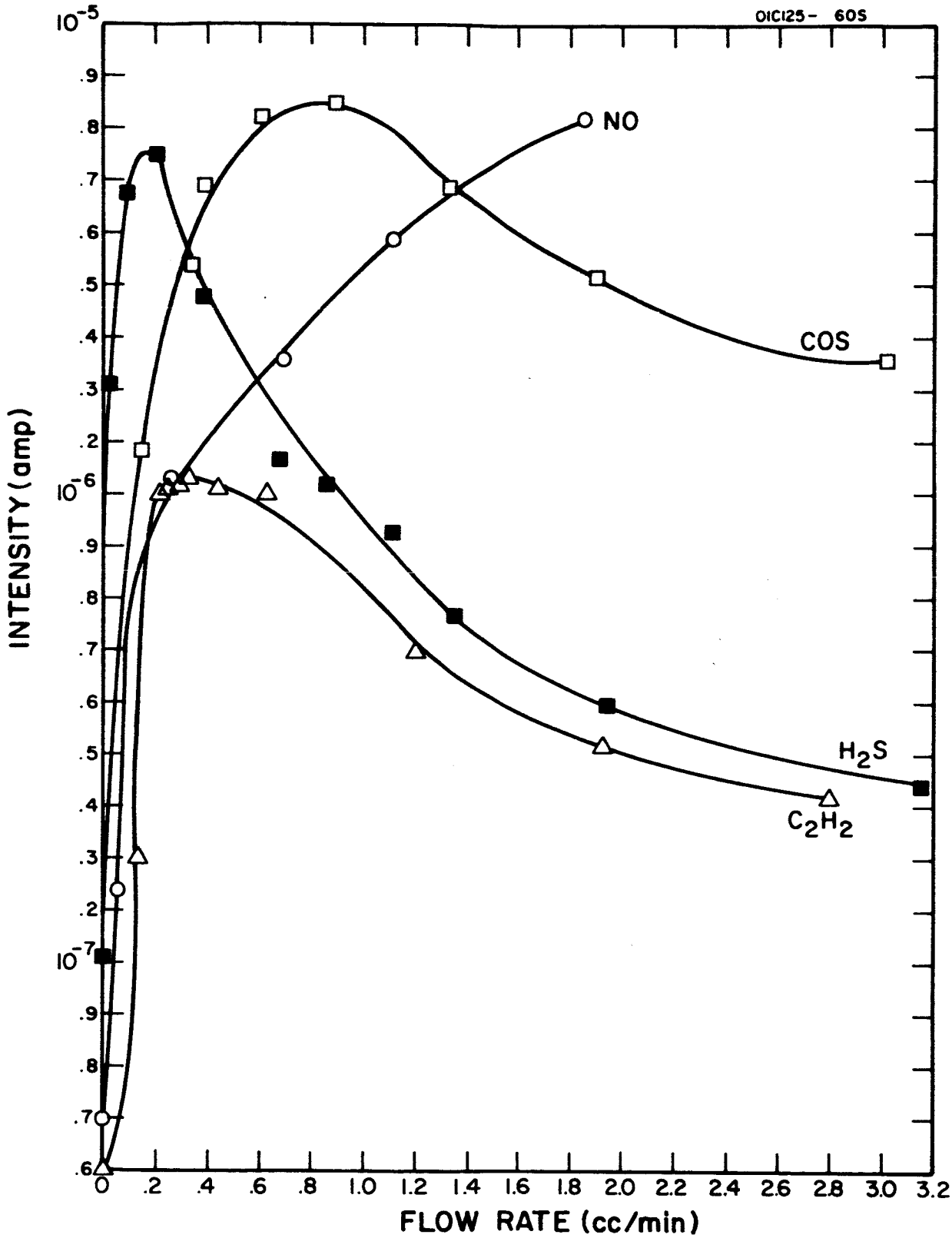

Figure 26. Intensity vs flow rate variation at low pressure.

5. RECOMMENDATIONS

In this section on the basis of work performed under this contract a series of recommendations for further work are made. These in general represent elaborations of the initial survey and also the movement into the field of rocket program representing the fruition of the conceptual studies on innovative atmospheric experiments. The theoretical efforts recommended are of a supportive nature.

Consequently, the following is recommended:

(1) Laboratory studies

(a) A further survey of the chemiluminous reactions and the inter-comparisons of the intensity of chemiluminous reactions between atmospheric constituents, atomic oxygen, ozone, and atomic nitrogen and such specific organo-metallic compounds as trimethyl bismuth, trimethyl phosphorous, dimethyl mercury and diethyl cadmium or similar compounds as available.

(b) Measurements on relative intensities reaction mechanisims, chemical consumption rates of compounds found suitable for chemical release as determined by our previous study. These compounds include (1) trimethyl antimony, (2) triethyl boron, (3) trimethyl aluminum, (4) diethyl zinc or similar compounds as available.

(c) An examination of the method of the measurement of temperature from the study of fluorescence excited in the suitable intermediate formed during the release of above suitable compound. The fluorescence efficiency and the effect of ambient conditions on the observed temperatures will be considered.

(d) Experiments directed toward the measurement by differential spectrophotometry of the ratios of active atmospheric species such as the ratio of atomic oxygen to ozone through their chemiluminescence with nitric oxide and the ratio of atomic oxygen to atomic nitrogen through this chemiluminescence with diethyl zinc.

(e) As back-up to the elucidation of the 6300Å atmospheric emission by release of oxygen into the atmosphere, measurements of the deactivation of $O(^1D)$ by molecular oxygen. Also the charge exchange cross-sections of O^+ with O_2^+ and N_2^+ should be measured.

(2) Theoretical studies

(a) Necessary calculations of Franck-Condon factors and transition probabilities should be made so as to ensure quantitative interpretation of intensity measurements.

(b) There should be analyzed for the selected compounds the governing set of differential equations which determine its optical behavior under atmospheric release.

(c) Theoretical studies should be continued on the analytical techniques necessary for the differential spectrophotometric measurement of ratios of atmospheric active species.

(3) Outline of projected priority rocket experiments

There are suggested here a list of five rocket experiments which it is considered will contribute to our understanding of upper atmospheric physics.

The list of priority experiments given below is only annotated briefly. They have been documented in the main body.

(a) Release of triethyl boron (TEB), a stronger source of luminescence with atomic oxygen.

(b) Release of molecular oxygen to test hypothesis of 6300Å mechanism.

(c) Simultaneous measurement of ratio of two minor constituent, e.g., 0 and 0_3 through differential chemilumenescent spectra. This technique can give us the ratio of two active constituents without the need of knowing the dynamics of expansion.

(d) NO (or other compounds) measurements of atomic oxygen and simultaneous ground measurement of 5577Å. A check on theories of 5577Å emission.

(e) Release of atomic hydrogen into region of hydroxyl emission. A check on theory of the natural hydroxyl emission by preturbing the concentration of atomic hydrogen.

REFERENCES

1. Slipher, V. M., "Emission in the Spectrum of the Light of the Night Sky," Publ. Ast. Soc. Pocif. 41m, 262-263 (1929a).

2. Packer, D. M., Ann. Geophys. 17, 67-74 (1961).

3. Tarasova, T. M., Space Research 3, 162-172, Amsterdam, North Holland Publishing Co. (1963).

4. Wallace, L. and Nidey, R. A., J. Geophys. Res. 69, 471-479.

5. Barbier, D., Compt.-Rend. 245, 1559-1561 (1957).

6. Barbier, D. and Glaime, J., Planetary Space Sci. 9, 133-148 (1962).

7. Barbier, D., Roach and Steiger, J. Res. NBS 66D(1), 145-152 (1962).

8. Carmon, E. H. and Kelfoyle, B. P., J. Geophys. Res. 68, 5605-5607 (1963).

9. Barbier, D., Ann. Geophys. 20, 22-33.

10. Pressman, J., GCA Technical Report No. 62-25-A (1962).

11. Jonathan, N. and Doherty, G., NASA Contractor Report No. NASA CR-67 (1964), GCA Technical Report No. 63-1-N (1963).

12. Jonathan, N. and Warneck, P., "Continuation of the Laboratory Chemiluminescent Experiments for Ballistic Missile Defense," GCA Technical Rpt. No. 64-12-A (1964).

13. Kiess, N. H. and Broida, H. P., Seventh Symposium on Combustion, p.217, (Butterworth, London) (1959).

14. Jennings, K. R. and Linnet, J. W., Trans. Faraday Soc. 56, 1737 (1960).

15. Barnes, R. H., Jung, R. G., Kircher, J. R., Ritzman, R. L., Smith, J. C. and Stenginsky, B., Battelle Memorial Institute Technical Report No. BMI-197-10-2 (1964).

16. Bernanose, A. J. and Rene, M. G., Ozone Chemistry and Technology: Advances in Chemistry Series 21, American Chemical Society, Washington (1959).

17. Stair, R., Schneider, W. E. and Jackson, J. K., Applied Optics 2, 1151 (1963).

18. Cook, G. A., Kiffer, A. D., Klumpp, C. V., Malik, A. H. and Spence, L. A., Ozone Chemistry and Technology Advances in Chemistry Series 21, p.44, American Chemical Society, Washington (1959).

19. Sharma, A. and Padur, J. P., GCA Technical Report No. 65-20-N (1965).

20. Sharma, A. and Padur, J. P., GCA Technical Report No. 65-19-N (1965).

21. Sharma, A., Padur, J. P. and Warneck, P., J. Chem. Phys. (1965).

22. Sharma, A. and Padur, J. P., GCA Technical Report No. 65-17-N (1965).

23. Pannetier, G., Goudmand, P., Dessaux, O. and Tavernier, N., Compt. Rend. 255, 91 (1962).

24. Benson, S. W., The Foundations of Chemical Kinetics, McGraw-Hill Book Co., New York (1960).

25. Harteck, P., Reeves, R. R., Jr. and Albers, E. W., Final Report of the Department of Chemistry, Rensselaer Polytechnic Institute, Troy, N. Y., Contract No. AF19(604)-6128 (1964).

APPENDIX A

RESUMÉ OF THE MATHEMATICAL DEVELOPMENT SPECIFIED IN THE "SNOW-PLOW" AND "INTERPENETRABILITY" MODELS FOR THE 6300Å PERTURBATION ROCKET EXPERIMENT

Preliminary Remarks

The following account is a brief resumé of the mathematical procedures followed in obtaining integral and explicit representations of the concentration field functions encountered in the "snowplow" and "interpenetrability" models.

The reader is referred to the discussion in the main body of this report for an explanation of the physico-chemical setting and motivation for the "snowplow" and "interpenetrability" models. Further, the reader is referred to the GCA internal report, "A Mathematical Study of the Mechanism of 6300Å Airglow due to Rocket Chemical Release of Molecular Oxygen between 250 - 300 km," by H. K. Brown and J. Pressman, for an account of the application of the formulas (derived in the resolution procedure) to nighttime releases in the Earth's upper atmosphere in order to obtain numerical values of the transient concentration fields associated with the red-line (6300Å) airglow (of the excited oxygen atoms).

Finally, in the account presented below, the outline of the presentation, the order in which the various topics are discussed, follows that of the cited GCA report. In this manner the reader can grasp readily the scope of the mathematical procedure used at any particular stage and if (full) detail is desired, he can easily refer back to the particular portion of the cited report.

With these preliminary remarks and words of explanation in mind, the reader can allow for (the omission of) the mathematical developments associated with the sequence of topics presented in the following sections.

A-1. THE "SNOWPLOW" MODEL WITH $\epsilon=0$; $[O^*(P, +0)] = 0$

A.1.1 Specification of "Snowplow" Model with $\epsilon=0$ and Outline of Iterative Procedure to Resolve System of Boundary Value Problems

A.1.1.1 Reactions and equations of continuity. Corresponding to the set of reaction equations

$$O_2 + O^+ \overset{k_1}{\rightarrow} O_2^+ + O \quad ,$$

$$O_2^+ + e \overset{k_2}{\rightarrow} O^* + O \quad ,$$

$$O^* \overset{k_3}{\rightarrow} h\nu + O \quad ,$$

is the following complete set of continuity equations:

$$\frac{\partial}{\partial t}[O_2] = \bar{\nabla} \cdot D_1 \bar{\nabla}[O_2] - k_1[O_2][O^+] \quad ,$$

$$\frac{\partial}{\partial t}[O^+] = \bar{\nabla} \cdot D_2 \bar{\nabla}[O^+] - k_1[O_2][O^+] \quad ,$$

$$\frac{\partial}{\partial t}[O_2^+] = \bar{\nabla} \cdot D_3 \bar{\nabla}[O_2^+] + k_1[O_2][O^+] - k_2[O_2^+][e] \quad ,$$

$$\frac{\partial}{\partial t}[e] = \bar{\nabla} \cdot D_4 \bar{\nabla}[e] - k_2[O_2^+][e] \quad ,$$

$$\frac{\partial}{\partial t}[O^*] = \bar{\nabla} \cdot D_5 \bar{\nabla}[O^*] + k_2[O_2^+][e] - k_3[O^*] \quad ,$$

in the concentration functions $[O_2] = [O_2(P,t)]$, $[O^+] = [O^+(P,t)]$, $[O_2^+] = [O_2^+(P,t)]$, $[e] = [e(P,t)]$, and $[O^*] = [O^*(P,t)]$, where $P:(x,y,z)$ is a point in the infinite space $R(P): -\infty < x < \infty$, $-\infty < y < \infty$, $-\infty < z < \infty$.

It is assumed that particles with electric charge, that is, $[O^+]$, $[O_2^+]$, and $[e]$, are transported by diffusion in vertical lines (following the magnetic lines of the Earth) while the particles without electric charge, that is, $[O_2]$ and $[O^*]$, are transported by diffusion along spherically symmetric radial lines issuing from the origin x=0, y=0, and z=0.

It is assumed that the diffusion coefficients $D_1, D_2, \ldots, D_5$ are all equal to the constant D.

Under these circumstances the complete set of continuity equations listed above is replaced by the following:

$$\frac{\partial}{\partial t}[O_2] = D\,\nabla^2[O_2] - k_1[O_2][O^+] \quad ,$$

$$\frac{\partial}{\partial t}[O^+] = D\frac{\partial^2}{\partial z^2}[O^+] - k_1[O_2][O^+] \quad ,$$

$$\frac{\partial}{\partial t}[O_2^+] = D\,\frac{\partial^2}{\partial z^2}[O_2^+] + k_1[O_2][O^+] - k_2[O_2^+][e] \quad ,$$

$$\frac{\partial}{\partial t}[e] = D\,\frac{\partial^2}{\partial z^2}[e] - k_2[O_2^+][e] \quad ,$$

$$\frac{\partial}{\partial t}[O^*] = D\,\nabla^2[O^*] + k_2[O_2^+][e] - k_3[O^*] \quad .$$

The Laplacian operator $\nabla^2(\ )$ in these equations has the axial symmetric form, in the coordinates $\xi = \sqrt{x^2 + y^2}$ and z, displayed below:

$$\nabla^2(\ ) = \frac{1}{\xi}\frac{\partial}{\partial \xi}\left(\xi\,\frac{\partial}{\partial \xi}(\ )\right) + \frac{\partial^2}{\partial z^2}(\ )$$

when $[O_2] = [O_2(P,t)]$ and $[O^*] = [O^*(P,t)]$ are considered as functions of ξ and z.

Under those circumstances where the functions $[O_2] = [O_2(P,t)]$ and $[O^*] = [O^*(P,t)]$ are considered to be spherically point symmetric in $r = \sqrt{x^2 + y^2 + z^2} = \sqrt{\xi^2 + z^2}$, then the spherically point symmetric form of the Laplacian operator $\nabla^2(\ )$ can be used:

$$\nabla^2(\ ) = \frac{1}{r^2}\frac{\partial}{\partial r}\left(r^2 \frac{\partial}{\partial r}(\ )\right) \quad .$$

A.1.1.2 Conservation of electric charge: $[e] = [O_2^+] + [O^+]$. At the point $P:(x,y,z)$ in $R(P): -\infty < x < \infty$, $-\infty < y < \infty$, $-\infty < z < \infty$, at all times $t > 0$, it is required that concentration field functions $[O_2^+] = [O_2^+(P,t)]$, $[e] = [e(P,t)]$, and $[O^+] = [O^+(P,t)]$ satisfy the conservation of electric charge law:

$$[O_2^+] \equiv [e] - [O^+] \quad ;$$

in particular at the boundary of R(P) it is required that

$$[O_2^+(\infty)] = [e(\infty)] - [O^+(\infty)] \quad .$$

A.1.1.3 Specification of initial configuration of concentration fields. The charged particles $[O^+]$, $[O_2^+]$, and $[e]$ are assumed to have an inverted Gaussian distribution in all space at the instant $t = +0$ when the molecular oxygen particles are released into free space with a Gaussian configuration:

$$[O_2(P,+0)] = [O_2(0)] \exp\left(-\frac{r^2}{h^2}\right) ,$$

$$[O^+(P,+0)] = [O^+(\infty)]\left[1 - \exp\left(-\frac{r^2}{h^2}\right)\right] ,$$

$$[O_2^+(P,+0)] = [O_2^+(\infty)]\left[1 - \exp\left(-\frac{r^2}{h^2}\right)\right] ,$$

$$[e(P,+0)] = [e(\infty)]\left[1 - \exp\left(-\frac{r^2}{h^2}\right)\right] ,$$

wherein

$$r^2 = x^2 + y^2 + z^2 = \xi^2 + z^2 , \quad \xi^2 = x^2 + y^2 .$$

The constant h is some appropriate Gaussian halfwidth.

The symbols $[O^+(\infty)]$, $[O_2^+(\infty)]$, and $[e(\infty)]$ designate the corresponding steady state values of the concentration fields $[O^+]$, $[O_2^+]$, and $[e]$ at the boundary of the space region R(P): $-\infty < x < \infty$, $-\infty < y < \infty$, and $-\infty < z < \infty$.

The symbol $[O_2(0)]$ designates the center-point value of the concentration field $[O_2(P,t)]$ at the instant $t = +0$.

The concentration field $[O^*] = [O^*(P,t)]$ is assumed to be null at the time $t = +0$:

$$[O^*(P,+0)] = 0 .$$

These assumptions regarding the initial configurations of the concentration fields $[O^+]$, $[O_2^+]$, and $[e]$ specify that the instantaneous

release of the molecular oxygen particles has had a "snowplow" effect in the ambient atmosphere in the 250 to 300 kilometer region.

Under the action of diffusion and the chemical reaction the initial Gaussian configuration of the molecular oxygen concentration field $[O_2]$ is changed into a transient axial symmetric field which evanesces in time.

The excited oxygen atoms, O^*, are generated by the O_2^+, e reaction and are destroyed by the airglow mechanism.

In time the transient fields, induced by the injected molecular oxygen, die out leaving the steady state ambient concentration fields.

A.1.1.4 Outline of iterative procedure to solve system of boundary value problems. It is proposed to find appropriate representations of the concentration field functions $[O_2]$, $[O^+]$, $[O_2^+]$, $[e]$, and $[O^*]$ by a suitably convergent iterative procedure.*

Consider the following preliminary remarks:

Let a sequence of functions:

$$[O_2^{(0)}],[O_2^{(1)}],[O_2^{(2)}],[O_2^{(3)}], \ldots , [O_2^{(i)}],[O_2^{(i+1)}], \ldots ,$$

$$[O^{+(0)}],[O^{+(1)}],[O^{2(2)}],[O^{+(3)}], \ldots , [O^{+(i)}],[O^{+(i+1)}], \ldots ,$$

$$[O_2^{+(0)}],[O_2^{+(1)}],[O_2^{+(2)}],[O_2^{+(3)}], \ldots , [O_2^{+(i)}],[O_2^{+(i+1)}], \ldots ,$$

*See Hildebrand, F. B., Advanced Calculus for Engineers, Prentice-Hall, New York, 1949, pp.218-224.

$$[e^{(0)}],[e^{(1)}],[e^{(2)}],[e^{(3)}], \ \ldots \ ,[e^{(i)}],[e^{(i+1)}], \ \ldots \quad ,$$

$$[O^{*(0)}],[O^{*(1)}],[O^{*(2)}],[O^{*(3)}], \ \ldots \ , \ [O^{*(i)}],[O^{*(i+1)}], \ \ldots$$

be introduced corresponding, respectively, to the concentration field functions

$$[O_2(P,t)],[O^{+}(P,t)],[O_2^{+}(P,t)],[e(P,t)], \text{ and } [O^{*}(P,t)] \quad .$$

Let it be assumed that the initial configurations correspond to the zero-order approximation of the concentration field functions:

$$[O_2^{(0)}] \equiv [O_2(P,+0)] \equiv [O_2(0)] \exp\left(-\frac{r^2}{h^2}\right) \quad ,$$

$$[O^{+(0)}] \equiv [O^{+}(P,+0)] \equiv [O^{+}(\infty)]\left[1 - \exp\left(-\frac{r^2}{h^2}\right)\right] \quad ,$$

$$[O_2^{+(0)}] \equiv [O_2^{+}(P,+0)] \equiv [O_2^{+}(\infty)]\left[1 - \exp\left(-\frac{r^2}{h^2}\right)\right] \quad ,$$

$$[e^{(0)}] \equiv [e(P,+0] \equiv [e(\infty)]\left[1 - \exp\left(-\frac{r^2}{h^2}\right)\right] \quad ,$$

$$[O^{*(0)}] \equiv [O^{*}(P,+0)] = 0 \quad .$$

Corresponding to the i^{-th} iterative functions $[O_2^{(i)}],[O^{+(i)}]$, $[O_2^{+(i)}],[e^{(i)}]$, and $[O^{*(i)}]$, for i=1,2,3, ... , are the equations of continuity displayed below:

$$\frac{\partial}{\partial t}[O_2^{(i)}] = D\,\nabla^2[O_2^{(i)}] - k_1[O_2^{(i-1)}][O^{+(i-1)}] \quad ,$$

$$\frac{\partial}{\partial t}[O^{+(i)}] = D\,\frac{\partial^2}{\partial z^2}[O^{+(i)}] - k_1[O_2^{(i-1)}][O^{+(i-1)}] \quad ,$$

$$\frac{\partial}{\partial t}[O_2^{+(i)}] = D \frac{\partial^2}{\partial z^2}[O_2^{+(i)}] - k_1[O_2^{(i-1)}][O^{+(i-1)}] ,$$

$$- k_2[O_2^{+(i-1)}][e^{(i-1)}] ,$$

$$\frac{\partial}{\partial t}[e^{(i)}] = D \frac{\partial^2}{\partial z^2}[e^{(i)}] - k_2[O_2^{+(i-1)}][e^{(i-1)}] ,$$

$$\frac{\partial}{\partial t}[O^{*(i)}] = D \nabla^2[O^{*(i)}] + k_2[O_2^{+(i-1)}][e^{(i-1)}] - k_3[O^{*(i)}] .$$

It is evident that the integrating factor $\exp(k_3 t)$ can be used to rewrite the last equation in $[O^{*(i)}]$ in the form:

$$\frac{\partial}{\partial t}(\exp(k_3 t)\ [O^{*(i)}]) = D \nabla^2 (\exp(k_3 t)\ [O^{*(i)}])$$

$$+ k_2 \exp(k_3 t)\ [O_2^{+(i-1)}][e^{(i-1)}] .$$

A.1.1.5 The boundary value problems associated with the i^{-th} approximation i=1,2,3, ... It is seen that if the function U = U(P,t) is used to represent any one of the charged particle concentration field functions $[O^{+(i)}] \equiv [O^{+(i)}(P,t)]$, $[O_2^{+(i)}] \equiv [O_2^{+(i)}(P,t)]$, and $[e^{(i)}] \equiv [e^{(i)}(P,t)]$, i = 1,2,3, ... , and if the function V = V(P,t) is used to represent either of the neutral particle concentration field functions $[O_2^{(i)}] \equiv [O_2^{(i)}(P,t)]$ and $\exp(k_3 t)\ [O^{*(i)}] \equiv [O^{*(i)}(P,t)] \exp(k_3 t)$, i = 1,2,3, ... , then the array of i^{-th} iterative equations of continuity can be represented by the following pair of nonhomogeneous partial differential equations in U = U(P,t) and V = V(P,t):

$$L_1(U) \equiv \frac{\partial}{\partial t} U - D \frac{\partial^2}{\partial z^2} U = u \quad , \quad u = u(P,t) \quad ,$$

and

$$L_3(V) \equiv \frac{\partial}{\partial t} V - D \nabla^2 V = v \quad , \quad v = v(P,t) \quad .$$

At the instant $t = +0$ the function $U = U(P,t)$ has the representation

$$U(P,+0) = U(\infty)\left[1 - \exp\left(-\frac{r^2}{h^2}\right)\right], \quad r^2 = x^2 + y^2 + z^2 = \xi^2 + z^2$$

while the function $V = V(P,t)$ has the representation

$$V(P,+0) = \epsilon\, V(0) \exp\left(-\frac{r^2}{h^2}\right) \quad ,$$

where $\epsilon \equiv 1$ for $V(P,t) \equiv [O_2^{(i)}(P,t)]$, $i = 1,2,3, \ldots$,

and $\epsilon \equiv 0$ for $V(P,t) \equiv \exp(k_3 t)[O^{*(i)}(P,t)]$, $i = 1,2,3, \ldots$.

The functions $u = u(P,t)$ and $v = v(P,t)$ are made up of linear combinations of products of the i^{-th} iterative functions $i = 1,2,3, \ldots$.

A.1.1.6 The Green's functions procedure for obtaining representations of the i^{-th} approximation functions. The Green's functions $G_1 = G_1(z,z';t,\tau)$ and $G_3 = G_3(P,P';t,\tau)$, defined below, can be used to set down Green's function integral formula representations of the functions $U = U(P,t)$ and $V = V(P,t)$, respectively.

In particular, the function $U = U(P,t)$ which satisfies the boundary value problem in $U = U(P,t)$:

$$L_1(U) = u, \quad U(P,t) \to U(P,+0) \quad \text{when } t \to +0 \ ,$$
$$U(P,t) \to U(\infty) \quad \text{when } P:(x,y,z) \to \infty \ ,$$

is defined by the following integral formula:

$$U(P,t) = \int_{-\infty}^{+\infty} U(P\ (x,y,z'),+0)\ G_1(z,z';t,0)\ dz'$$
$$+ \int_0^t d\tau \int_{-\infty}^{+\infty} u(P\ (x,y,z')\ \tau)\ G_1(z,z';t,\tau)\ dz' \ .$$

Further, the function $V = V(P,t)$ which satisfies the boundary value problem in $V = V(P,t)$:

$$L_3(V) = v, \quad V(P,t) \to V(P,+0) \quad \text{when } t \to +0 \ ,$$
$$V(P,t) \to 0 \quad \text{when } P:(x,y,z) \to \infty \ ,$$

is defined by the following integral formula:

$$V(P,t) = \int_0^{\infty} 4\pi r'^2\ V(P\ (r,r'),+0)\ G_3^{(1)}(r,r';t,0)\ dr'$$
$$+ \int_0^t d\tau \int_0^{\infty} 4\pi r'^2\ v(P\ (r,r'),\tau)\ G_3^{(1)}(r,r';t,\tau)\ dr' \ ,$$

otherwise,

$$V(P,t) = \int_0^\infty 4\pi r'^2\, V(P\ (r,r'),+0)\ G_3^{(1)}(r,r';t,0)\ dr'$$

$$+ \int_0^t d\tau \int_{-\infty}^{\infty} dz' \int_0^\infty 2\pi\ \xi' d\xi'\ v(P\ (\xi',z'),\tau)\ G_3^{(2)}(P,P';t,\tau) \quad .$$

The Green's functions $G_1(z,z';t,\tau)$ and $G_3(P,P';t,\tau)$ are defined as follows:

$$G_1(z,z';t,\tau) \equiv \frac{1}{2\sqrt{\pi D(t-\tau)}} \exp\left(-\frac{z^2+z'^2}{4D(t-\tau)}\right) \cosh\left(\frac{zz'}{2D(t-\tau)}\right) \quad ,$$

$$G_2(\xi,\xi';t,\tau) \equiv \frac{1}{4\pi D(t-\tau)} \exp\left(-\frac{\xi^2+\xi'^2}{4D(t-\tau)}\right) I_o\left(\frac{\xi\xi'}{2D(t-\tau)}\right) \quad ,$$

$$G_3(r,r';t,\tau) \equiv \frac{1}{4\pi rr'\sqrt{\pi D(t-\tau)}} \exp\left(\frac{r^2+r'^2}{4D(t-\tau)}\right) \sinh\left(\frac{rr'}{2D(t-\tau)}\right) \quad ,$$

with

$$G_3^{(1)}(r,r';t,\tau) \equiv G_3(r,r';t,\tau) \quad , \quad r^2 = x^2 + y^2 + z^2 = \xi^2 + z^2 \quad ,$$

$$G_3^{(2)}(P,P';t,\tau) \equiv G_1(z,z';t,\tau)\ G_2(\xi,\xi';t,\tau) \quad .$$

A.1.1.7 Specification of first approximation system of boundary value problems in $[O_2^{(1)}]$, $[O^{+(1)}]$, $[e^{(1)}]$, and $[O^{*(1)}]$. According to the iterative scheme outlined above, the concentration field functions $[O_2^{(1)}]$, $[O^{+(1)}]$, $[O_2^{+(1)}]$, $[e^{(1)}]$, and $[O^{*(1)}]$ are first order approximations to the corresponding concentration field functions $[O_2]$, $[O_2^+]$, $[e]$, and $[O^*]$.

The first order functions $[O_2^{(1)}] = [O_2^{(1)}(P,t)]$, $[O^{+(1)}] = [O^{+(1)}(P,t)]$, $[e^{(1)}] = [e^{(1)}P[,t)]$, and $[O^{*(1)}] = [O^{*(1)}(P,t)]$ are defined by the following array of initial value problems:

$$L_3([O_2^{(1)}]) \equiv \frac{\partial}{\partial t}[O_2^{(1)}] - D\frac{1}{r^2}\frac{\partial}{\partial r}\left(r^2\frac{\partial}{\partial r}[O_2^{(1)}]\right) = -k_1[O_2^{(0)}][O^{+(0)}] \quad ,$$

with

$$[O_2^{(0)}] \equiv [O_2(0)]\exp\left(-\frac{r^2}{h^2}\right) \equiv [O_2(P,+0] \quad ,$$

$$[O^{+(0)}] \equiv [O^+(\infty)]\left[1 - \exp\left(-\frac{r^2}{h^2}\right)\right] \equiv [O^+(P,+0)] \quad ,$$

and

$$[O_2^{(1)}]_{t=+0} \equiv [O_2^{(1)}(r,+0)] = [O_2(0)]\exp\left(-\frac{r^2}{h^2}\right) \quad ;$$

$$L_1([O^{+(1)}]) \equiv \frac{\partial}{\partial T}[O^{+(1)}] - D\frac{\partial^2}{\partial z^2}[O^{+(1)}] = -k_1[O_2^{(0)}][O^{+(0)}] \quad ,$$

with

$$k_1[O_2^{(0)}][O^{+(0)}] \equiv k_1[O_2(0)][O^+(\infty)]\left[\exp\left(-\frac{r^2}{h^2}\right) - \exp\left(-\frac{2r^2}{h^2}\right)\right] ,$$

and

$$[O^{+(1)}]_{t=+0)} = [O^{+(1)}(P,+0)] = [O^+(\infty)]\left[1 - \exp\left(-\frac{r^2}{h^2}\right)\right] \quad ,$$

with

$$r^2 = \xi^2 + z^2$$

so that

$$\exp\left(-\frac{r^2}{h^2}\right) \equiv \exp\left(-\frac{\xi^2}{h^2}\right)\exp\left(-\frac{z^2}{h^2}\right) \quad ;$$

$$L_1([e^{(1)}]) \equiv \frac{\partial}{\partial t}[e^{(1)}] - D\frac{\partial^2}{\partial z^2}[e^{(1)}] = -k_2[e^{(0)}][O_2^{+(0)}] \quad ,$$

with

$$[e^{(0)}] \equiv [e(\infty)]\left[1 - \exp\left(-\frac{\xi^2}{h^2}\right)\exp\left(-\frac{z^2}{h^2}\right)\right]$$

$$\equiv [e(P,+0] \quad ,$$

$$[O_2^{+(0)}] \equiv [O_2^{+}(\infty)]\left[1 - \exp\left(-\frac{\xi^2}{h^2}\right)\exp\left(-\frac{z^2}{h^2}\right)\right]$$

$$\equiv [O_2^{+}(P,+0)] \quad ,$$

and

$$[e^{(1)}]_{t=+0} \equiv [e^{(1)}(P,+0)] = [e(P,+0)] \quad ;$$

and

$$L_3([O^{*(1)}]) \equiv \frac{\partial}{\partial t}[O^{*(1)}] - D\frac{1}{r^2}\frac{\partial}{\partial r}\left(r^2\frac{\partial}{\partial r}[O^{*(1)}]\right) = -k_3[O^{*(1)}]$$

$$+ k_2[O_2^{+(0)}][e^{(0)}]$$

or else

$$L_3\{\exp(k_3t)[O^{*(1)}]\} \equiv \frac{\partial}{\partial t}\{e(k_3t)[O^{*(1)}]\} - D\frac{1}{r^2}\left[r^2\frac{\partial}{\partial r}\{\exp(k_3t)[O^{*(1)}]\}\right] = k_2\exp(k_3t)[O_2^{+(0)}][e^{(0)}] \quad ,$$

with

$$[O_2^{+(0)}] \equiv [O_2^{+}(P,+0)] \equiv [O_2^{+}(\infty)]\left[1 - \exp\left(-\frac{r^2}{h^2}\right)\right] \quad ,$$

$$[e^{(0)}] \equiv [e(P,+0)] \equiv [e(\infty)]\left[1 - \exp\left(-\frac{r^2}{h^2}\right)\right] \quad ,$$

and

$$\{\exp(k_3t)[O^{*(1)}]\}_{t=+0} = [O^{*(1)}(P,+0)] = 0 \quad .$$

These initial value problems in $[O_2^{(1)}]$, $[O^{+(1)}]$, $[e^{(1)}]$, and $[O^{*(1)}]$ are resolved by Green's function techniques in the discussion to follow.

A.1.2 Resolution of the Boundary Value Problem in $[O_2^{(1)}]$ and Properties of $[O_2^{(1)}(O,z,t)]$.

A.1.2.1 Green's function integral formula for $[O_2^{(1)}] = V_1(r,t) + V_2(r,t)$. Reference is made to the partial differential equation

$$\frac{\partial}{\partial t}[O_2^{(1)}] = D\frac{1}{r^2}\frac{\partial}{\partial r}\left(r^2\frac{\partial}{\partial r}[O_2^{(1)}]\right) - k_1[O_2^{(0)}][O^{+(0)}] \quad ,$$

where

$$k_1[O_2^{(0)}][O^{+(0)}] = k_1[O_2(0)][O^{+}(\infty)]\left[\exp\left(-\frac{r^2}{h^2}\right) - \exp\left(-\frac{2r^2}{h^2}\right)\right]$$

with the initial condition

$$[O_2^{(1)}]_{t=+0} = [O_2(P,+0)] = [O_2(0)] \exp\left(-\frac{r^2}{h^2}\right) .$$

The spherically point symmetric Green's function $G_3(r,r';t,\tau)$,

$$G_3(r,r';t,\tau) = \frac{1}{4\pi rr' \sqrt{\pi D(t-\tau)}} \exp\left(-\frac{r^2 + r'^2}{}\right) \sinh\left(\frac{rr'}{2D(t-\tau)}\right) ,$$

can be used to define a function $[O_2^{(1)}(P,t)] = V_1(r,t) + V_2(r,t)$

which resolves the initial value problem in $[O_2^{(1)}] = [O_2^{(1)}(P,t)]$.

A.1.2.2 Explicit formulas for $[O_2^{(1)}(P,t)]$, $V_1(r,t)$, $V_2^{(1)}(r,t)$, and $V_2^{(2)}(r,t)$. It can be demonstrated that the concentration field function $[O_2^{(1)}(P,t)]$ can be represented by the explicit formula displayed below:

$$[O_2^{(1)}(P,t)] = [O_2(0)]\left(\frac{h}{T_1}\right)^3 \exp\left[-\left(\frac{r}{T_1}\right)^2\right]$$

$$- k_1[O_2(0)][O^+(\infty)] \frac{\sqrt{\pi}h^3}{4rD} \left\{\left[\operatorname{erf}\left(\frac{r}{h}\right) - \operatorname{erf}\left(\frac{r}{T_1}\right)\right]\right.$$

$$\left. - \frac{1}{2\sqrt{2}}\left[\operatorname{erf}\left(\frac{\sqrt{2}r}{h}\right) - \operatorname{erf}\left(\frac{\sqrt{2}r}{T_2}\right)\right]\right\} .$$

In deriving this formula for $[O_2^{(1)}(P,t)]$ the following reduced integral Green's function formulas were obtained:

$$V_1(r,t) = [O_2(0)] \int_0^\infty 4\pi r'^2 \exp\left(-\frac{r'^2}{h^2}\right) G_3(r,r';t,0)dr' \quad ,$$

$$= [O_2(0)] \left(\frac{h}{T_1}\right)^3 \exp\left(-\frac{r^2}{T_1^2}\right) \quad ;$$

$$V_2^{(1)}(r,t) \equiv -k_1[O_2(0)][O^+(\infty)] \int_0^t dt' \int_0^\infty 4\pi r'^2 \exp\left(-\frac{r'^2}{h^2}\right) G_3(r,r';t,t'')dr',$$

$$\equiv -k_1[O_2(0)][O^+(\infty)] \int_0^t \left(\frac{h}{T_1'}\right)^3 \exp\left(-\frac{r^2}{T_1'^2}\right) dt' \quad ,$$

$$\equiv -k_1[O^+(\infty)] \int_0^t V_1(r,t')\, dt' \quad ,$$

$$\equiv -k_1[O_2(0)][O^+(\infty)] \left(\frac{\sqrt{\pi}h^3}{4rD}\right)\left[\mathrm{erf}\left(\frac{r}{h}\right) - \mathrm{erf}\left(\frac{r}{T_1}\right)\right] \quad ;$$

$$V_2^{(2)}(r,t) \equiv k_1[O_2(0)][O^+(\infty)] \int_0^t dt' \int_0^\infty 4\pi r'^2 \exp\left(\frac{2r'^2}{h^2}\right) G_3(r,r';t,t'')dt',$$

$$\equiv k_1[O_2(0)][O^+(\infty)] \int_0^t \left(\frac{h}{T_2'}\right)^3 \exp\left(-\frac{2r^2}{T_2'^2}\right) dt' \quad ,$$

$$\equiv k_1[O_2(0)][O^+(\infty)] \left(\frac{\sqrt{\pi}h^3}{4rD}\right) \frac{1}{2\sqrt{2}} \left[\mathrm{erf}\left(\frac{\sqrt{2}r}{h}\right) - \mathrm{erf}\left(\frac{\sqrt{2}r}{T_2}\right)\right] \quad .$$

A.1.2.3 The function $[O_2^{(1)}(0,z,t)]$. For points along the vertical z axis one has $\xi = \sqrt{x^2 + y^2} = 0$ and $r = \sqrt{\xi^2 + z^2} = z$ for $z > 0$ and $r = -|z|$ for $z < 0$.

The concentration field function $[O_2^{(1)}(P,t)]$ for points on the vertical z axis, $\xi = 0$, can be designated as $[O_2^{(1)}(0,z,t)]$ and is defined by the rational formula displayed below:

$$[O_2^{(1)}(0,z,t)] = [O_2(0)]\left(\frac{h}{T_1}\right)^3 \exp\left(-\frac{z^2}{T_1^2}\right) - k_1[O_2(0)][O^+(\infty)]\left(\frac{\sqrt{\pi}h^3}{4D}\right)\left\{\left(\frac{\operatorname{erf}\left(\frac{z}{h}\right) - \operatorname{erf}\left(\frac{z}{T_1}\right)}{z}\right.\right.$$
$$\left.\left. - \frac{1}{2\sqrt{2}}\left(\frac{\operatorname{erf}\left(\frac{\sqrt{2}z}{h}\right) - \operatorname{erf}\left(\frac{\sqrt{2}z}{T_2}\right)}{z}\right)\right\} .$$

At the origin $\xi = 0$, $z = 0$, it is seen that the center-point value of the concentration field function $[O_2^{(1)}]$, designated by $[O_2^{(1)}(0,0,t)]$, is defined by the expression in the right-hand side of the above equation for $[O_2^{(1)}(o,z,t)]$ when $z \to 0$. Since $\operatorname{erf}(0) = 0$ it is seen that the indeterminate form $\frac{0}{0}$ appears in this specification of $[O_2^{(1)}(0,0,t)]$ with $z \to 0$.

A.1.2.4 The center-point value function $[O_2^{(1)}(0,0,t)]$. By reference to l'Hospital's rule it is seen that

$$\left.\frac{\operatorname{erf}\left(\frac{z}{h}\right) - \operatorname{erf}\left(\frac{z}{T_1}\right)}{z}\right]_{z \to 0} = \left.\frac{\frac{2}{\sqrt{\pi}}\frac{1}{h}\exp\left(-\frac{z^2}{h^2}\right) - \frac{2}{\sqrt{\pi}}\frac{1}{T_1}\exp\left(-\frac{z^2}{T_1^2}\right)}{1}\right]_{z \to 0}$$
$$= \frac{2}{\sqrt{\pi}}\left(\frac{1}{h} - \frac{1}{T_1}\right) ,$$

and

$$\left.\frac{\operatorname{erf}\left(\frac{\sqrt{2}z}{h}\right) - \operatorname{erf}\left(\frac{\sqrt{2}z}{T_2}\right)}{z}\right]_{z \to 0} = \frac{2\sqrt{2}}{\sqrt{\pi}}\left(\frac{1}{h} - \frac{1}{T_2}\right) \quad .$$

Accordingly, at the origin $\xi = 0$, $z = 0$, $r = 0$, the concentration field function $[O_2^{(1)}(P,t)]$ has the center-point value $[O_2^{(1)}(0,0,t)]$ defined by the following formula:

$$[O_2^{(1)}(0,0,t)] = [O_2(0)]\left(\frac{h}{T_1}\right)^3 - \left(\frac{k_1 h^2}{4D}\right)[O_2(0)][O^+(\infty)]\left(\frac{h}{T_2} - \frac{2h}{T_1} + 1\right),$$

where

$$T_1 = \sqrt{h^2 + 4Dt} \quad \text{and} \quad T_2 = \sqrt{h^2 + 8Dt} \quad .$$

A.1.3 Resolution of the Boundary Value Problem in $[O^{+(1)}]$ and Properties of $[O^{+(1)}(0,z,t)]$.

A.1.3.1 Green's function integral formula for $[O^{+(1)}] = U_1(P,t) + U_2(P,t)$. Reference is made to the partial differential equation

$$\frac{\partial}{\partial t}[O^{+(1)}] = D\frac{\partial^2}{\partial z^2}[O^{+(1)}] - k_1[O_2^{(0)}][O^{+(0)}] \quad ,$$

where

$$k_1[O_2^{(0)}][O^{+(0)}] = k_1[O_2(0)][O^+(\infty)]\exp\left(-\frac{\xi^2}{h^2}\right)\left[\exp\left(-\frac{z^2}{h^2}\right)\right.$$

$$\left. - \exp\left(-\frac{\xi^2}{h^2}\right)\exp\left(-\frac{2z^2}{h^2}\right)\right] \quad ,$$

with the initial condition

$$[O^{+(1)}]_{t=+0} = [O^{+}(\infty)]\left[1 - \exp\left(-\frac{\xi^2}{h^2}\right)\exp\left(-\frac{z^2}{h^2}\right)\right] .$$

The one-dimensional Cartesian Green's function $G_1(z,z';t,\tau)$,

$$G_1(z,z';t,\tau) = \frac{1}{2\sqrt{\pi D(t-\tau)}}\exp\left(-\frac{z^2+z'^2}{4D(t-\tau)}\right)\cosh\left(\frac{zz'}{2D(t-\tau)}\right) ,$$

can be used to define a function $[O^{+(1)}(P,t)]$ in the form

$$[O^{+(1)}(P,t)] = U_1(P,t) + U_2(P,t)$$

which resolves the initial value problem in $[O^{+(1)}(P,t)]$.

A.1.3.2 Explicit formula for $[O^{+(1)}(P,t)]$ in terms of the integral of the error function, ierfc(x). The concentration field function $[O^{+(1)}(P,t)]$, can be represented in the following form:

$$[O^{+(1)}(P,t)] = [O^{+}(\infty)]\left[1 - \frac{h}{T_1}\exp\left(-\frac{\xi^2}{h^2}\right)\exp\left(-\frac{z^2}{T_1^2}\right)\right]$$

$$- 2\sqrt{\pi}\, k_1[O_2(0)][O^{+}(\infty)]\frac{h^2}{4D}\exp\left(-\frac{\xi^2}{h^2}\right)\left\{\left[\left(\frac{T_1}{h}\right)\text{ierfc}\left(\frac{z}{T_1}\right)\right.\right.$$

$$\left.\left. - \text{ierfc}\left(\frac{z}{h}\right)\right] - \frac{1}{2}\exp\left(-\frac{\xi^2}{h^2}\right)\left[\left(\frac{T_2}{h}\right)\text{ierfc}\left(\frac{\sqrt{2}z}{T_2}\right) - \text{ierfc}\left(\frac{\sqrt{2}z}{h}\right)\right]\right\}$$

wherein

$$T_1 = \sqrt{h^2 + 4Dt} \quad , \quad T_2 = \sqrt{h^2 + 8Dt}$$

$$\text{ierfc}(x) = \int_x^\infty \text{erfc}(x')\, dx' = \frac{1}{\sqrt{\pi}} \exp(-x^2) - x\,\text{erfc}(x) \quad ,$$

and

$$\text{erfc}(x) = \frac{2}{\sqrt{\pi}} \int_x^\infty \exp(-\lambda^2)\, d\lambda = 1 - \text{erf}(x) \quad .$$

A.1.3.3 The function $[O^{+(1)}(0,z,t)]$ and the center-point value function $[O^{+(1)}(0,0,t)]$. For points on the vertical z axis, $\xi = 0$, the concentration field function $[O^{+(1)}(P,t)]$ is designated by $[O^{+(1)}(0,z,t)]$ and is defined by the following formula:

$$[O^{+(1)}(0,z,t)] = [O^{+}(\infty)]\left[1 - \frac{h}{T_1} \exp\left(-\frac{z^2}{T_1^2}\right)\right]$$

$$- 2\sqrt{\pi}\left(\frac{k_1 h^2}{4D}\right)[O_2(0)][O^{+}(\infty)]\left\{\left[\left(\frac{T_1}{h}\right)\text{ierfc}\left(\frac{z}{T_1}\right) - \text{ierfc}\left(\frac{z}{h}\right)\right]\right.$$

$$\left. - \frac{1}{2}\left[\left(\frac{T_2}{h}\right)\text{ierfc}\left(\frac{\sqrt{2}z}{T_2}\right) - \text{ierfc}\left(\frac{\sqrt{2}z}{h}\right)\right]\right\} \quad .$$

At the origin $\xi = 0$, $z = 0$, $r = 0$ the center-point value of the concentration field function $[O^{+(1)}(P,t)]$ is designated as $[O^{+(1)}(0,0,t)]$ and has the value specified by the following formula:

$$[O^{+(1)}(0,0,t)] = [O^{+}(\infty)]\left(1 - \frac{h}{T_1}\right) - \left(\frac{k_1 h^2}{4D}\right)[O_2(0)][O^{+}(\infty)]\left(\frac{2T_1}{h} - \frac{T_2}{h} - 1\right).$$

This representation of $[O^{+(1)}(P,t)]$ at the origin $\xi = 0$, $z = 0$, $r = 0$, follows from the specification of the function ierfc(x) at x = 0:

$$\text{ierfc}(x) = \int_x^\infty \text{erfc}(x')\,dx' = \frac{1}{\sqrt{\pi}} \exp(-x^2) - x\,\text{erfc}(x) \quad ,$$

with $\text{ierfc}(0) = \frac{1}{\sqrt{\pi}}$, since erfc(0) = 1 - erf(0) = 1.

A.1.4 Resolution of the Boundary Value Problem in $[e^{(1)}]$ and Properties of $[e^{(1)}(0,z,t)]$.

A.1.4.1 Explicit formula for $[e^{(1)}(P,t)]$ in terms of ierfc(x).

Reference is made to the partial differential equation

$$\frac{\partial}{\partial t}[e^{(1)}] = D\frac{\partial^2}{\partial z^2}[e^{(1)}] - k_2[e^{(0)}][O_2^{+(0)}]$$

where

$$k_2[e^{(0)}][O_2^{+(0)}] = k_2[e(\infty)][O_2^{+}(\infty)]\left[1 - 2\exp\left(-\frac{\xi^2}{h^2}\right)\exp\left(-\frac{z^2}{h^2}\right) + \exp\left(-\frac{2\xi^2}{h^2}\right)\exp\left(-\frac{2z^2}{h^2}\right)\right]$$

with the initial condition

$$[e^{(1)}]_{t=+0} = [e(\infty)]\left[1 - \exp\left(-\frac{\xi^2}{h^2}\right)\exp\left(-\frac{z^2}{h^2}\right)\right] \quad .$$

The resolution of this initial value problem in $[e^{(1)}(P,t)]$ patterns after the scheme used for obtaining a representation of the function $[O^{+(1)}(P,t)]$ with the addition of a single time-space Green's function

integral to account for the constant term in the nonhomogeneous (forcing function) term in the partial differential equation in $[e^{(1)}] = [e^{(1)}(P,t)]$.

A.1.4.2 The function $[e^{(1)}(0,z,t)]$ and the center-point value function $[e^{(1)}(0,0,t)]$. For points along the vertical z axis, $\xi = 0$, the concentration field function $[e^{(1)}(P,t)]$ is designated by the symbol $[e^{(1)}(0,z,t)]$ and is defined by the formula below:

$$[e^{(1)}(0,z,t)] = [e(\infty)]\left[1 - \frac{h}{T_1}\exp\left(-\frac{z^2}{T_1^2}\right)\right] - k_2 t[e(\infty)][O_2^+(\infty)]$$

$$+ 4\sqrt{\pi}\left(\frac{k_2 h^2}{4D}\right)[e(\infty)][O_2^+(\infty)]\left\{\left[\left(\frac{T_1}{h}\right)\text{ierfc}\left(\frac{z}{T_1}\right)\right.\right.$$

$$\left.\left. - \text{ierfc}\left(\frac{z}{h}\right)\right] - \frac{1}{4}\left[\left(\frac{T_2}{h}\right)\text{ierfc}\left(\frac{\sqrt{2}z}{T_2}\right) - \text{ierfc}\left(\frac{\sqrt{2}z}{h}\right)\right]\right\} .$$

At the origin $\xi = 0$, $z = 0$, $r = 0$ the center-point value $[e^{(1)}(0,0,t)]$ of the concentration field function $[e^{(1)}(P,t)]$ is defined by the simple formula displayed below:

$$[e^{(1)}(0,0,t)] = [e(\infty)]\left(1 - \frac{h}{T_1}\right) - k_2 t[e(\infty)][O_2^+(\infty)]$$

$$+ \left(\frac{k_2 h^2}{4D}\right)[e(\infty)][O_2^+(\infty)]\left(\frac{4T_1}{h} - \frac{T_2}{h} - 3\right) .$$

This representation of $[e^{(1)}(P,t)]$ at the origin $z = 0$, $\xi = 0$, $r = 0$, depends on the specification of the function ierfc(x) at $x = 0$:

$$\text{ierfc}(x)]_{x=0} = \left[\frac{1}{\sqrt{\pi}}\exp(-x^2) - x\,\text{erfc}(x)\right]_{x=0} = \frac{1}{\sqrt{\pi}} \quad .$$

A.1.5 Resolution of the Boundary Value Problem in $[O^{*(1)}]$ and Properties of $[O^{*(1)}(0,z,t)]$.

A.1.5.1 Green's function integral formula for $\exp(k_3 t)\,[O^{*(1)}(P,t)]$.

Reference is made to the partial differential equation

$$\frac{\partial[O^{*(1)}]}{\partial t} = \frac{D}{r^2}\frac{\partial}{\partial r}\left(r^2\frac{\partial}{\partial r}[O^{*(1)}]\right) - k_3[O^{*(1)}] + k_2[O_2^{+(0)}][e^{(0)}] \quad ,$$

where

$$[e^{(0)}] \equiv [e(P,+0)] = [e(\infty)]\left[1 - \exp\left(-\frac{r^2}{h^2}\right)\right]$$

and

$$[O_2^{+(0)}] \equiv [O_2^{+}(P,+0)] = [O_2^{+}(\infty)]\left[1 - \exp\left(-\frac{r^2}{h^2}\right)\right] \quad ,$$

with the initial condition

$$[O^{*(1)}] \to 0 \quad \text{as} \quad t \to 0 \quad \text{for all} \quad r \text{ in } 0 \leq r < \infty \quad ,$$

where

$$r^2 = \xi^2 + z^2 \quad , \quad \xi^2 = x^2 + y^2 \quad .$$

By use of the spherically point symmetric Green's function $G_3(r,r';t,\tau)$

$$G_3(r,r';t,\tau) = \frac{1}{4\pi rr'\sqrt{\pi D(t-\tau)}}\exp\left(-\frac{r^2+r'^2}{4D(t-\tau)}\right)\sinh\left(\frac{rr'}{2D(t-\tau)}\right) \quad ,$$

the concentration function $[O^{*(1)}(P,t)]$ can be defined by the integral formula

$$\exp(k_3 t)\ [O^{*(1)}(P,t)] = \int_0^t d\tau \int_0^\infty 4\pi r'^2\, dr'\ k_2 \exp(k_3\tau)\ [e(\infty)][O_2^+(\infty)]$$

$$\left[1 - \exp\left(-\frac{r'^2}{h^2}\right)\right]^2 \cdot G_3(r,r';t,\tau) \quad .$$

A.1.5.2 Representation of $[O^{*(1)}(r,t)]$ as an indefinite time integral. The repeated integral formula for $[O^{*(1)}(r,t)]$ can be represented by the single integral formula:

$$[O^{*(1)}(r,t)] = k_2[e(\infty)][O_2^+(\infty)] \int_0^t \frac{\exp(-k_3 t')}{4\sqrt{\pi D t'}} \exp\left(-\frac{r^2}{4Dt'}\right)$$

$$[\varphi_o - 2\varphi_1 + \varphi_2]\ dt'$$

$$\equiv k_2[e(\infty)][O_2^+(\infty)] \int_0^t \exp(-k_3 t') \exp\left(-\frac{r^2}{4Dt'}\right)\left\{\exp\left(\frac{r^2}{4Dt'}\right)\right.$$

$$\left. - 2\left(\frac{h}{T_1'}\right)^3 \exp\left[\frac{r^2}{4Dt'}\left(\frac{h}{T_1'}\right)^2\right] + \left(\frac{h}{T_2'}\right)^3 \exp\left[\frac{r^2}{4Dt'}\left(\frac{h}{T_2'}\right)^2\right]\right\} dt'$$

$$= k_2[e(\infty)][O_2^+(\infty)] \int_0^t \exp(-k_3 t')\left[1 - 2\left(\frac{h}{T_1'}\right)^3\right.$$

$$\exp\left(-\frac{r^2}{4Dt'T_1'^2}\,(T_1'^2 - h^2)\right) + \left(\frac{h}{T_2'}\right)^3$$

$$\left.\exp\left(-\frac{r^2}{4Dt'T_2^2}\,(T_2^2 - h^2)\right)\right] dt'$$

so that

$$[O^{*(1)}(r,t)] = k_2[e(\infty)][O_2^{+}(\infty)]\int_o^t \exp(-k_3t')\left[1 - 2\left(\frac{h}{T_1'}\right)^3 \exp\left(-\frac{r^2}{T_1'^2}\right) + \left(\frac{h}{T_2'}\right)^3 \exp\left(-\frac{2r^2}{T_1'^2}\right)\right] dt' ,$$

wherein

$$T_1^2 = h^2 + 4Dt \quad , \qquad T_2^2 = h^2 + 8Dt \quad .$$

A.1.5.3 Reduction of the time integrals $\psi_1(r,t)$ and $\psi_2(r,t)$:

$$\psi_1(r,t) = \int_o^t \exp(-k_3t')\left(\frac{h}{T_1'}\right)^3 \exp\left(-\frac{r^2}{T_1'^2}\right) dt'$$

$$\psi_2(r,t) = \int_o^t \exp(-k_3t')\left(\frac{h}{T_2'}\right)^3 \exp\left(-\frac{2r^2}{T_2'^2}\right) dt' \quad ,$$

In this time integral formula for $[O^{*(1)}(r,t)]$ let the auxiliary functions $\psi_1(r,t)$ and $\psi_2(r,t)$ be introduced by the definitions

$$\psi_1(r,t) = \int_o^t \exp(-k_3t')\left(\frac{h}{T_1'}\right)^3 \exp\left(-\frac{r^2}{T_1'^2}\right) dt'$$

and

$$\psi_2(r,t) = \int_o^t \exp(-k_3t')\left(\frac{h}{T_2'}\right)^3 \exp\left(-\frac{2r^2}{T_2'^2}\right) dt'$$

in order to represent the concentration field function $[O^{*(1)}(r,t)]$ by the linear form:

$$[O^{*(1)}(r,t)] = k_2[e(\infty)][O_2^+(\infty)]\left\{\frac{1}{k_3}\left(1 - \exp(-k_3 t)\right) - 2\psi_1(r,t) + \psi_2(r,t)\right\}.$$

The reduction of the integrals for $\psi_1(r,t)$ and $\psi_2(r,t)$ is complicated by the presence of the exponential decay term $\exp(-k_3 t')$.

Nevertheless, the auxiliary functions ψ_1 and ψ_2 can be represented in terms of exponential and error functions.

A.1.5.4 Explicit formulas for $\psi_1(r,t)$ and $\psi_2(r,t)$. It is convenient to introduce the parameter α by the substitution

$$\alpha \equiv \frac{h}{2}\sqrt{\frac{k_3}{D}}$$

in the following specification of the auxiliary function $\psi_1(r,t)$:

$$\psi_1(r,t) \equiv \frac{\sqrt{\pi}}{8}\left(\frac{h^3}{rD}\right)\exp(\alpha^2)\left\{\exp\left(\frac{2\alpha r}{h}\right)\left[\operatorname{erf}\left(\frac{r}{h} + \alpha\right) - \operatorname{erf}\left(\frac{r}{T_1} + \frac{T_1}{h}\alpha\right)\right]\right.$$

$$\left. + \exp\left(-\frac{2\alpha r}{h}\right)\left[\operatorname{erf}\left(\frac{r}{h} - \alpha\right) - \operatorname{erf}\left(\frac{r}{T_1} - \frac{T_1}{h}\alpha\right)\right]\right\} .$$

By analogous procedures it can be demonstrated that the auxiliary function $\psi_2(r,t)$ has the following specification:

$$\psi_2(r,t) \equiv \frac{\sqrt{\pi}}{16\sqrt{2}}\left(\frac{h^3}{rD}\right)\exp\left(\frac{1}{2}\alpha^2\right)\left\{\exp\left(\frac{2\alpha r}{h}\right)\left[\operatorname{erf}\left(\frac{\sqrt{2}r}{h} + \frac{\alpha}{\sqrt{2}}\right) - \operatorname{erf}\left(\frac{\sqrt{2}r}{T_2}\right.\right.\right.$$

$$\left.\left.\left. + \frac{T_2}{h}\frac{\alpha}{\sqrt{2}}\right)\right] + \exp\left(-\frac{2dr}{h}\right)\left[\operatorname{erf}\left(\frac{\sqrt{2}r}{h} - \frac{\alpha}{\sqrt{2}}\right) - \operatorname{erf}\left(\frac{\sqrt{2}r}{T_2} - \frac{T_2}{h}\frac{\alpha}{\sqrt{2}}\right)\right]\right\}$$

wherein

$$T_1^2 \equiv h^2 + 4Dt \quad \text{and} \quad T_2^2 \equiv h^2 + 8Dt \quad .$$

A.1.5.5 Explicit formulas for $\psi_1(0,0,t)$ and $\psi_2(0,0,t)$ and the center-point value function $[O^{*(1)}(0,0,t)]$. In order to specify the center-point value $[O^{*(1)}(0,0,t)]$ of the concentration field function $[O^{*(1)}(P,t)]$, at the origin $z = 0$, $\xi = 0$, it is required to specify the values of $\psi_1(0,z,t)$ and $\psi_2(0,z,t)$ when $z \to 0$.

Note that when $z = 0$ the function $\psi_1(0,z,t)$ assumes the form $\frac{0}{0}$ since $\text{erf}(-x) = -\text{erf}(x)$. Accordingly, in the formulas for $\psi_1(0,z,t)$ and $\psi_2(0,z,t)$ it is required to apply l'Hospital's rule in order to assign a value to $\psi_1(0,z,t)$ and $\psi_2(0,z,t)$ when $z \to 0$:

$$\psi_1(0,z,t)]_{z \to 0} = \frac{\sqrt{\pi}}{2}\left(\frac{h^3}{4D}\right)\exp(\alpha^2)\left\{\frac{2\alpha}{h}\left[\text{erf}(\alpha) - \text{erf}\left(\frac{T_1}{h}\alpha\right)\right]\right.$$

$$- \frac{2\alpha}{h}\left[-\text{erf}(\alpha) + \text{erf}\left(\frac{T_1}{h}\alpha\right)\right]$$

$$+ \frac{2}{\sqrt{\pi}}\left[\frac{1}{h}\exp(-\alpha^2) - \frac{1}{T_1}\exp\left(-\frac{T_1^2\alpha^2}{h^2}\right)\right]$$

$$\left. + \frac{2}{\sqrt{\pi}}\left[\frac{1}{h}\exp(-\alpha^2) - \frac{1}{T_1}\exp\left(-\frac{T_1^2\alpha^2}{h^2}\right)\right]\right\} \quad ,$$

$$= 2\sqrt{\pi}\left(\frac{h^2}{4D}\right)\exp(\alpha^2)\left\{\left(\frac{1}{\sqrt{\pi}}\exp(-\alpha^2) - \alpha\,\mathrm{erfc}(\alpha)\right) - \frac{h}{T_1}\left[\frac{1}{\sqrt{\pi}}\exp\left(-\frac{T_1^2\alpha^2}{h^2}\right) - \frac{T_1\alpha}{h^2}\,\mathrm{erfc}\left(\frac{T_1\alpha}{h}\right)\right]\right\} ,$$

so that

$$\psi_1(0,0,t) \equiv 2\sqrt{\pi}\left(\frac{h^2}{4D}\right)\exp(\alpha^2)\left\{\mathrm{ierfc}(\alpha) - \frac{h}{T_1}\,\mathrm{ierfc}\left(\frac{T_1\alpha}{h}\right)\right\} ;$$

furthermore

$$\psi_2(0,z,t)]_{z\to 0} = \frac{\sqrt{\pi}}{4\sqrt{2}}\left(\frac{h^3}{4D}\right)\exp\left(\frac{1}{2}\alpha^2\right)\left\{\frac{2\alpha}{h}\left[\mathrm{erf}\left(\frac{\alpha}{\sqrt{2}}\right) - \mathrm{erf}\left(\frac{T_2}{h}\frac{\alpha}{\sqrt{2}}\right)\right] - \frac{2\alpha}{h}\left[-\mathrm{erf}\left(\frac{\alpha}{\sqrt{2}}\right) + \mathrm{erf}\left(\frac{T_2}{h}\frac{\alpha}{\sqrt{2}}\right)\right] + \frac{2}{\sqrt{\pi}}\left[\frac{\sqrt{2}}{h}\exp\left(\frac{1}{2}\alpha^2\right) - \frac{\sqrt{2}}{T_2}\exp\left(-\frac{T_2^2\alpha^2}{2h}\right)\right] + \frac{2}{\sqrt{\pi}}\left[\frac{\sqrt{2}}{h}\exp\left(\frac{1}{2}\alpha^2\right) - \frac{\sqrt{2}}{T_2}\exp\left(-\frac{T_2^2\alpha^2}{2h}\right)\right]\right\}$$

$$= \sqrt{\pi}\left(\frac{h^2}{4D}\right)\exp\left(\frac{1}{2}\alpha^2\right)\left\{\left[\frac{1}{\sqrt{\pi}}\exp\left(\frac{1}{2}\alpha^2\right) - \frac{\alpha}{\sqrt{2}}\,\mathrm{erfc}\left(\frac{\alpha}{\sqrt{2}}\right)\right] - \frac{h}{T_2}\left[\frac{1}{\sqrt{\pi}}\exp\left(-\frac{T_2^2\alpha^2}{2h}\right) - \frac{T_2\alpha}{\sqrt{2h}}\,\mathrm{erfc}\left(\frac{T_2\alpha}{\sqrt{2h}}\right)\right]\right\}$$

so that

$$\psi_2(0,0,t) = \sqrt{\pi}\left(\frac{h^2}{4D}\right)\exp\left(\frac{1}{2}\alpha^2\right)\left\{\mathrm{ierfc}\left(\frac{\alpha}{\sqrt{2}}\right) - \frac{h}{T_2}\,\mathrm{ierfc}\left(\frac{T_2\alpha}{\sqrt{2h}}\right)\right\} .$$

By direct substitution into the center-point formula

$$[O^{*(1)}(0,0,t)] = k_2[e(\infty)][O_2^+(\infty)]\left\{\frac{1}{k_3}\left(1 - \exp(-k_3 t) - 2\psi_1(0,0,t) + \psi_2(0,0,t)\right)\right\}$$

it is implied the concentration field function $[O^{*(1)}(P,t)]$ has the center-point value $[O^{*(1)}(0,0,t)]$ defined by the integral of the error function formula displayed below:

$$[O^{*(1)}(0,0,t)] = \left(\frac{k_2}{k_3}\right)[e(\infty)][O_2^+(\infty)]\left\{1 - \exp(-k_3 t) - 4\sqrt{\pi}\alpha^2 \exp(\alpha^2)\left[\text{ierfc}(\alpha) - \frac{h}{T_1}\,\text{ierfc}\left(\frac{T_1\alpha}{h}\right)\right] + \sqrt{\pi}\alpha^2 \exp\left(\frac{1}{2}\alpha^2\right)\left[\text{ierfc}\left(\frac{\alpha}{\sqrt{2}}\right) - \frac{h}{T_2}\,\text{ierfc}\left(\frac{T_2\alpha}{\sqrt{2h}}\right)\right]\right\},$$

wherein

$$\alpha = \frac{h}{2}\sqrt{\frac{R_3}{D}}\,, \quad T_1 = \sqrt{h^2 + 4Dt}\,, \quad T_2 = \sqrt{h^2 + 8Dt}\,.$$

A.1.5.6 The line integral density function $S^{(1)}_{[O^*]}(t,\lambda,h)$ defined by $S^{(1)}_{[O^*]} = \int_0^{\lambda h} [O^{*(1)}(0,z,t)]dz$. Let an integrated line density particle count per unit cross sectional area, defined by the symbol $S^{(1)}_{[O^*]}(t,\lambda h)$, be made along the z axis, $\xi = 0$, from $\xi = 0$, $z = 0$ $(r = 0)$ to $\xi = 0$, $z = \lambda h$, in the concentration field $[O^{*(1)}(P,t)]$.

That is to say, consider the function $S^{(1)}_{[0^*]}(t,\lambda h)$ defined by the integral formula:

$$S^{(1)}_{[0^*]}(t,\lambda h) = \oint_L [0^{*(1)}(P,t)]ds = \int_0^{\lambda h} [0^{*(1)}(P,t)]_{\xi=0}\, dz \ ;$$

specifically consider the function $S^{(1)}_{[0^*]}(t,\lambda h)$ defined by

$$S^{(1)}_o(t,\lambda h) \equiv k_2[e(\infty)][O_2^+(\infty)] \int_0^{\lambda h} dz \int_0^t \exp(-k_3 t' \left[1 - 2\left(\frac{h}{T_1'}\right)^3 \right.$$

$$\left. \exp\left(-\frac{z^2}{T_1'^2}\right) + \left(\frac{h}{T_2'}\right)^3 \exp\left(-\frac{2z^2}{T_2'^2}\right) \right] dt'$$

$$\equiv k_2[e(\infty)][O_2^+(\infty)] \int_0^t \exp(-k_3 t')\, dt' \left\{\lambda h - 2\left(\frac{h}{T_1'}\right)^3 \right.$$

$$\left. \int_0^{\lambda h} \exp\left(-\frac{z^2}{T_1'^2}\right) dz + \left(\frac{h}{T_2'}\right)^3 \int_0^{\lambda h} \exp\left(-\frac{2z^2}{T_2'^2}\right) dz' \right\}$$

A.1.5.6.1 Canonical form of the function $S^{(1)}_{[0^*]}(t,\lambda h)$ as a function of $\alpha = \frac{h}{2}\sqrt{\frac{k_3}{D}}$ and t. The formula for $S^{(1)}_{[0^*]}(t,\lambda h)$ can be expressed in the following canonical form:

$$S^{(1)}_{[O^*]}(t,\lambda h) = \int_0^{\lambda h} [O^{*(1)}[0,z,t)]dz$$

$$= h\left(\frac{k_2}{k_3}\right)[e(\infty)][O_2^+(\infty)]\left\{\lambda\left(1 - \exp(-k_3 t)\right)\right.$$

$$- \sqrt{\pi}\,\alpha^2 \exp(\alpha^2) \int_{\alpha^2}^{\alpha^2+k_3 t} \frac{\exp(-u)}{u} \operatorname{erf}\left(\frac{\lambda\alpha}{\sqrt{u}}\right)du$$

$$\left. + \frac{\sqrt{\pi}}{4\sqrt{2}}\,\alpha^2 \exp\left(\frac{1}{2}\alpha^2\right) \int_{\frac{1}{2}\alpha^2}^{\frac{1}{2}\alpha^2+k_3 t} \frac{\exp(-u)}{u} \operatorname{erf}\left(\frac{\lambda\alpha}{\sqrt{u}}\right)du \right\} ,$$

wherein

$$\alpha^2 = \frac{h^2 k_3}{4D} , \qquad \alpha = \frac{h}{2}\sqrt{\frac{k_3}{D}} .$$

The factor $(k_2/k_3)[e(\infty)][O_2^+(\infty)]$, which appears in this explicit formula for $S^{(1)}_{[O^*]}(t,\lambda h)$, has the value $[O^{*(1)}(\infty)] = [O^*(\infty)]$. That this is so is evident by an inspection of the equation of continuity in $[O^*]$,

$$\frac{\partial}{\partial t}[O^*] = D\nabla^2[O^*] + k_2[O_2^+][e] - k_3[O^*] ,$$

and the reiterative equation of continuity for $[O^{*(1)}]$,

$$\frac{\partial}{\partial t}[O^{*(1)}] = D\,\frac{1}{r^2}\,\frac{\partial}{\partial r}\left(r^2\,\frac{\partial}{\partial r}\,[O^{*(1)}]\right) + k_2\,[O_2^{+(0)}][e^{(0)}] - k_3[O^{*(1)}] .$$

A.2 THE "SNOWPLOW" MODEL WITH $\epsilon=1$: $[O^*(P,+0)] = [O^*(\infty)]\left[1 - \exp\left(-\frac{r^2}{h^2}\right)\right]$

A.2.1 Resolution of the Boundary Value Problem in $[O^*(P,t)]$ and $[O^{*(1)}(P,t)]$ when $\epsilon=1$ with $[O^*(P,+0)] = [O^*(\infty)]\left[1 - \exp\left(-\frac{r^2}{h^2}\right)\right]$. It is now proposed to solve the partial differential equation in $[O^*] = [O^*(P,t)]$

$$\frac{\partial}{\partial t}[O^*] = D\nabla^2[O^*] - k_3[O^*] + k_2[O_2^+][e]$$

when the functions $[O^*]$, $[O_2^+]$, and $[e]$ initially have the inverted Gaussian forms:

$$[O^*]_{t=0} = [O^*(\infty)]\left[1 - \exp\left(-\frac{r^2}{h_2}\right)\right], \quad [O_2^+]_{t=0} = [O_2^+(\infty)]\left[1 - \exp\left(\infty\frac{r^2}{h^2}\right)\right]$$

and

$$[e]_{t=0} = [e(\infty)]\left[1 - \exp\left(-\frac{r^2}{h^2}\right)\right] .$$

Under steady state conditions at the boundary of the region $R(P): -\infty < x < \infty$, $-\infty < y < \infty$, $-\infty < z < \infty$, it is required that

$$[O^*](\infty)] = \left(\frac{k_2}{k_3}\right)[O_2^+(\infty)][e(\infty)].$$

As a first approximation $[O^*(P,t)]$ to the concentration function $[O^*(P,t)]$ consider the partial differential equation in $[O^{*(1)}] = [O^{*(1)}(P,t)]$:

$$\frac{\partial}{\partial t}[O^{*(1)}] = D\nabla^2[O^{*(1)}] - k_3[O^{*(1)}] + k_2[O_2^+]_{t=0}[e]_{t=0}$$

with the initial condition

$$[O^{*(1)}]_{t=0} = [O^{*}(\infty)]\left[1 - \exp\left(-\frac{r^2}{h^2}\right)\right] .$$

A.2.1.1 Green's function integral formula for $\exp(k_3 t)[O^{*(1)}] = I_1 + I_2$. The Green's function

$$G_3(r,r';t,\tau) = \frac{1}{4\pi r r' \sqrt{\pi D(t-\tau)}} \exp\left(-\frac{r^2 + r'^2}{4D(t-\tau)}\right) \sinh\left(\frac{rr'}{2D(t-\tau)}\right)$$

can be used to define the following representation of the concentration field function $[O^{*(1)}(P,t)]$:

$$\exp(k_3 t)[O^{*(1)}(P,t)] = \int_0^\infty 4\pi r'^2 \left\{\exp(k_3 t)[O^{*(1)}]\right\}_{t=0} G_3(r,r';t,0)dr'$$

$$+ \int_0^t d\tau \int_0^\infty 4\pi r'^2 dr' \; k_2 \exp(k_3 \tau)[O_2^+]_{t=0}[e]_{t=0} \; G_3(r,r';t,\tau) .$$

The definite integral identity

$$\int_0^\infty x \exp(-a^2 x^2) \sinh bx \, dx = \frac{\sqrt{\pi}}{4} \frac{b}{a^3} \exp\left(\frac{b^2}{4a^2}\right)$$

can be used to reduce the space integral in the above Green's integral formula for $[O^{*(1)}(P,t)]$.

For note that $\exp(k_3 t)[O^{*(1)}] \equiv I_1 + I_2$ where

$$I_1 \equiv \int_0^\infty 4\pi r'^2 \left\{\exp(k_3 t)[O^{*(1)}]\right\}_{t=0} G_3(r,r';t,0)\, dr'$$

$$\equiv \frac{4\pi}{4\pi r\sqrt{\pi Dt}}[O^*(\infty)] \exp\left(-\frac{r^2}{4Dt}\right)\int_0^\infty r'\left[1 - \exp\left(-\frac{r'^2}{h^2}\right)\right]\exp\left(-\frac{r'^2}{4Dt}\right) \sinh\left(\frac{rr'}{2Dt}\right) dr'$$

and

$$I_2 \equiv \int_0^t d\tau \int_0^\infty 4\pi r'^2 dr'\, k_2 \exp(k_3\tau)\, [O_2^+]_{t=0}[e]_{t=0} G_3(r,r';t,\tau) \quad .$$

A.2.1.2 Representation of $[O^{*(1)}(P,t)]$ as an indefinite time integral. It is concluded that the concentration field function $[O^{*(1)}(P,t)]$ is defined by the following integral formula with $[O^{*(1)}(P,+0)] = [O^*(0)]\left[1 - \exp\left(-\frac{r^2}{h^2}\right)\right]$:

$$[O^{*(1)}(P,t)] = [O^*(\infty)]\left[1 - \left(\frac{h}{T_1}\right)^3 \exp\left(-\frac{r^2}{T_1^2}\right)\right] \exp(-k_3 t)$$

$$+ k_2[O_2^+(\infty)]\int_0^t \exp(-k_3 t') \left\{1 - 2\left(\frac{h}{T_1'}\right)^3 \exp\left(-\frac{r^2}{T_1'^2}\right) + \left(\frac{h}{T_2'}\right)^3 \exp\left(-\frac{2r^2}{T_2'^2}\right)\right\} dt' \quad ,$$

wherein

$$T_1'^2 \equiv h^2 + 4Dt' \quad \text{and} \quad T_2'^2 \equiv h^2 + 8Dt' \quad \text{and}$$

$$k_2[O_2^+(\infty)][e(\infty)] = k_3[O^*(\infty)] \quad .$$

A.2.1.3 The integrated line density function $S_o^{(1)}(t,\lambda h) = \int_o^{\lambda h} [O^{*(1)}(P,t)]_{\xi=0}\, dz$. Let an integrated line density particle count per unit cross-sectional area, defined by the symbol $S_o^{(1)}(t,\lambda h)$, be made along the z axis, $\xi=0$, $z=0$ ($r=0$) to $\xi=0$, $z=\lambda h$, in the concentration field $[O^{*(1)}(P,t)]$ with $P:(x,y,z)$, $\xi^2 = x^2 + y^2$, $r^2 = \xi^2 + z^2$.

That is to say, consider the function $S_o^{(1)}(t,\lambda h)$ defined by the line-integral formula:

$$S_o^{(1)}(t,\lambda h) \equiv \oint_L [O^{*(1)}(P,t)]\, ds \equiv \int_o^{\lambda h} [O^{*(1)}(P,t)]_{\xi=0}\, dz \quad .$$

A.2.1.3.1 Canonical form of the function $S_o^{(1)}(t,\lambda h)$ as a function of $\alpha = \frac{h}{2}\sqrt{k_3/D}$ and t and $\sigma_\lambda(u)$. The formula for $S_o^{(1)}(t,\lambda h)$ can be expressed in the form:

$$S_o^{(1)}(t,\lambda h) = \lambda h[O^*(\infty)] \exp(-k_3 t)$$

$$- \frac{\sqrt{\pi}}{2} [O^*(\infty)] \frac{h^3}{T_1^2} \exp(-k_3 t') \operatorname{erf}\left(\frac{\lambda h}{T_1}\right)$$

$$+ k_2[O_2^+(\infty)][e(\infty)] \int_o^t \exp(-k_3 t')\, dt' \left\{ \lambda h - \frac{2\sqrt{\pi}}{2} \frac{h^3}{T_1'^2} \right.$$

$$\left. \operatorname{erf}\left(\frac{\lambda h}{T_1'}\right) + \frac{\sqrt{\pi}}{2\sqrt{2}} \frac{h^3}{T_2'^2} \operatorname{erf}\left(\frac{\sqrt{2}\lambda h}{T_2'}\right) \right\} .$$

With the introduction of the parameter α defined by the substitution

$$\alpha = \frac{h}{2}\sqrt{\frac{k_3}{D}}$$

this formula for $S_o^{(1)}(t,\lambda h)$ can be rewritten as

$$S_o^{(1)}(t,\lambda h) = h[O^*(\infty)] \exp(-k_3 t) \left[\lambda - \frac{\sqrt{\pi}}{2} \left(\frac{h}{T_1}\right)^2 \operatorname{erf}\left(\frac{\lambda h}{T_1}\right) \right]$$

$$+ \frac{k_2}{k_3}[e(\infty)][O_2^+(\infty)]\, h \left\{ \lambda \left(1 - \exp(-k_3 t)\right) \right.$$

$$- \sqrt{\pi}\alpha^2 \exp(\alpha^2) \int_{h^2}^{T_1^2} \frac{\exp\left(-\frac{k_3}{4D} u\right)}{u_1} \operatorname{erf}\left(\frac{\lambda h}{\sqrt{u_1}}\right) du ,$$

$$\left. + \frac{\sqrt{\pi}}{4\sqrt{2}} \alpha^2 \exp\left(\frac{1}{2}\alpha^2\right) \int_{h^2}^{T_2^2} \frac{\exp\left(-\frac{k_3}{2D} u_2\right)}{u_2} \operatorname{erf}\left(\frac{\sqrt{2}\lambda h}{\sqrt{u_2}}\right) du_2 \right\} .$$

A.2.1.3.2 Alternate canonical formula for $S_o^{(1)}(t,\lambda h)$ in terms of $\alpha, t, H_\lambda(\alpha^2 + k_3 t)$, and $F_\lambda\left(\frac{1}{2}\alpha^2 + k_3 t\right)$. An alternate formula for $S_o^{(1)}(t,\lambda h)$ is displayed below:

$$S_o^{(1)}(t,\lambda h) = \int_o^{\lambda h} [O^{*(1)}(0,z,t)]\, dz$$

$$- h[O^*(\infty)]\left\{\lambda - \frac{\sqrt{\pi}}{2}\left(\frac{h}{T_1}\right)^2 \exp(-k_3 t)\ \mathrm{erf}\left(\frac{\lambda h}{T_1}\right)\right.$$

$$- \sqrt{\pi}\alpha^2 \exp(\alpha^2)\ H_\lambda(\alpha^2 + k_3 t)$$

$$\left. + \frac{\sqrt{\pi}}{4\sqrt{2}}\alpha^2 \exp\left(\frac{1}{2}\alpha^2\right)\ F_\lambda\left(\frac{1}{2}\alpha^2 + k_3 t\right)\right\} ,$$

wherein

$$F_\lambda(x) = \int_{\frac{1}{2}\alpha^2}^{x} \sigma_\lambda(u)\, du$$

and

$$H_\lambda(x) = \int_{\alpha^2}^{x} \sigma_\lambda(u)\, du$$

with

$$\sigma_\lambda(u) \equiv \frac{\exp(-u)}{u}\ \mathrm{erf}\left(\frac{\lambda\alpha}{\sqrt{u}}\right) ,$$

with

$$T_1^2 = h^2 + 4Dt, \qquad \alpha = \frac{h}{2}\sqrt{\frac{k_3}{D}} .$$

When $k_3 t > \frac{1}{2}\alpha^2$ then $x = \frac{1}{2}\alpha^2 + k_3 t > \alpha^2$ with $F_\lambda(x) = F_\lambda(\alpha^2) + H_\lambda(x)$, so that for times

$$t > \frac{1}{2}\frac{\alpha^2}{k_3} = \frac{1}{2}\frac{h^2 k_3}{4Dk_3} = \frac{h^2}{8D}$$

one can define $S_o^{(1)}(t,\lambda h)$ by the rule:

$$S_o^{(1)}(t,\lambda h)]_{t>\frac{h^2}{8D}} = h[0^*(\infty)]\left\{\lambda - \frac{\sqrt{\pi}}{2}\left(\frac{h}{T_1}\right)^2 \exp(-k_3 t)\ \mathrm{erf}\left(\frac{\lambda h}{T_1}\right)\right.$$

$$+ \frac{\sqrt{\pi}}{4\sqrt{2}}\alpha^2 \exp\left(\frac{1}{2}\alpha^2\right) F_\lambda(\alpha^2) - \sqrt{\pi}\,\alpha^2 \exp(\alpha^2)$$

$$H_\lambda(\alpha^2 + k_3 t) + \frac{\sqrt{\pi}}{4\sqrt{\pi}}\alpha^2 \exp\left(\frac{1}{2}\alpha^2\right)$$

$$\left. H_\lambda\left(\frac{1}{2}\alpha^2 + k_3 t\right)\right\}.$$

A.2.2 Resolution of the Boundary Value Problem in $[0^{*(2)}(P,t)]$, the Second Approximation to $[0^*(P,t)]$, when $\epsilon=0$ or $\epsilon=1$.

A.2.2.1 Explicit representation of the equation of continuity in $[0^{*(2)}(P,t)]$. The second approximation $[0^{*(2)}(P,t)]$ to the concentration field function $[0^*(P,t)]$ is required to satisfy the equation of continuity

$$\frac{\partial}{\partial t}[O^{*(2)}] = \frac{D}{r^2}\frac{\partial}{\partial r^2}\left(r^2\frac{\partial}{\partial r}[O^{*(2)}]\right) - k_3[O^{*(2)}] + k_2[O_2^{+(1)}][e^{(1)}]$$

where the concentration field functions $[e^{(1)}] = [e^{(1)}(P,t)]$ and $[O_2^{+(1)}] = [O_2^{+(1)}(P,t)]$ are the first approximations to the concentration field functions $[e(P,t)]$ and $[O_2^{+}(P,t)]$, respectively.

It has been demonstrated that $[e^{(1)}(P,t)]$ and $[O_2^{+(1)}(P,t)]$ have the following specific forms:

$$[e^{(1)}] \equiv [e^{(1)}(P,t)] = [e(\infty)]\left[1 - \left(-\frac{h}{T_1}\right)\exp\left(-\frac{\xi^2}{h^2}\right)\exp\left(-\frac{z^2}{T_1^2}\right)\right.$$

$$- k_2 t[e(\infty)][O_2^{+}(\infty)] + 4\sqrt{\pi}\left(\frac{k_2 h^2}{4D}\right)[e(\infty)][O_2^{+}(\infty)]\exp\left(-\frac{\xi^2}{h^2}\right)$$

$$\left\{\left[\left(\frac{T_1}{h}\right)\text{ierfc}\left(\frac{z}{T_1}\right) - \text{ierfc}\left(\frac{z}{h}\right)\right] - \frac{1}{4}\exp\left(-\frac{\xi^2}{h^2}\right)\left[\left(\frac{T_2}{h}\right)\text{ierfc}\left(\frac{\sqrt{2}z}{T_2}\right)\right.\right.$$

$$\left.\left. - \text{ierfc}\left(\frac{\sqrt{2}z}{h}\right)\right\}\right.$$

$$[O_2^{+(1)}] \equiv [O_2^{+(1)}(P,t)] \equiv [e^{(1)}] - [O^{+(1)}]$$

where

$$[O^{+(1)}] \equiv [O^{+(1)}(P,t)] = [O^{+}(\infty)]\left[1 - \frac{h}{T_1}\exp\left(-\frac{\xi^2}{h^2}\right)\exp\left(-\frac{z^2}{T_1^2}\right)\right]$$

$$- 2\sqrt{\pi}\left(\frac{k_1 h^2}{4D}\right)[O_2(0)][O^{+}(\infty)]\exp\left(-\frac{\xi^2}{h^2}\right)\left\{\left[\left(\frac{T_1}{h}\right)\text{ierfc}\left(\frac{z}{T_1}\right)\right.\right.$$

$$\left.\left. - \text{ierfc}\left(\frac{z}{h}\right)\right] - \frac{1}{2}\exp\left(-\frac{\xi^2}{h^2}\right)\left[\left(\frac{T_2}{h}\right)\text{ierfc}\left(\frac{\sqrt{2}z}{T_2}\right) - \text{ierfc}\left(\frac{\sqrt{2}z}{h}\right)\right]\right\} .$$

A.2.2.2 The substitutions $\Omega_j(P,t)$, λ_j, μ_j, and γ_j. Let the auxiliary functions $\Omega_j(P,t)$ be introduced by the substitutions

$$\Omega_1(P,t) = 1 \ , \ \Omega_2(P,t) = \frac{h}{T_1} \exp\left(-\frac{\xi}{T_1}\right) \exp\left(-\frac{z^2}{T_1^2}\right) \ ,$$

$$\Omega_3(P,t) = t \ , \ \Omega_4(P,t) = \exp\left(-\frac{\xi^2}{h^2}\right)\left[\left(\frac{T_1}{h}\right) \text{ierfc}\left(\frac{z}{T_1}\right) - \text{ierfc}\left(\frac{z}{h}\right)\right] \ ,$$

$$\Omega_5(P,t) = \exp\left(-\frac{2\xi^2}{h^2}\right)\left[\left(\frac{T_2}{h}\right) \text{ierfc}\left(\frac{\sqrt{2}z}{T_2}\right) - \text{ierfc}\left(\frac{\sqrt{2}z}{h}\right)\right] \ .$$

Further let the set of constants λ_j be introduced (in the specification of $[e^{(1)}]$):

$$\lambda_1 = [e(\infty)] \ , \ \lambda_2 = -[e(\infty)] \ , \ \lambda_3 = -k_2[e(\infty)][O_2^+(\infty)] \ ,$$

$$\lambda_4 = 4\sqrt{\pi}\left(\frac{k_2h^2}{4D}\right)[e(\infty)][O_2^+(\infty)] \ ,$$

$$\lambda_5 = \sqrt{\pi}\left(\frac{k_2h^2}{4D}\right)[e(\infty)][O_2^+(\infty)] \ ,$$

and let the set of constants μ_j be introduced (in the specification of $[O^{+(1)}]$):

$$\mu_1 = [O^+(\infty)] \ , \ \mu_2 = -[O^+(\infty)] \ , \ \mu_3 = 0 \ ,$$

$$\mu_4 = -2\sqrt{\pi}\left(\frac{k_1h^2}{4D}\right)[O_2(0)][O^+(\infty)] \ ,$$

$$\mu_5 = +\sqrt{\pi}\left(\frac{k_1h^2}{4D}\right)[O_2(0)][O^+(\infty)] \ .$$

In terms of $\Omega_j = \Omega_j(P,t)$, λ_j, and μ_j it is seen that:

$$[e^{(1)}] \equiv \sum_{j=1}^{j=5} \lambda_j \Omega_j \qquad \text{and} \qquad [O^{+(1)}] \equiv \sum_{j=1}^{j=5} \mu_j \Omega_j \quad .$$

Furthermore, by the introduction of the constants γ_j by the rule

$$\gamma_j \equiv \lambda_j - \mu_j$$

it is seen that

$$[O_2^{+(1)}] \equiv [e^{(1)}] - [O^{+(1)}] \equiv \sum_{j=1}^{j=5} \gamma_j \Omega_j(P,t)$$

with

$$k_2[O_2^{+(1)}][e^{(1)}] \equiv k_2 \sum_{j_1=1}^{j_1=5} \sum_{j_2=1}^{j_2=5} \gamma_{j_1} \lambda_{j_2} \Omega_{j_1}(P,t) \Omega_{j_2}(P,t) \quad .$$

This means that the equation of continuity in $[O^{*(2)}] = [O^{*(2)}(P,t)]$ can be expressed in the explicit form

$$\frac{\partial}{\partial t}\left(\exp(k_3 t)[O^{*(2)}]\right) = \frac{D}{r^2}\frac{\partial}{\partial r^2}\left[r^2 \frac{\partial}{\partial r}\left(\exp(k_3 t)[O^{*(2)}]\right)\right]$$

$$+ k_2 \sum_{j_1=1}^{j_1=5} \sum_{j_2=1}^{j_2=5} \gamma_{j_1} \lambda_{j_2} \exp(k_3 t) \Omega_{j_1}(P,t) \Omega_{j_2}(P,t) \quad .$$

The concentration field function $[0^{*(2)}] = [0^{*(2)}(P,t)]$ has the initial form $[0^{*(2)}(P,+0)$ which can be taken to be an inverted Gaussian with an off-on factor ϵ:

$$0^{*(2)}(P,+0) = \epsilon[0^{*}(\infty)]\left[1 - \exp\left(-\frac{r^2}{h^2}\right)\right] ,$$

with $\epsilon = 0$ or $\epsilon = 1$.

A.2.2.3 Green's function integral formula for $\exp(k_3 t)[0^{*(2)}(P,t)]$. Since the functions $\Omega_j(P,t)$ are defined in terms of $P:(\xi,z)$ it is required to use the Green's function $G_3^{(2)}(P,P';t,\tau)$,

$$G_3^{(2)}(P,P';t,\tau) \equiv G_1(z,z';t,\tau)\, G_2(\xi,\xi';t,\tau) ,$$

$$G_1(z,z';t,\tau) \equiv \frac{1}{2\sqrt{\pi D(t-\tau)}} \exp\left(-\frac{z^2 + z'^2}{4D(t-\tau)}\right) \cosh\left(\frac{zz'}{2D(t-\tau)}\right) ,$$

$$G_2(\xi,\xi';t,\tau) \equiv \frac{1}{4\pi\, D(t-\tau)} \exp\left(-\frac{\xi^2 + \xi'^2}{4D(t-\tau)}\right) I_o\left(\frac{\xi\xi'}{2D(t-\tau)}\right),$$

in addition to the spherical-point symmetric Green's function $G_3^{(1)}(P,P';t,0)$

$$G_3^{(1)}(P,P';t,0) \equiv G_3(r,r';t,0) = \frac{1}{4\pi rr'\sqrt{Dt}} \exp\left(-\frac{r^2 + r'^2}{4Dt}\right) \sinh\left(\frac{rr'}{2Dt}\right)$$

in the following Green's function integral formula for $[0^{*(2)}] = [0^{*(2)}(P,t)]$:

$$\exp(k_3 t)[0^{*(2)}(P,t)] = \int_0^\infty 4\pi r'^2 \left\{\exp(k_3 t)\epsilon[0^{*}(\infty)]\left[1 - \exp\left(-\frac{r'^2}{h^2}\right)\right]\right\}_{t=0} G_3(r,r';t,0)dr' + \int_0^t d\tau \iiint_{-\infty}^{\infty} q(P',\tau)\, G_3^{(2)}(P,P';t,\tau)dV(P') .$$

That is to say,

$$[O^{*(2)}(P,t)] = \epsilon[O^{*}(\infty)]\exp(-k_3 t)\left[1-\left(\frac{h}{T_1}\right)^3\exp\left(-\frac{r^2}{T_1^2}\right)\right]$$
$$+ k_2\exp(-k_3 t)\sum_{j_1=1}^{j_1=5}\sum_{j_2=1}^{j_2=5}\gamma_{j_1}\lambda_{j_2}\int_0^t \exp(k_3\tau)\,d\tau$$
$$\int_{-\infty}^{\infty} dz'\int_0^{\infty} 2\pi\,\xi' d\xi'\Omega_{j_1}(P',\tau)\,\Omega_{j_2}(P',\tau)\cdot G_1(z,z';t,\tau)$$
$$G_2(\xi,\xi';t,\tau)\ .$$

A.2.2.4 Concluding remarks about the reduction of the integral formula for $\exp(k_3 t)[O^{*(2)}(P,t)]$. A casual inspection of complexity of the integrand of the time-space integral in this integral formula for the concentration field function $[O^{*(2)}(P,t)]$, the second approximation of the field function, $[O^{*}(P,t)]$, reveals the enormity of the analytic task in attempting to obtain an explicit closed-form representation of $[O^{*(2)}(P,t)]$.

The authors (particularly the first (H.K.Brown)) have not given consideration at the present time to putting this presentation of the problem (to find numerical values of $O^{*(2)}(P,t)$ in some suitable lattice in space-time) on a large-scale computer.

Values of $[O^{*(1)}(P,t)]$ (as well as $S^{(1)}_{[O^*]}(t,h)$) are presented in the computational section of this report.

In an effort to push the investigation, at the present time, to a stage where the approximation to the concentration field $[O^*(P,t)]$ reflects the influence of the transient molecular oxygen field (that is, values of $[O_2]$ are introduced into the specification of $[O^*(P,t)]$), the problem is approached anew, as described in the next section of this resumé.

A.3 THE "INTERPENETRABILITY" MODEL FOR $[O^*(P,t)]$ with $[O^*(P, +0)] = [O^*(\infty)]$

It is now proposed to investigate the concentration field, $[O^*(P,t)]$, of the excited oxygen atoms, under assumed conditions that permit the boundary value problem in $[O^*(P,t)]$ to be resolved explicitly without recourse to iterative procedures.

To this end, let it be assumed that the ambient region between 250 km and 300 km is sparse enough that the ambient particles are not initially disturbed when the molecular oxygen particles are introduced (at the time $t = +0$) with an initial Gaussian distribution.

That is to say, the "snow-plow" assumption is replaced by an "interpenetrability" assumption: the injected molecular oxygen particles establish transient fields which are superimposed on the steady-state ambient concentration fields.

In order to keep the mathematical analysis in a manageable state it has been assumed that the O^* particles are not transported by diffusion.

A.3.1 Specification of the Boundary Value Problems in $[O_2^+(P,t)]$ and $[O^*(P,t)]$.

A.3.1.1 The reaction equations and the equations of continuity. Corresponding to the reaction equations

$$O_2 + O^+ \xrightarrow{k_1} O_2^+ + O \ ,$$

$$O_2^+ + e \xrightarrow{k_2} O^* + O \ ,$$

$$O^* \xrightarrow{k_3} h\nu + O \ ,$$

are the equations of continuity

$$\frac{\partial[O^*]}{\partial t} = - k_3[O^*] + k_2[O_2^+]\ [e]$$

and

$$\frac{\partial[O_2^+]}{\partial t} = D\frac{\partial^2}{\partial z^2}[O_2^+] + k_1[O_2]\ [O^+] - k_2[O_2^+]\ [e]$$

for the concentration field functions $[O^*] = [O^*(P,t)]$ and $[O_2^+] = [O_2^+(P,t)]$.

It is assumed that the concentration field functions $[e] = [e(P,t)]$ and $[O^+] = [O^+(P,t)]$ have constant values for all times t and space positions P:(x,y,z) in the region $\mathcal{R}$: $0 \leq t \leq t_\infty$, $0 \leq r \leq r_\infty$, $r^2 = x^2 + y^2 + z^2$.

A.3.1.2 Specification of $[e]$, $[O^+]$, and $[O_2]$ in the equations of continuity. That is to say it is assumed that

$$[e] = [e(P,t)] = [e(\infty)]$$

and

$$[O^+] = [O^+(P,t)] = [O^+(\infty)]$$

for all t and P:(x,y,z) in $\mathcal{R}$: $0 \leq t \leq t_\infty$, $0 \leq r \leq r_\infty$, $r^2 = x^2 + y^2 + z^2$.

It is assumed that the concentration field function $[O_2] = [O_2(P,t)]$ is defined by the spherically point symmetric Gaussian form

$$[O_2] = [O_2(P,t)] = [O_2(o)]\left(\frac{h}{T_1}\right)^3 \exp\left(-\frac{r^2}{T_1^2}\right) + [O_2(\infty)]$$

for all t and P:(x,y,z), $r^2 = x^2 + y^2 + z^2$, in $\mathcal{R}$: $0 \leqq t \leqq t_\infty$, $0 \leqq r \leqq r_\infty$ wherein h is some Gaussian half-width and T_1 is defined by the quadratic form

$$T_1 = T_1(t) = \sqrt{h^2 + 4Dt} \ , \quad 0 \leqq t \leqq t_\infty \ ,$$

where D is a Fickian diffusion constant.

A.3.1.3 Explicit specifications of the boundary value problems in $[O_2^+] = [O_2^+(P,t)]$ and $[O^*] = [O^*(P,t)]$. The concentration field function $[O_2^+] = [O_2^+(P,t)]$ is defined as the solution of the boundary value problem in $[O_2^+(P,t)]$:

$$L_1([O_2^+]) \equiv \frac{\partial}{\partial t}[O_2^+] - D\frac{\partial^2}{\partial z^2}[O_2^+] + k_2[e(\infty)][O_2^+] - k_1[O^+(\infty)][O_2(\infty)]$$

$$- k_1[O_2(o)][O^+(\infty)]\left(\frac{h}{T_1}\right)^3 \exp\left(-\frac{r^2}{T_1^2}\right) = 0 \ ,$$

with

$$[O_2^+]_{t=0} = [O_2^+(P,t)]_{t=0} = [O_2^+(\infty)] \ , \quad P \text{ in } \mathcal{R}$$

and

$$[O_2^+]_{r=r_\infty} = [O_2^+(P,t)]_{r=r_\infty} = [O_2^+(\infty)] \ , \quad t \text{ in } \mathcal{R}.$$

The concentration field function $[O^*] = [O^*(P,t)]$ is defined as the solution of the boundary value problem in $[O^*(P,t)]$:

$$L_2([O^*]) \equiv \frac{\partial}{\partial t}[O^*] + k_3[O^*] - k_2[e(\infty)]\,[O_2^+] = 0 \ ,$$

with $[O_2^+] = [O_2^+(P,t)]$ defined by the boundary value problem in $[O_2^+(P,t)]$ and with

$$[O^*]_{t=0} = [O^*(P,t)]_{t=0} = [O^*(\infty)] \ , \quad P \text{ in } \mathcal{R}$$

and

$$[O^*]_{r=r_\infty} = [O^*(P,t)]_{r=r_\infty} = [O^*(\infty)] \ , \quad t \text{ in } \mathcal{R}.$$

A.3.2 Resolution of the Boundary Value Problem in $[O_2^+(P,t)]$

A.3.2.1 The substitution $U(P,t) = \exp(k_2' t)\,[O_2^+(P,t)]$. Let the function $U = U(P,t)$ be introduced by the substitution

$$U = U(P,t) = \exp(k_2' t)\,[O_2^+] = \exp(k_2[e(\infty)]t)\,[O_2^+(P,t)]$$

wherein the constant k_2' is defined by

$$k_2' \equiv k_2[e(\infty)] \ .$$

For $t = 0$ the function $U = U(P,t)$ has the representation required of the substitution $U = \exp(k_2' t)\,[O_2^+]$:

$$U(P,+0) = U(P,t)]_{t\to 0} = \left\{\exp(k_2' t)\,[O_2^+]\right\}_{t\to 0} = [O_2^+(\infty)] \ .$$

A.3.2.2 Green's function integral formula for $U(P,t) = U_1(P,t)+U_2(P,t)$.

The Green's function $G_1(z,z';t,\tau)$,

$$G_1(z,z';t,\tau) = \frac{1}{2\sqrt{\pi D(t-\tau)}} \exp\left(\frac{z^2 + z'^2}{4D(t-\tau)}\right) \cosh\left(\frac{z\,z'}{2D(t-\tau)}\right),$$

for z, z', t, τ in $\mathcal{R}$: $0 \leq t \leq t_\infty$, $0 \leq r \leq r_\infty$, $r^2 = x^2 + y^2 + z^2 = \xi^2+z^2$, $\xi^2 = x^2 + y^2$, can be used to write down a functional form for the function $U = U(P,t)$ which satisfies the boundary value problem in $U(P,t)$.

A.3.2.3 Representation of $[O_2^+(o,z,t)]$ in terms of the exponential integral function $E_1(-x) = \int_{-x}^{\infty} e^{-u}\, u^{-1}\, du$. For points $P:(x,y,z)$, $r^2 = \xi^2+z^2$, $\xi^2 = x^2 + y^2$, along the vertical z-axis, $\xi = 0$, the function $[O_2^+(P,t)]$ takes on the following value $[O_2^+(o,z,t)]$:

$$[O_2^+(o,z,t)] = \exp(-k_2' t)\; U(o,z,t)$$

$$= [O_2^+(\infty)] + q_o \frac{h^3}{T_1} \exp\left(-\frac{z^2}{T_1^2}\right) V_2^{(3)}(o,t) \exp(-k_2' t)$$

$$= [O_2^+(\infty)] + \frac{q_o h^3}{4DT_1} \exp\left(-\frac{z^2}{T_1^2}\right) \exp\left(-\frac{h^2}{4D}\right) \exp(-k_2' t) \cdot$$

$$\cdot \left[E_1(-\beta^2) - E_1\left(-\frac{T_1^2}{h^2}\beta^2\right)\right],$$

where $\beta^2 = \frac{h^2}{4}\frac{k_2'}{D}$.

A.3.2.4 The integrated line density function $S_{[O_2^+]}(o,\lambda h,t) = \int_o^{\lambda h} [O_2^+(o,z,t)]\,dz$. Along the vertical z axis, $\xi = 0$, the integrated line particle count function $S_{[O_2^+]}(o,\lambda h,t)$ for the concentration field $[O_2^+(P,t)]$, is defined by the line integral of $[O_2^+(o,z,t)]$ from $\xi = 0$, $z = 0$ to $\xi = 0$, $z = \lambda h$:

$$S_{[O_2^+]}(o,\lambda h,t) = \int_o^{\lambda h} [O_2^+(o,z,t)]dz$$

so that

$$S_{[O_2^+]}(o,\lambda h,t) = (\lambda h[O_2^+(\infty)]) \left\{1 + \frac{\sqrt{\pi}\, h^2}{8D\lambda} k_2' \frac{[O_2(o)]}{[O_2(\infty)]} \exp(-\beta^2) \exp(-k_2' t) \operatorname{erf}\left(\frac{\lambda h}{T_1}\right)\right.$$

$$\left. \cdot \left[E_1(-\beta^2) - E_1\left(-\frac{T_1^2}{h^2}\beta^2\right)\right]\right\} .$$

A.3.3 Properties of the Function $[O^*] = [O^*(P,t)]$.

A.3.3.1 Resolution of the boundary value problem in $[O^*(P,t)]$.

Attention is now directed towards the concentration field function $[O^*] = [O^*(P,t)]$ which is the solution of the boundary value problem in $[O^*(P,t)]$:

$$L_2([O^*]) \equiv \frac{\partial}{\partial t}[O^*] + k_3[O^*] - k_2[e(\infty)]\,[O_2^+] = 0$$

with

$$[O^*]_{t=0} = [O^*(\infty)] \ , \quad P:(x,y,z) \text{ in } \mathcal{R} \ ,$$

$$[O^*]_{r=r_\infty} = [O^*(\infty)] \ , \quad t \text{ in } \mathcal{R} \ .$$

The integrating factor $\exp(k_3 t)$ can be used to rewrite the equation of continuity in $[O^*]$, $L_1([O^*]) = 0$, in the form

$$\frac{\partial}{\partial t}\left(\exp(k_3 t)\ [O^*]\right) = k_2[e(\infty)]\ [O_2^+]\ \exp(k_3 t)\ .$$

By integration of both sides with respect to t and by use of the initial condition $[O^*]_{t=0} = [O^*(\infty)]$ it is evident that this partial differential equation has the reduced form

$$\exp(k_3 t)\ [O^*(P,t)] = [O^*(\infty)] + k_2[e(\infty)] \int_o^t \exp(k_3 t')\ [O_2^+(P,t')]\ dt'$$

so that the concentration field function $[O^*(P,t)]$ can be represented by the simple formula

$$[O^*(P,t)] = [O^*(\infty)]\ \exp(-k_3 t) + k_2[e(\infty)] \int_o^t \exp[-k_3(t-t')]\ [O_2^+(P,t')]dt'\ .$$

The function $[O_2^+(P,t)]$, which appears in the integrand of this integral formula for $[O^*(P,t)]$, is defined by the formula

$$[O_2^+(P,t)] = \exp(-k_2' t)\ U(P,t)$$

where

$$U(P,t) = [O_2^+(\infty)]\ \exp(k_2' t) + q_o \frac{h^3}{T_1} \exp\left(-\frac{z^2}{T_1^2}\right) \int_o^t \frac{\exp(k_2' t')}{T_1'^2} \exp\left(-\frac{\xi^2}{T_1'^2}\right) dt'\ .$$

with $T_1 = \sqrt{h^2 + 4Dt}$.

A.3.3.2 Representation of $[O^*(o,z,t)]$ as an indefinite time integral with an exponential integral kernel. For points P:(x,y,z), $r^2 = \xi^2 + z^2$, $\xi^2 = x^2 + y^2$, along the vertical z axis, $\xi = 0$, $[O_2^+(P,t)]$ takes on the form:

$$[O_2^+(o,z,t)] = [O_2^+(\infty)] \left\{1 + \frac{h^3 k_2'}{4DT_1} \frac{[O_2(o)]}{[O_2(\infty)]} \exp(-\beta^2) \exp(-k_2' t) \exp\left(-\frac{z^2}{T_1^2}\right) \cdot \right.$$

$$\left. \cdot \left[E_1(-\beta^2) - E_1\left(-\frac{T_1^2}{h^2}\right)\right]\right\} ,$$

so that along $\xi = 0$ the concentration function $[O^*(P,t)]$ is defined by the integral formula:

$$[O^*(o,z,t)] = [O^*(\infty)] \exp(-k_3 t) + k_2'[O_2^+(\infty)] \left\{-\frac{1}{k_3}[\exp(-k_3 t) - 1]\right\}$$

$$+ k_2'[O_2^+(\infty)]\, h\beta^2 \frac{[O_2(o)]}{[O_2(\infty)]} \exp(-\beta^2) \int_o^t \exp(-k_2' t') \exp[-k_3(t-t')]$$

$$\exp\left(-\frac{z^2}{T_1'^2}\right) \cdot \frac{1}{T_1'} \left[E_1(-\beta^2) - E_1\left(-\frac{T_1'^2}{h^2}\beta^2\right)\right] dt' .$$

A.3.3.3 Representation of $S_{[O^*]}(o,\lambda h,t) = \int_o^{\lambda h} [O^*(o,z,t)]\, dz$ as a time integral of the exponential integral function. In the concentration field $[O^*(P,t)]$, for points P:(x,y,z), $r^2 = \xi^2 + z^2$, $\xi^2 = x^2 + y^2$, along the vertical z-axis, $\xi = 0$, the integrated line particle count (per unit cross-sectional area), designated by the symbol $S_{[O^*]}(o,\lambda h,t)$, from $\xi = 0$, $z = 0$ to $\xi = 0$, $z = \lambda h$, is defined by the line integral formula

$$S_{[O^*]}(o,\lambda h,t) = \int_o^{\lambda h} [O^*(o,z,t)]\, dz$$

$$= \lambda h[O^*(\infty)] \exp(-k_3 t) \left\{1 - \frac{k_2'}{k_3} [1 - \exp(+k_3 t)] \frac{[O_2^+(\infty)]}{[O^*(\infty)]}\right.$$

$$+ \frac{\sqrt{\pi}\, k_2'}{2\lambda} \beta^2 \exp(-\beta^2) \frac{[O_2^+(\infty)]}{[O^*(\infty)]} \frac{[O_2(o)]}{[O_2(\infty)]} \int_o^t \exp[-(k_2'-k_3)t']$$

$$\left. \operatorname{erf}\left(\frac{\lambda h}{T_1'}\right) \cdot \left[E_1(-\beta^2) - E_1\left(-\frac{T_1'^2}{h^2}\beta^2\right)\right] dt'\right\} .$$

It is to be noted that the equation of continuity in $[O^*] = [O^*(P,t)]$, $L_2([O^*]) = 0$ (see Section A.3.1.3)

$$\frac{\partial}{\partial t}[O^*] = - k_3[O^*] + k_2[O_2^+]\,[e] ,$$

requires that, for times $t \to t_\infty$ and for points $r \to r_\infty$,

$$[O^*(\infty)] = \frac{k_2}{k_3} [O_2^+(\infty)]\,[e(\infty)] \equiv \frac{k_2'}{k_3} [O_2^+(\infty)] .$$

In other words, the boundary conditions in the region : $0 \leqq t \leqq t_\infty$, $0 \leqq r \leqq r_\infty$, imposed on the concentration field function $[O^*] = [O^*(P,t)]$, require that

$$\frac{k_2'}{k_3} \frac{[O_2^+(\infty)]}{[O^*(\infty)]} \equiv 1 .$$

This equilibrium condition can be used to cast the formula for $S_{[O^*]}(o,\lambda h,t)$ into the somewhat simpler form:

$$S_{[O^*]}(o,\lambda h,t) = \lambda h[O^*(\infty)]\left\{1 + \frac{\sqrt{\pi}}{2\lambda} k_3 \beta^2 \exp(-\beta^2) \frac{[O_2(o)]}{[O_2(\infty)]} \exp(-k_3 t) \cdot \right.$$

$$\left. \cdot \int_o^t dt' \exp[-(k_2'-k_3)t'] \operatorname{erf}\left(\frac{\lambda h}{T_1'}\right)\left[E_1(-\beta^2) - E_1\left(-\frac{T_1'^2}{h^2}\beta^2\right)\right]\right\},$$

wherein

$$\beta^2 = \frac{h^2 k_2'}{4D},$$

$$T_1 = \sqrt{h^2 + 4Dt},$$

$$E_1(x) \equiv \int_x^\infty \frac{\exp(-u)}{u}\, du,$$

$$k_2'[O_2^+(\infty)] \equiv k_2[e(\infty)]\,[O_2^+(\infty)] = k_1[O_2(\infty)]\,[O^+(\infty)] = k_3[O^*(\infty)].$$